

A STUDY ON MUONS ASSOCIATED WITH
EXTENSIVE AIR SHOWERS

Thesis presented

by

Y.C. SAXENA

to the

Gujarat University
for the Ph.D. degree

December 1971

043



B4313

Physical Research Laboratory
Ahmedabad-9

P R E F A C E

An experiment, to study high energy muons (Energy ≥ 150 Gev) associated with Extensive Air Showers (EAS) of cosmic rays, has been conducted by the author, at Kolar Gold Fields (K.G.F.), India, in collaboration with the Tata Institute of Fundamental Research (TIFR), Bombay. The thesis incorporates the results from this experiment.

The basic aim of such a study is to derive information about the characteristics of nuclear interactions in which such high energy muon component of EAS is produced. The muon component of EAS arises mainly through the decay of the parent particles e.g. pions and kaons. High energy pions and Kaons, in turn, are produced in the first few high energy ($\geq 10^{13}$ eV) interactions in the upper regions of the atmosphere. These muons, after being produced, maintain their direction and spectrum very closely and hence carry information, about the various features of the high energy interactions as well as about the nature of the particles participating in the interactions. Thus a study, such as the present one, is helpful in obtaining information about the nuclear interactions and the composition of the primary cosmic rays at high energies.

The experimental set-up consists of

- i) an air shower array at the surface, consisting of 20 plastic scintillators arranged along the

peripheries of concentric circles of increasing radii; and

- ii) a penetrating particle detector located at a depth of 194 m underground.

The author, working at Physical Research Laboratory, Ahmedabad, under the guidance of Dr. Bibha Chowdhuri and Prof. V.A. Sarabhai was responsible for the fabrication, setting-up and maintenance of the penetrating particle detector and the associated electronic circuits used in the present experiment. The EAS array and associated circuitry, used in the present experiment, form part of the experimental set-up of the TIFR EAS group at K.G.F. The data reduction and the analysis of the EAS data to fit shower parameters was done by the author, on CDC 3600/160A computer installation at TIFR, in collaboration with and using a computer programme of the TIFR EAS group. Further analysis, to obtain the results presented in the thesis, was done by author himself using CDC 3600/160A computer system at TIFR and IBM 1620 computer at Physical Research Laboratory, Ahmedabad. The author is responsible for the results and the conclusions presented in the thesis. The material presented in the thesis is divided into seven chapters.

The first chapter contains a brief review of the present knowledge about the various components of EAS. Some of the aspects of EAS studies, the importance of the muon component of EAS and the scope of the present work are outlined together with a brief description of the theories and models of high energy interactions, involved in the development of EAS.

The second chapter deals with the experimental set-up used in the present experiment. Triggering, recording and selection procedures are described.

The third chapter describes the data reduction procedure and gives details of the analysis done to obtain the various parameters of the recorded showers. Results of an error analysis are presented.

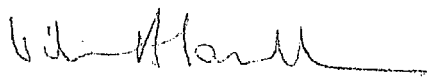
The fourth chapter gives the results obtained from the experiment. The main results relate to the size spectra of the EAS recorded with and without the associated muons, the number of muons of energy ≥ 150 Gev in showers of different sizes and the energy spectrum of the muons in EAS.


The results of Monte-Carlo calculations, carried out for some of the models on muon component of EAS are presented in the fifth chapter. A comparison of the predictions of the models with the results from present experiment is given. The implications of the results are discussed.

In sixth chapter results from the data obtained with neon flash tube hodoscope are presented. A discussion of these results along with their comparison with the results obtained in other similar experiments is given. The results are also compared with the predictions of the known theories.

The seventh chapter contains a summary of the results and the conclusions from the present experiment.

The thesis presents new results on the muons of energy ≥ 150 Gev in EAS, having sizes in the range $10^5 \leq N \leq 5.10^6$ particles, which may be helpful in better understanding of the high energy interactions and the composition of primary cosmic rays in relevant energy range (10^{14} eV - 5.10^{15} eV)


(Vikram A. Sarabhai)
Professor-in-charge


(Y.C. Saxena)
Author

ACKNOWLEDGEMENTS

The author wishes to acknowledge with gratitude his indebtedness to Dr. Bibha Chowdhuri for guidance and supervision of this work in all its facets, and to Prof. Vikram A. Sarabhai for guidance, encouragement and many helpful suggestions during this investigation.

The author is grateful to Prof. B.V. Sreekantan and his colleagues of TIFR EAS group for extremely helpful collaboration throughout the present investigation. Thanks are due to Prof. S. Naranan, Dr. K. Sivaprasad and Dr. M.V. Sreenivas Rao for many useful discussions and suggestions.

The author is grateful to Prof. S.P. Pandya who read the manuscript and suggested many improvements. Constant encouragement and advices given by Profs R.P.Kane, U.R. Rao and Satya Prakash are gratefully acknowledged.

Author is extremely thankful to Shri S.R. Thakore, Head of the computer centre, Physical Research Laboratory, and his colleagues for the help in computations and data processing. Thanks are due to M/s M.A. Gandhi, P.S. Shah and Atchuta Rao for help in computer programming and to M/s C.R.T. Nair and V.P. Nair for the job processing on CDC 3600/160 A at TIFR, Bombay. The assistance rendered

by Miss K.B. Vijayakar in data processing at TIFR, Bombay is gratefully acknowledged.

The author is grateful to the authorities of "Kolar Gold Mining Undertakings" for providing various facilities during the course of the present investigation.

It is a pleasure to acknowledge the help rendered by M/s K.P. Kamath, C.K. Viswanathan and A.R.S. Pandian in maintainence and running of the experiment at its various stages. The efforts put up by M/s K.G. Sharma and C.S. Panchal in making the neon-flash-tubes are thankfully acknowledged.

The author is thankful to the personnel of the drafting and photographing section of the Physical Research Laboratory for help in making the diagrams presentable.

The financial help provided by the Ministry of Education, Government of India and the Department of Atomic Energy is gratefully acknowledged.

The author is thankful to Miss Lakshmi for neat typing of the draft and to Mr. T.E. John for the patient and excellent job of typing the thesis.

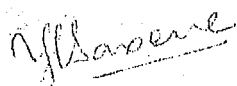

(Y.C. SAXENA)

TABLE OF CONTENTS

	<u>Page</u>
PREFACE	i
ACKNOWLEDGEMENT	v
<u>CHAPTER I</u> : Introduction ..	1
I.1 Extensive Air Showers (Historical)	1
I.2 Development of EAS in the atmosphere	4
I.3 Electron Component of EAS	6
I.4 The Penetrating Component of EAS	10
I.5 N-Component of EAS ..	12
I.6 Muon - Component of EAS ..	14
I.7 Objectives of EAS Studies	24
I.8 High Energy Interactions	26
I.9 Importance of Muon Component of EAS	30
<u>CHAPTER II</u> : Experimental Arrangement	33
II.1 Experimental Set-up ..	33
II.2 Air Shower Array ..	33
II.3 The underground Detector	37
II.4 Electronics Used With UG Detector	40
II.5 Detection Efficiency for the Underground Detector	41

	<u>Page</u>
<u>CHAPTER III: Data Reduction and Analysis</u>	43
III.1 Data Reduction ..	43
III.2 Evaluation of Shower Parameters	45
III.3 Initial Estimates of Shower Parameters	48
III.4 Errors in the Fitted Parameters	49
<u>CHAPTER IV: Experimental Results</u>	55
IV.1 Shower Data ..	55
IV.2 The 100% area for Showers	56
IV.3 The Size Spectra ..	58
IV.4 Number of Muons of Energy ≥ 150 Gev, in Showers of Different sizes	66
IV.5 Energy Spectra of Muons in EAS	75
IV.6 Primary Cosmic Ray Spectrum	76
<u>CHAPTER V: Discussion and Conclusion</u>	79
V.1 Comparison of Present Experimental Results of Other Experiments	79
V.2 Monte Carlo Calculations	83
V.3 Results of Monte Carlo Calculations	88
V.4 Comparison of Experimental results with the Predictions of the Models	92
V.5 Consequences of Observed η_{μ^-} Ne Variation	94

Page

V.6	Primary Mass Composition and n_{μ} - Ne Relation	95
V.7	Change in the nature of the Characteristics of the nuclear Interaction and the n_{μ} - Ne Relation	101
V.8	Energy Spectrum of Muons in EAS	102
V.9	Conclusions ..	105
V.10	Suggestions for future Investigations	106
CHAPTER VI: NFT Hodoscope Data Results and Discussion		108
VI.1	The NFT Data ..	108
VI.2	The Single-track Events ..	111
VI.3	Pair-track Events ..	118
VI.4	Multiple-track Events ..	126
VI.5	Electromagnetic Interactions of the High Energy Muons	127
VI.6	Large Size Bursts ..	130
VI.7	Conclusion and Summary ..	131
VI.8	Suggestions for Further Investigations	133
CHAPTER VII: Summary ..		138
List of References ..		R1

CHAPTER I

INTRODUCTION

I.1 Extensive Air Showers: (Historical)

Extensive Air Showers, characterised by the simultaneous incidence of a large number of coherent particles from the atmosphere, over large areas, were discovered independently by Auger et al. (1938) and Kolhorster et al. (1938) by observing coincidence between the coherent particles with separations varying from 40 cm to few tens of meters. Auger et al. (1939a) obtained coincidences between particles separated by distances of the order of 300 m while Skobelt'syn et al. (1947) presented evidence of the existence of coherent particles separated by distances ~ 1 Km. These and other similar experiments demonstrated the extensive nature of the phenomenon which was appropriately named Extensive Air showers abbreviated EAS.

A predominantly electronic nature of the particles in the EAS was inferred by Auger et al. (1939b) from the study of the secondary effects of these particles. Plate cloud Chamber photographs of the EAS particles (Janossy and Lovell 1938; Auger et al. 1939c) also showed concentration of the tracks, implying production of secondary showers by electrons and photons forming part of the EAS.

Indications of the presence of a penetrating component of the EAS, capable of traversing 20 cm of lead, were already available in the experiments of Auger et al. (1938, 1939b) and the presence of this component was confirmed by Daudin (1945), Rogo~~g~~isky(1944), Cocconi et al. (1946) and Broadbent and Janossy (1947a, 1947b, 1948). A number of slow proton tracks were seen in cloud chamber photographs of the EAS particles, by Auger et al. (1939b). V.C. Tongiorgi (1948a, 1948b, 1949) in a series of experiments, using BF3 counters, gave evidence of the presence of neutrons in EAS. The presence of a nuclear active component (N-Component) was thus established. Thus, within a short period of the discovery EAS were known to consist of i) an electron-photon component and ii) a penetrating component a part of which contained nuclear active particles.

Extensive Air showers are initiated by the primary cosmic ray particles of energy $\geq 10^{12}$ eV incident on the earth's atmosphere. The primary particles, which initiate EAS, could either be i) electronic in nature, i.e. consist of electrons and/or photons or ii) nucleons and to a certain extent heavy nuclei.

Because of the predominance of the electron-photon components, the EAS were initially believed to be produced by electrons or photons forming part of primary cosmic rays.

Hulsizer and Rossi (1948), however, gave an upper limit of 1% for the fraction of the electrons of energy $\geq 4.5 \times 10^9$ eV in the primary cosmic rays. The possibility of electrons initiating EAS was also ruled out on the ground that bremsstrahlung radiation from the electrons in the galactic magnetic field will not allow the electrons to have energies $> 10^{12}$ eV. A search for 'the photon initiated EAS' was undertaken, in Bolivian Air Shower Joint Experiment (BASJE), based on the idea that such showers will contain extremely small numbers of penetrating particles. Though the results from this experiment (K. Suga et al. 1963; V. Toyoda et al 1965) as well as the experiment of Polish group (R. FirKowski et al. 1962a, 1962b, 1963; J. Gawin et al. 1968) confirmed the existence of a separate group of such showers, the flux of the primary photons obtained on the basis of the rate of such showers was found to be too small to account for the observed EAS flux, the estimated flux being $\sim 2.0 \times 10^{-11} \text{ cm}^{-2} \text{ Sec}^{-1}$ for primary γ -rays of energy $\geq 3 \times 10^{13}$ eV (Kamata et al. 1968) and $(6 \pm 4) \times 10^{-9} \text{ m}^{-2} \text{ Sec}^{-1} \text{ Sr}^{-1}$ for the primary gamma-ray energy $\geq 8 \times 10^{14}$ eV (Gawin et al 1968). The primary cosmic ray electrons and photons could, then, not be considered as responsible for the production of the majority of the EAS and the only other possibility is

the production through the interactions of primary nucleons and heavy nuclei in the atmosphere. Cloud chamber photographs by various workers (Daudin 1944; Rochester 1946; Bridge et al. 1948) demonstrated that the electrons and photons could be generated through nuclear interactions. The results on the distribution of the ionizing particles in the EAS were also in agreement with the distributions for the showers developed through a process of nuclear cascade (Section I.3; Greisen 1960). It is now, therefore, widely accepted that the majority of Extensive Air showers originate in the nuclear interactions of the primary cosmic ray nuclei, high in the atmosphere.

I.2 Development of EAS in the Atmosphere:

The majority of primary cosmic ray particles, which initiate EAS, are protons with a small fraction of α -particles and heavy nuclei. The primaries undergo nuclear interactions with air nuclei. The interactions being inelastic, a fraction η of the primary energy is given to the interaction which results in the production of new particles, e.g. pions, Kaons, nucleon - antinucleon pairs, hyperons etc. Pions are the most abundant among the created particles and the neutral pions, having a very short life time ($\sim 2 \times 10^{-16}$ sec) decay almost instantly into two γ -rays.

The primary particle survives either as a proton or a neutron or in some excited non-strange isobar state with an energy $(1 - \eta)$ of the total energy. The surviving particle together with other nuclear-active particles, produced in the proceeding interactions, undergoes further interactions in the atmosphere giving rise to more particles. A nuclear cascade is, thus, generated.

For unstable charged particles, e.g. pions and kaons there is a competition between the nuclear interaction and the decay. A fraction of these particles then decays into muons. Muons have very high penetrating power, since their interactions with matter are weak. Most of the accurate muon-nucleon scattering experiments give limits to the cross-section which are at least three orders of magnitude smaller than the geometric cross-section. Moreover, the decay probabilities for the high energy muons, during their traversal through the atmosphere, are practically negligible because of a rather large life time ($\sim 2 \times 10^{-6}$ Sec) and the relativistic time dilation. The mu-mesons thus form a highly penetrating component of EAS.

The γ -rays of sufficient energy, produced by the decaying neutral pions, initiate electron-photon cascade. The number of particles in these cascades keeps on multiplying till i) the electron energies are

oreduced below ϵ_c , the critical energy of electrons, ii) the photon energies are in the region where Compton-scattering and photo-ionization processes predominate over the pair-production process and iii) the energy source, i.e. the nuclear cascade, becomes depleted.

The particles, at the time of their production, acquire transverse momenta and are also subjected to deflections due to Coulomb - scattering and magnetic field of the earth. Hence, they are distributed in lateral plane and are spread over large areas around the axis or core of the EAS. The core preserves the direction of the initiating primary and exhibits a high density of the particles.

The particles in the EAS can then be classified into following categories:

a) a soft component consisting of electrons and photons which form a majority of the particles and

b) a penetrating component comprised of i) the N-component containing particles capable of undergoing nuclear interactions and ii) the muons and neutrinos.

I.3 Electron Component of EAS:

A large amount of experimental as well as theoretical effort, in the studies of EAS, has been

directed to the study of electron - photon component and is confined, to a great extent, to the understanding of the distribution of the electrons around the axis of the EAS and the measurements of the frequency of EAS as a function of total number of ionizing particles.

The experimental results on the lateral distribution of the ionizing particles (consisting, mainly, of electrons) in the EAS indicate a near invariance of the distribution with respect to the size of the shower as well as the altitude of their observation. The main source of the lateral spread of the electrons in EAS is the multiple Coulomb - scattering and the lateral spread is generally expressed in terms of Moliere unit defined as

$$r_1 = E_S X_0 / \epsilon_c = \frac{73.5}{P} \cdot \frac{T}{273} \text{ m} \quad \dots(1.3.1)$$

where $E_S = 21 \text{ MeV}$ is the characteristic scattering energy of the electrons, ϵ_c the critical energy and X_0 is the radiation length. P is the atmospheric pressure and T the temperature in $^{\circ}\text{K}$. The density $\rho(r)$ of a particle at distance r from the axis can be written as

$$\rho(r) = (N/r_1^2) \cdot f(s, r/r_1) \quad \dots(1.3.2)$$

The function $f(s, r/r_1)$ is known as the lateral distribution function normalised such that

$$\int_0^{\infty} f(s, r/r_1) \cdot 2\pi(r/r_1) d(r/r_1) = 1 \quad \dots(1.3.3)$$

The parameter s is called the age parameter of the shower and is related to the longitudinal development of the shower.

Theoretical calculations, based on the electromagnetic cascade theory, have been done by a number of authors. Moliere (1946) derived the lateral distribution functions for the showers at the maxima of their development. The calculations were limited by inaccuracies at low energy. Nishimura and Kamata (1950, 1951, 1952) have derived the distribution functions for showers at all stages of their development and following Greisen (1956) the Nishimura - Kamata (NK) distribution function can be written as

$$f(s, r/r_1) = C(s) (r/r_1)^{s-2} (1 + r/r_1)^{s-4.5} \quad \dots (1.3.4)$$

$$C(s) = (4.5 - s) / 2 \Gamma(s) \cdot \Gamma(4.5 - 2s)$$

This formula, known as NKG-formula, gives a good fit to the NK-distribution function for $0.6 \leq s \leq 1.8$ and $0.01 \leq r/r_1 \leq 10$. Derivation of NK-distribution function involves following definition of s

$$s = 3t / (t + 2 \ln(E_0/\epsilon_C) + 2 \ln(r/r_1)) \quad \dots (1.3.5)$$

which implies a variation of s with r . However, the r dependence of s is rather weak for $-1 \leq r/r_1 \leq 1$ and a single value of s can be used in this region of r .

The most extensive measurements of the lateral distribution of the ionizing particles in EAS have been carried out by Russian workers (Dobrovolsky et al. 1956; Dovchenko and Nikol'skii 1955; Khristiansen et al. 1956; Zatsepin et al. 1963). Measurements have also been done by M.I.T group (Clark et al. 1957) and a number of other groups. The experimentally obtained lateral distributions can be fitted to the NK-distribution with the age parameter $s \sim 1.2$ to 1.3 (Cocconi 1958; Khristiansen 1958; Greisen 1960)

It is thus seen that the lateral distribution of all ionizing particles in EAS resembles closely the one obtained on the basis of a pure electromagnetic cascade. However, it is also observed that the variation in the shape of the distribution with the altitude of the observation of the showers is extremely slow contrary to what one would expect on the basis of a pure electromagnetic cascade. Also the variation of s with r is not in confirmation with the predicted one.

Thus the electron - photon component in EAS is not a pure electromagnetic cascade but an admixture of a number of such cascades generated during the longi-

tudinal development of EAS. The source of the electromagnetic cascade is a line source continuously feeding the energy to the cascade and, thus, maintaining a near constant shape of the distribution (Greisen 1960).

I.4 The penetrating component of EAS:

a) Percentage of penetrating particles:

Various investigations, (e.g., those of Broadbent et al. (1947), Chowdhuri (1948), Cocconi et al. (1949a), McCusker (1950) and McCusker and Millar (1951) at sea level and those of Treat and Greisen (1948), Sitte (1950, 1952) and Kasnitz and Sitte (1954) at mountain elevations) to study the penetrating component of EAS, involved the detection of EAS, by means of unshielded counters, and examining the penetrating particle detector in coincidence with the showers. Majority of experiments were aimed at obtaining the ratio " R_p " of the penetrating particles to the total number of ionizing particles. A value of $(2 \pm 0.2) \%$ was obtained for R_p by Chowdhuri (1948) and other experiments were in broad agreement with this value. However, results of McCusker and Millar (1951) gave an average value of 6% for R_p . It was also shown that under certain conditions R_p approached 100%. Later experiments of Eidus et al. (1952) at sea level and of Zatsepin et al. (1953) at mountain

elevations demonstrated a variation of R_p with distance r from the axis of the shower. At large distances R_p increases linearly with r the variation becoming less rapid at small distances with the R_p value levelling off to $\sim 1\%$ near the axis, (Greisen 1956).

Size variation of R_p was demonstrated by Cocconi et al. (1949b) and Ise and Fretter (1952) at mountain elevations and by Milone (1952) at sea level and could be expressed as

$$R_p \propto N_e^{-0.13} \quad \text{or} \quad N_p \propto N_e^{0.87}$$

where N_p is the total number of penetrating particles in showers of size N_e . It is thus seen that the number of penetrating particles in a shower increases less rapidly than the total number of particles.

b) Ratio of Interacting to non-interacting penetrating Particles in EAS:

The penetrating particles of the EAS consist, mostly, of nucleons, π - mesons and muons. A part of the penetrating particles produce local showers, as was evident from experiments of Brown and McKay (1949), Ise and Fretter (1949) and Chowdhuri (1950). The penetrating particles can then be divided into "the interacting" and "the non-interacting" components. The former consists of N-particles and later mostly of mu-meson

The percentage of N-particles in the penetrating component of EAS was investigated in a number of early experiments. McCusker (1950) gave a 1:2 ratio for interacting to non-interacting particles. Greisen et al. (1950) found the intensity of N-component to be 60% that of non-interacting component near shower axis. Experimental results of Chowdhuri et al. (1952) gave a ratio of N-component to μ -mesons as high as 88%, taking all low energy events into consideration, for showers of primary energy 10^{15} eV. The high energy N-component (> 10 GeV) was found to be 29% as abundant as μ -meson. Fujicka (1953) obtained the abundances of the N-component among penetrating particles at various core distances and found that the values varied from 0.64 at 5 m to 0.37 at 47 m.

Most of the above mentioned experiments, however, lacked in details, e.g. the energy of the detected particles, the size of the showers detected etc. and so a consistent picture could not be obtained from these experimental results.

I.5 N-Component of EAS:

The behaviour of nuclear active particles in EAS can be understood in terms of N-cascade of EAS. The studies of N-component of EAS, conducted by a number of workers, are mainly related to i) the lateral distribution

of the particles around EAS core, ii) the dependence of N-particle number N_n on shower size N_e and iii) the energy spectrum of the N-particles.

In energy range of 0.9 Gev - 3 Gev Danilova and Nikol'ski (1963) have obtained a lateral distribution which is well represented by

$$\rho_n(r) = \frac{\Lambda}{r} \exp \left(- \frac{r}{r_0} \right)$$

for $3 \times 10^4 \leq N_e \leq 10^7$ particles, with $r_0 = 70$ m for 2 Gev particles and 50 m for 3 Gev ones. Chatterjee et al. (1968a) give following form of lateral distribution of N-particles of energies between 50 Gev to 1600 Gev for showers of size $3 \cdot 10^4 \leq N_e \leq 3 \times 10^6$ at 800 gm/cm^2 .

$$\rho_n(N_e, r, E_n) = A \exp(-r/r_0)$$

$$\Lambda = 8.2 \left(\frac{N_e}{2 \cdot 10^7} \right)^{0.097} E_n^{0.28}$$

$$r_0 = 13.3 \left(\frac{N_e}{2 \cdot 10^7} \right)^{0.39-0.49} E_n^{0.28}$$

$$0 \leq r \leq 15 \text{ m}$$

The integral energy spectrum obtained in various investigations agrees well with a power law having an index of -1.0. Chatterjee et al. (1968a) give an index

of -1.1 for the energy spectrum in the above mentioned energy range.

The ratio of the N-particles to the total number of particles in EAS decreases with increasing size. Danilova and Nikol'skii (1963) give following relation for particles of energy 0.2 Gev - 3 Gev at 3300 m elevation.

$$N_n / N_e = (1.2 \pm 0.4) 10^{-2} (N_e / 10^6)^{-0.34 \pm 0.01}$$

for $3 \times 10^3 \leq N_e \leq 10^7$. A similar results is obtained by Chatterjee et al. (1963) for N- particles of energy ≥ 1 Gev at 800 gm/cm² for sizes $10^5 \leq N_e \leq 10^7$

$$N_n / N_e = 2.1 \times 10^{-3} \left(\frac{N_e}{10^6} \right)^{-0.35 \pm 0.05}$$

At higher energies (50 Gev - 1600 Gev) Chatterjee et al. (1968a) give the following relation

$$N_n (\geq E_n, N_e) = 1.75 N_e^{0.78} E_n^{-1.1}$$

I.6 Muon Component of EAS:

The main emphasis in experiments to study EAS problems has slowly changed from the electron-photon component to muon component, as it has become clear that the latter component carries a large share of the

original energy. Various features of muons, associated with EAS, which have been studied are a) the lateral distribution of muons, b) their energy spectrum, c) variation of total number of muons with shower size, d) the fluctuation of muons at observation level and e) the phenomena of multiple penetrating particles and muon beams.

Various investigations on the muons associated with EAS may be classified into three different categories.

- i) Experiments in which muons of energy greater than a given energy E_μ are selected through detectors shielded by appropriate amount of absorber and the detectors examined in coincidence with EAS. These experiments may be termed as "absorption experiments".
- ii) Experiments using magnetic spectrographs with a muon detector in coincidence with EAS.
- iii) The experiments studying the e-m bursts produced by muons associated with EAS.

Pioneering work in this field was done by Barret et al. (1952) who studied the muon intensities at a depth of ~ 1600 m.w.e underground, corresponding to $E_\mu = 560$ Gev, in association with air showers at the surface. The most extensive measurements in this regard

are those of Bennett and Greisen (1961) and Earnshaw et al. (1967, 1968). A number of experiments at energies $E_\mu \sim 40$ Gev, have been done by Russian group using absorption, underground for selecting muons. Following paragraphs summarise the present information available on muons in EAS:

a) The Lateral Distribution of Muons:

Fig.1.1 to Fig 1.4 show lateral distribution of muons of energy ≥ 1 Gev, ≥ 10 Gev, ≥ 40 Gev and ≥ 100 Gev as obtained by various workers, mentioned therein, and normalised to showers of size 10^6 particles. Measurements show that the muons, in EAS, have a broader-distribution than electrons. Also the distribution becomes steeper for higher energy muons. Nikol'skii (1962) has fitted following formula to the lateral distribution obtained by Vavilov et al (1957), Khernov (1961) and Fukui et al (1960) for muons of energy ≥ 440 Mev in showers of size 7.7×10^5 particles.

$$\rho_\mu(r) = A(N, E_\mu) (r+2)^{-0.7} \exp(-r/r_0(E_\mu))$$

with $r_0(\geq 440 \text{ Mev}) = 330 \text{ m}$, $r_0(\geq 1 \text{ Bev}) = 220 \text{ m}$ and $r_0(\geq 5 \text{ Bev}) = 100 \text{ m}$.

Greisen (1960), on the basis of the available experimental results, has given the following formula for the lateral distribution of muons of various energies.

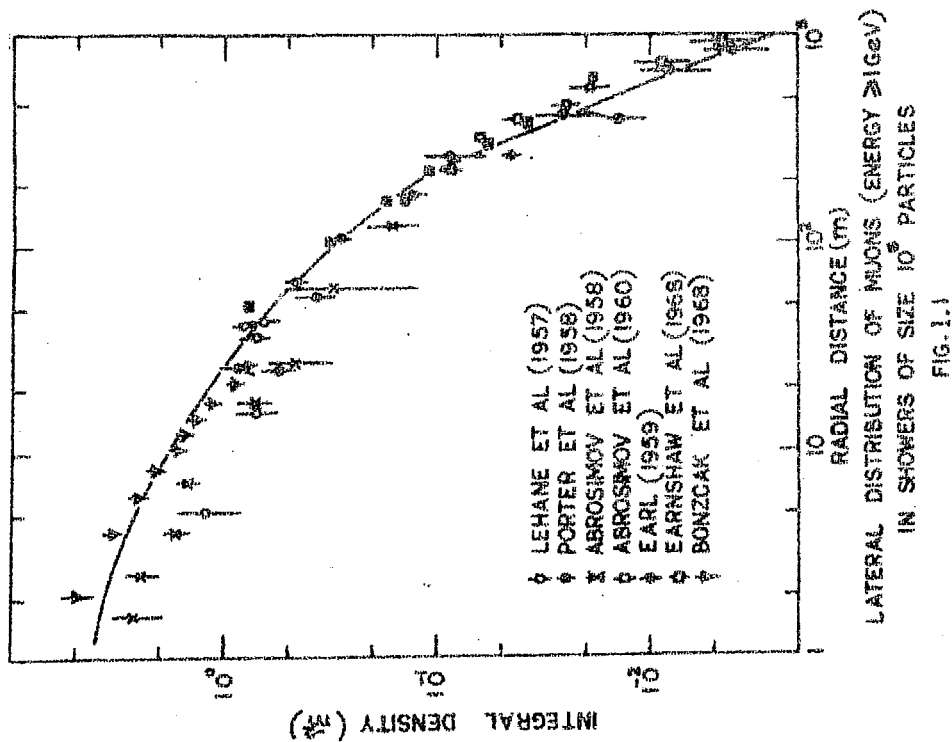


FIG. 1.1

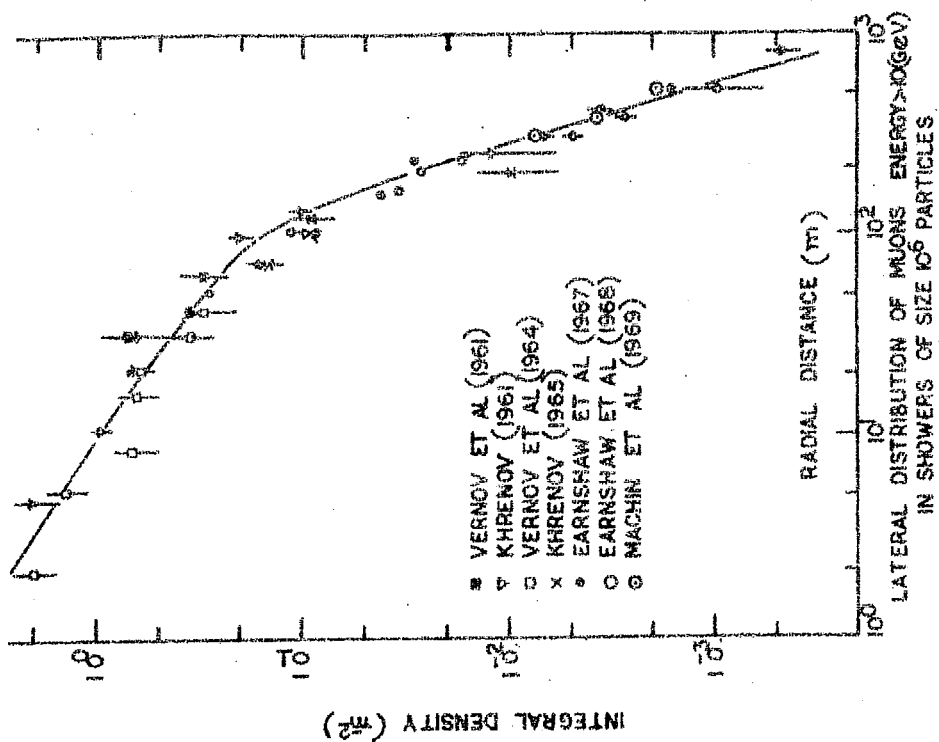
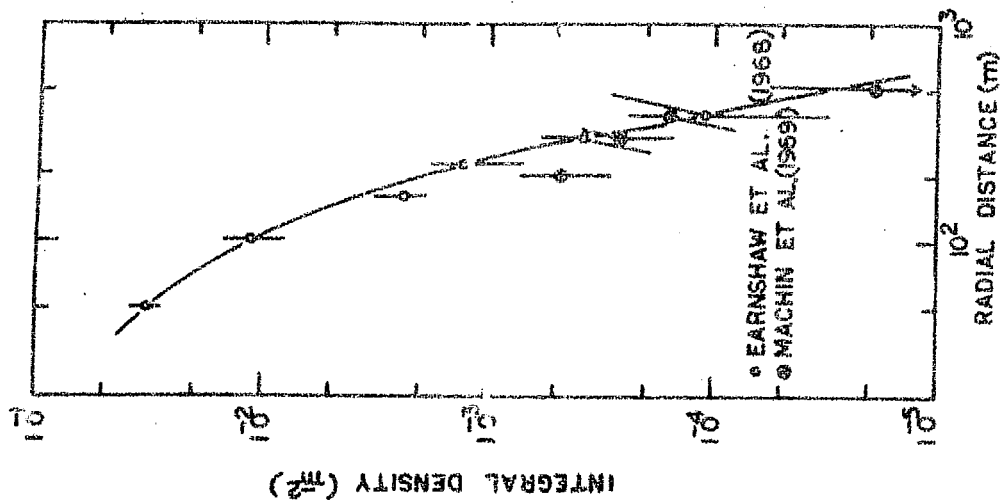
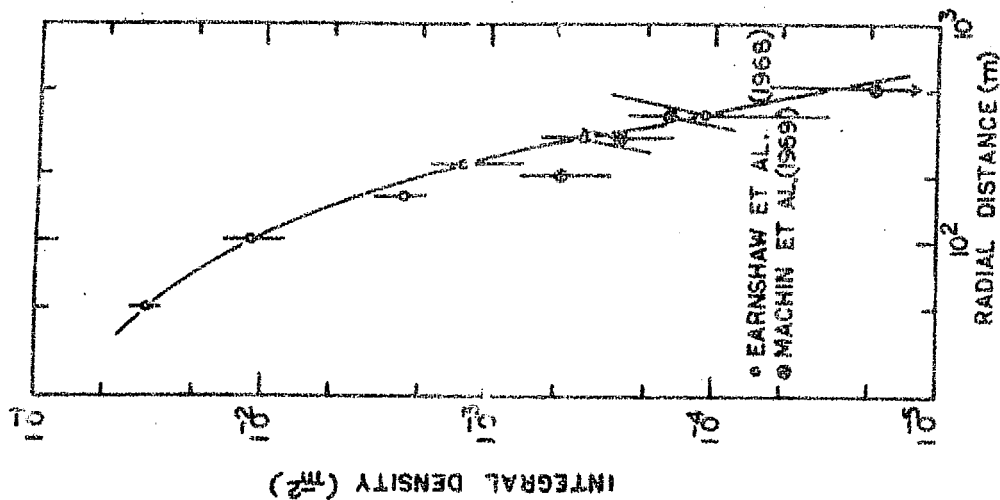


FIG. 1.2



LATERAL DISTRIBUTION FOR MUONS (ENERGY $> 40 \text{ GeV}$)
IN SHOWERS OF SIZE 10^6 PARTICLES

FIG.1.3



LATERAL DISTRIBUTION FOR MUONS (ENERGY $> 100 \text{ GeV}$)
IN SHOWERS OF SIZE 10^6 PARTICLES

FIG.1.4

$$\rho_{\mu}(r, N, \geq E_{\mu}) = A(N, \geq E_{\mu}) r^{-0.75} \left(1 + \frac{r}{520}\right)^{-2.5}$$

$$20 \leq r \leq 500 \text{ m} \quad \& \quad 1 \leq E \leq 20 \text{ GeV.}$$

The experimental results of Earnshaw et al (1968) for the threshold energies upto 100 GeV are in agreement with the above formula. Barrett et al. give a mean lateral distance of 9.7 m for muons of energy ≥ 560 GeV whereas Sivaprasad (1970) has obtained a mean distance of (12 ± 2) m for muons of energy ≥ 220 GeV.

Hara et al. (1970) have obtained the lateral distribution of muons above 5 GeV. The distribution goes as $r^{-2.6 \pm 2.5}$ for $200 \leq r \leq 800$ m. For the size range $10^4 - 10^8$ particles Staubert et al (1970) measured the lateral distribution of muons with energies ≥ 2 GeV. The lateral distribution was found to go as $r^{-0.85 \pm 0.02}$ and was found to be independent of the shower size within limits of error.

b) Size dependence of muon number:

Measurements done as early as 1949 by Cocconi et al. have shown that the relative number of muons decreases with increasing shower size. Results of majority of experiments, summarised by Greisen (1960) are in agreement with a dependence of the type

$$N \propto N_e^{0.75}$$

for threshold energies ≤ 40 GeV.

However, the results of Barrett et al. (1952) give a dependence of the type

$$N \quad (\geq 560 \text{ GeV}) \propto N_e^{0.45 \pm 0.13}$$

which indicates that the increase in number of muons of higher energies is much flatter. Recent measurements by Hara et al. (1970) for muons with energies ≥ 5 GeV give a size dependence of the type $N_e^{0.85 \pm 0.10}$ whereas the experiments of Vernov et al. (1970) and Staubert et al. (1970) yield a size dependence of the type $N_e^{0.78}$. However, Catz et al (1970) have demonstrated, for muons with energies ≥ 1 GeV, a characteristic oscillation in the value of $\alpha = \partial \ln N_\mu / \partial \ln N_e$ in the size range $10^5 - 10^6$. The authors indicate a possible change in the primary composition on the basis of this oscillation in α . However, there are also significant errors on the values of α .

Sivaprasad (1970) has obtained a size dependence for muons of energies ≥ 220 GeV and ≥ 640 GeV in showers of size $10^5 - 10^6$ particles. The relationship is a power law with power index (0.41 ± 0.14) . The earlier results of TIFR group (Chatterjee et al. (1965) and Chatterjee et al. (1968b) were in error and the modified results have been presented by Sivaprasad (1970) and summarised by Sreekantan (1971).

c) Energy Spectrum of Muons in EAS:-

On the basis of various experimental results Greisen (1960) gives an energy spectrum of the type

$$N_{\mu} (\geq E_{\mu} , N) = 1.7 \times 10^5 \left(\frac{N}{10^6} \right)^{0.75} \left(\frac{2}{E_{\mu} + 2} \right)^{1.37}$$

The spectral index obtained by Sivaprasad (1970) for $E_{\mu} \geq 220$ Gev is (1.35 ± 0.15) which is similar to that obtained by Greisen (1960) but the absolute values of muon numbers at $E_{\mu} \geq 220$ Gev and $E_{\mu} \geq 640$ Gev are much smaller than expected on the basis of the above formula. Results of Earnshaw et al (1968) give an energy spectrum of the type very much similar to that obtained by Greisen in the range $1 \leq E_{\mu} \leq 100$ Gev and $10^5 \leq N \leq 10^8$ particles.

There are no experimental results on energies between 100 Gev and 200 Gev at present. The present experiment deals with muons of energy ≥ 150 Gev and the details of the energy spectrum will be discussed in later chapter.

d) The Fluctuations in muon number at observation level.

Studies of fluctuations in the number of muons in showers of a given size as well as fluctuations in the shower size for showers having a given muon number have

been done by Moscow state university group (Vernov et al 1968, Vernov et al 1970). It is seen that for showers of a given size N_e the dispersions DN_μ/N do not change within the range error and within the whole range of N_e studied viz. $10^5 \leq N \leq 10^7$. The relation between \bar{N}_μ the average number of muons, and N_e at fixed N_e and the relation between N_μ and \bar{N}_e at fixed N_μ are described by a power law with the same exponent $\alpha = 0.78$. However, the proportion of muons in the showers with fixed N_μ is greater by a factor of (1.51 ± 0.18) than for the showers with fixed N_e . Firkowski et al (1970) have also investigated the fluctuations in EAS development on the basis of the ratio N_μ/N_e for two muon energy thresholds (0.5 Gev and 5 Gev). From the investigation of the electron and muon component of EAS Khristiansen et al. (1970) have shown that the dependence of the average number of muons \bar{N}_μ on the size N_e can be approximated by a single power law in a large interval of N_e . The dispersions of the distributions of N_μ/N_e for the showers with fixex N_e have large values in the interval of $N_e = 10^5 \div 10^7$. From these studies the authors conclude that protons make up a considerable part of the primary cosmic radiation at energies of $10^{15} - 10^{17}$ eV.

From the very narrow distribution of the number of muons observed in large EAS Linsley and Scarci (1962), Suga et al (1970) and others have concluded that the primary cosmic ray particles above 10^{17} eV are mainly protons.

e) Multiple Penetrating Particles and Muon Beams:

The phenomenon of multiple penetrating particles (mpp) has been of considerable interest in studies of EAS. Barret et al. (1952) were the first to report such events in which more than one parallel particles separated by distances ~ 1 m were incident on the underground detector simultaneously. Since then a number of workers have reported this type of events both in experiments associated with EAS as well as in experiments not associated with EAS. Barton (1968) has compiled alongwith his data, the data obtained by others and has calculated the rate of variation of multiple penetrating particles with depth. The observed rate of variation is slower than expected on the basis of number spectrum of the showers. This presumably means that the average energy of the muon, observed as a part of parallel particles, is higher than that of a single muon.

A class of phenomenon essentially similar to mpp but involving rather a larger number of muons has been consistently reported by Moscow State University Air

Shower group in their experiments at rather shallower depths ~ 40 m.w.e./Vernov et al. (1960, 1962, 1963, 1965), Vernov (1967) and Vernov et al. (1969)/. This phenomenon has been named by these workers as muon beams. Higashi et al (1957, 1960, 1962) were the first to observe this phenomenon in cloud chamber pictures at a depth of 30 m.w.e. Vernov et al.(1960) reported the observation of muon beams in Air Showers at sea level. Higashi et al. (1962) and Hasegawa et al (1963) suggest that the muon beams are the results of Poisson fluctuations on muon trajectories in the composition of EAS. In contrast Vernov et al. (1962) have shown that muon beams observed by Moscow State University group could not be ascribed to these fluctuations.

Details of the muon beams are given by Vernov et al. (1967). The mean energy of the muons in beams turns out to be 10^{13} ev. Vavilov (1962) gives an independent estimate of 10^{12} ev for the energy. Blake et al. (1971) have looked for the muon bundles in EAS. The results are, however, inconclusive. Wdowczy and Wolfendale (1971) suggest that such muon beams (bundles) might arise from the coherent production of pions.

I.7 Objectives of EAS Studies:

The studies of EAS are mainly related to the studies of very high energy primary cosmic ray particles

1.8 High Energy Interactions:

The EAS studies, particularly those related to the high energy muons and N-component, provide indirect information about the nuclear interactions at high energies ($> 10^{12}$ eV). A characteristic feature of the nuclear interactions at these energies is the phenomenon of multiple production of the particles. Fermi (1950) advanced a theory of multiple particle production in which the nucleons are assumed to interact and deposit their energies in C.M. system in a volume surrounding the two nucleons. Particles are supposed to be produced in this volume in which thermal equilibrium is attained. The theory predicts a quarter power law for the multiplicity. Some of the features expected on the basis of this theory are in contradiction with the experimental observations.

i) The theory predicts totally inelastic collisions, whereas experimentally it is known that the incident nucleon retains a large fraction of its energy after the interaction.

ii) An increase in the transverse momenta of the created particles with increasing energy of the primary particle is implied by the theory whereas experiments show a near constancy of the transverse momenta.

iii) The experiments indicate an anisotropic emission of the created particles in the CM - system whereas an isotropic emission is expected from the theory. Further the theory evokes a high temperature for the system of interacting nucleons and hence the emission of particles heavier than pions should be as much probable, as that of pions. This is not observed experimentally.

The main objection to Fermi's theory came from Landau (1953) who argued that because of the high temperature of the system the coupling between the particles inside the interaction volume must be very strong and the concept of independent particles existing in the interaction volume is not valid. He, therefore, envisaged a non-equilibrium behaviour of the system in the initial stage which could be described in terms of relativistic hydrodynamics. An expansion of the system in forward - backward direction in the CM - system takes place accompanied by reduction in the temperature. The multiplicity law in Landau's theory is similar to that obtained by Fermi. However, as the emission of the particles takes place when the system has cooled to a sufficiently low temperature the last two difficulties (mentioned above) in Fermi's theory, which arise because of the high temperature of the system, can be overcome.

However, the experimental results have repeatedly shown that only a part of its energy is given by the incident particle to the interaction and the angular distribution of the secondaries becomes more and more peaked as the energy of the incident particles increases, implying an increase in the longitudinal momentum with the energy. On the basis of these results two-fire-ball models have been proposed (Ciok et al. 1958; K. Niu (1958), Cocconi 1958a). In such a model it is assumed that as a result of interaction, two fire-balls are produced moving in forward and backward directions, in the CM-system, together with two survival particles. Particles are produced isotropically in the rest system of the fire-ball.

Cocconi, Koester and Perkins (1961) have proposed a numerical model, on the lines of the fire-ball model and based on the data at machine - energies ($\lesssim 30$ Gev). The model envisages a quarter power law for multiplicity, and exponential distributions for the energy and momenta of the produced particles and is in good agreement with the data at the accelerator energies ($\lesssim 30$ Gev).

Experiments have indicated the presence of a group of particles, among the secondaries of high - energy interactions, which carry higher energies than majority of the secondaries. To explain this, models envisaging

an excitation of the surviving particle to a resonance state have been proposed (Kraushar and Mark 1954; Takagi 1952, Peters 1962, Zatsepin 1962). Such models are known as Isobar models and involve the production of particles in two separate groups. The first group contains particles resulting from the evaporation of a fire-ball, the process being known as the "pionization". The second group corresponds to the nucleons in the fire-ball model. It is assumed that each of the nucleons comes out in an isobar state of πN system which subsequently decays into several pions, emitted isotropically in the rest system of the respective isobar.

Pal and Peters (1964) have put forward a phenomenological model having the essential features of an Isobar model. It is assumed that $\sim 20\%$ of the energy of incident nucleon is given for pionization and the incident nucleon emerges, with $\sim 80\%$ energy, in an isobar state with a high probability. The excited nucleon subsequently decays into pions. The multiplicity law in this model is

$$n_t = S n_B + n_f E_p^{1/2}$$

where the first term gives the average number of decay mesons from Isobar state and 2nd term is the contribution of the fire-ball process.

The various models and theories, described above explain some of the experimental observations at comparatively lower energies, especially at machine energies. The success of a given model depends upon the number of experimental facts which can be accounted for by the model. The applicability of these models at ultra high energies ($> 10^{12}$ ev) is yet to be investigated. Experimental observations at these energies are still very meagre.

I.9 Importance of the muon component of EAS:

Muon component, especially the high energy muons, of EAS has a unique importance in probing the high energy interactions occurring near the origin of EAS. Because of near inertness, these particles are able to maintain (approximately) their initial directions, as well as other characteristics while traversing the atmosphere. These muons originate more or less near the origin of the EAS because of the reduction in their production probabilities at larger depths due to i) the degradation of N-Cascade energy and ii) the increase in the density of the atmosphere, with increasing depth. A detailed study of these muons, therefore, reflects features of the first few collisions at the top of the atmosphere. In recent years there has been an increasing emphasis on the study of this component.

The high energy muon component can be studied by operating detectors at underground levels in association with the air shower arrays at surface. The surface array provides information about the energy of the primary particle. A simple consideration shows that the percentage of association of muons with EAS is related to the total number of these muons in EAS. Also variation of the percentage of association with depth of the observation of the muons gives information about the energy spectrum of the muons in EAS. The information obtained thus can be used to derive various characteristics of the high energy collisions e.g. multiplicity, inelasticity, transverse momenta of secondaries etc. This becomes feasible because the number of collisions involved are few and hence the cascade calculations, using known models, are easy to perform.

Keeping these possibilities in view an experiment has been carried out to study some of the characteristics of the muons of energy ≥ 150 Gev in association with EAS. We have also used one neon flash-tube hodoscope to get information about the multiple production and angular distribution of these high energy muons as well as about their interactions with the matter.

The subsequent chapters give the details of the experimental arrangement and the data analysis and present the results obtained from the experiment. The results are examined in light of some of the known models of the high energy interactions and the implications of the results are discussed.

CHAPTER II

EXPERIMENTAL ARRANGEMENT

II.1 Experimental set-up:

The experimental set up to study muons of energy > 150 Gev associated with EAS, consists of two parts.

- i) Air Shower array at surface
- ii) A penetrating particle detector at the underground level.

The present experiment has been carried out at Kolar Gold Fields, India (11°N ; 920 gm/cm^2 atmosphere depth) in collaboration with the EAS Group of the Tata Institute of Fundamental Research (TIFR), Bombay.

II.2 Air Shower Array:

The air shower array and the associated electronic equipment, used in the present experiment for recording EAS, form part of the EAS set up of TIFR, Bombay at Kolar Gold Fields. The array, shown in Fig.II.1 and described by Chatterjee et al. (1965), consists of 20 plastic scintillator detectors arranged in concentric circles of increasing radii. 19 of the detectors are within 100 m of the centre of the array, the 20th being at 200 m from the array centre.

K.G.F. EAS ARRAY

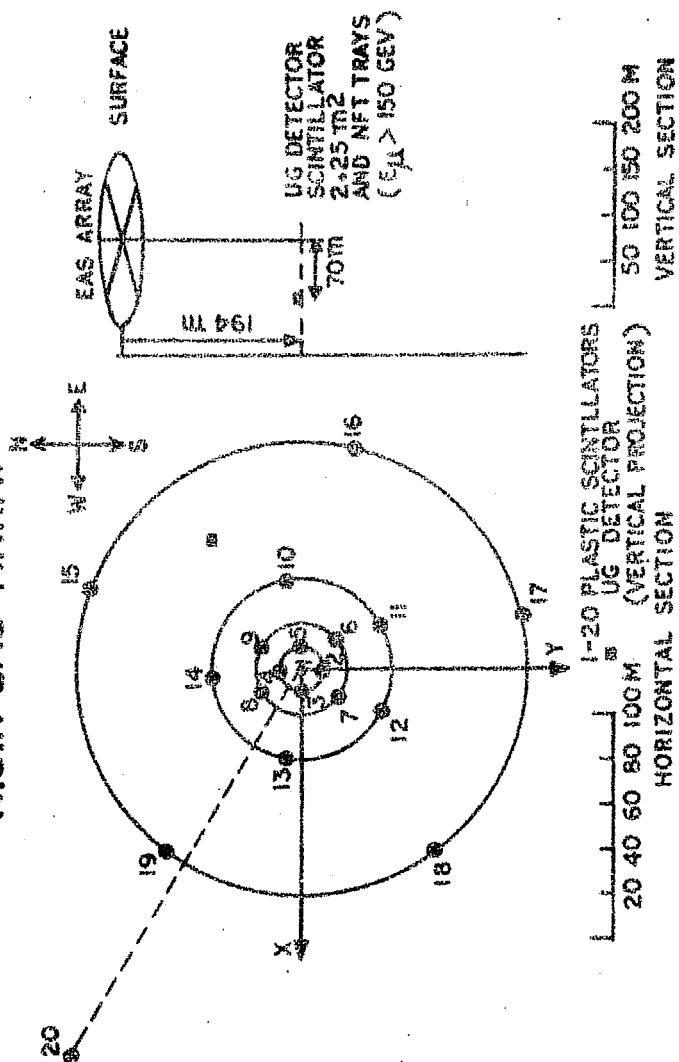


FIG. 11-1

Note:- The EAS-array shown in this Figure forms part of the experimental set-up of the TIFR EAS Group at K.G.F.

These detectors are used to sample the density of the particles forming part of EAS and will hereafter be referred to as density detectors. The area of each of the density detectors is 1 m^2 . Pulses from the preamplifiers attached to these detectors are taken to a central recording station by means of co-axial cables. Fig.II.2 shows the block diagramme of the electronics used for recording EAS. The details have been discussed by Manchanda (1967) and Sivaprasad (1970). The preamplifier outputs of each density detector are connected to corresponding log-amplifier and are also fed to a selection system used for selecting EAS. The selection criterion for an EAS requires a four fold coincidence between the density detectors with inner nine scintillators biased so as to record a minimum of two particles per m^2 and outer ten required to register a minimum of 1 particle / m^2 . 20th detector is not included in selection system and is used only for sampling densities at large distances from shower cores. When an EAS is detected, information regarding the particle densities in various density detectors is stored in the form of voltages across condensers, which are proportional to the output pulse heights of the Log-amplifiers and, hence, are related to the particle densities in the density detectors. Whenever the master pulse generator is triggered, a scanner scans the amplifiers and an analog to digital convertor transforms amplifier pulse heights into

BLOCK DIAGRAM OF ELECTRONICS USED FOR RECORDING
EXTENSIVE AIR SHOWERS

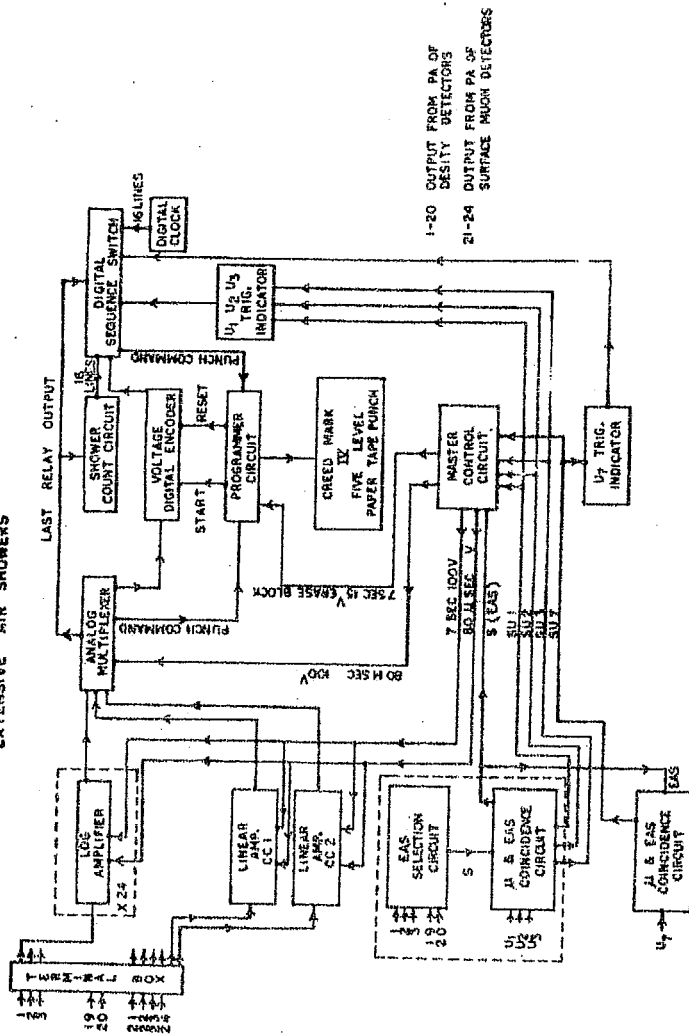


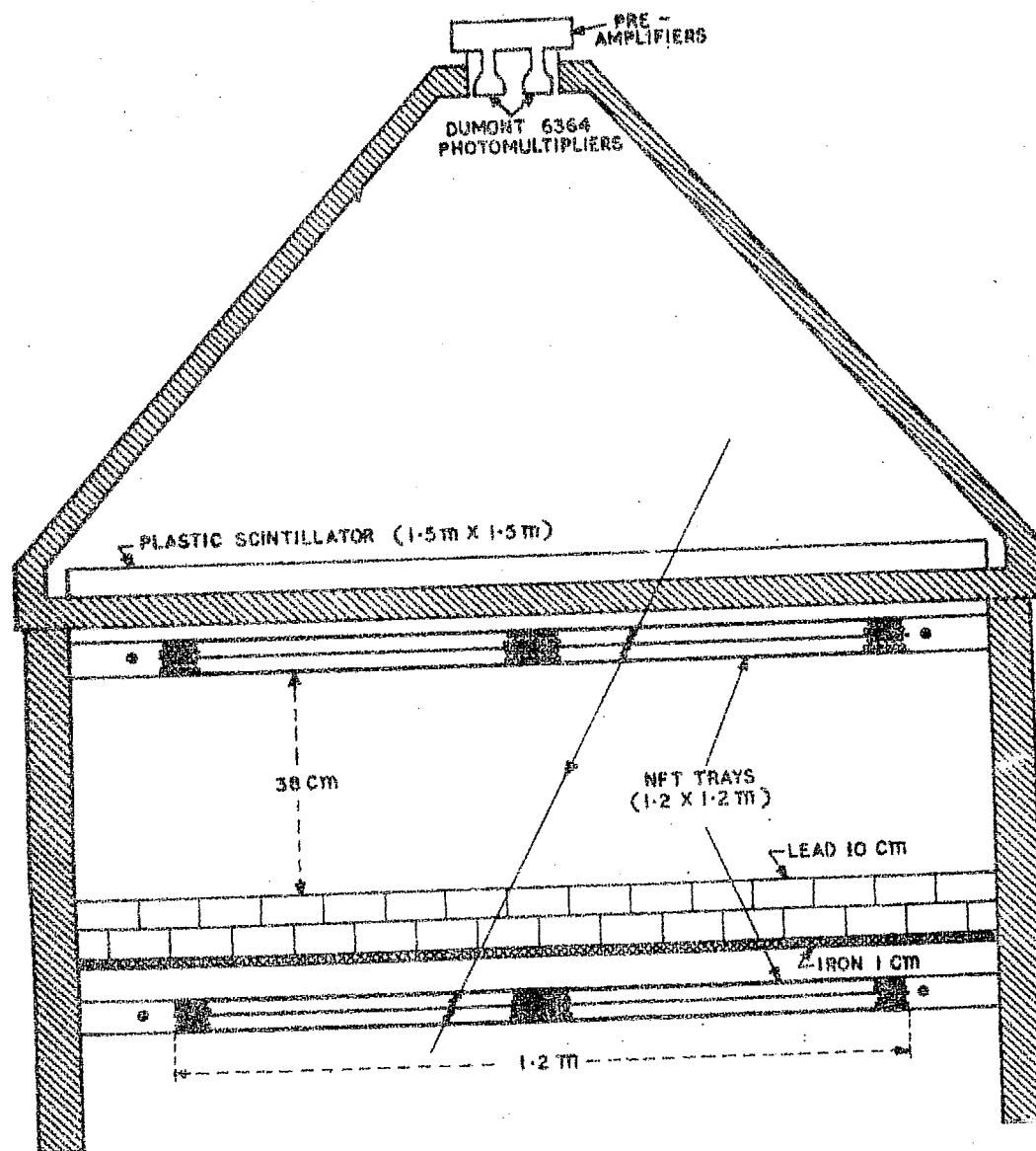
FIG. 13-2

NOTE:- The electronic-circuits shown here form
part of the EAS array of TIFD at K.G.P.

corresponding binary digits. This information together with time and number of the trigger is then punched on a paper tape in binary code.

II.3 The Underground Detector.

The underground detector (to be called UG-detector), used for detecting mu-mesons of energy ≥ 150 Gev, is situated at a depth of 194 m. underground at the 7th level of the Bullen's shaft of Kolar Gold Fields, (INDIA). As shown in Fig.II.1, the UG-detector is located ~ 70 m north-east of the vertical projection of the air shower array centre on the underground plane. Shown in Fig. II.3 (a) the UG-Detector consists of a plastic scintillator detector, of area $1.5 \text{ m} \times 1.5 \text{ m}$, viewed by two Dumont 6364 photomultipliers in coincidence. The coincidence between the two photomultipliers helps in reducing the radio-active background and the photomultiplier noises. In addition to the scintillator detector, there are two trays, containing neon-flash tubes, arranged under the scintillator as illustrated in Fig.II.3 (a). The neon flash tubes used in the present investigation are each $\sim 1.2 \text{ m}$ in length and of $\sim .98 \text{ cm}$ diameter. Each tray contains four horizontal layers of these tubes, there being ~ 120 tubes in each layer flash tubes are placed lengthwise in East-West direction. The two trays are separated vertically



UNDERGROUND MUON DETECTOR
(FRONT VIEW)

FIG. II. 3(a)

SIDE VIEW

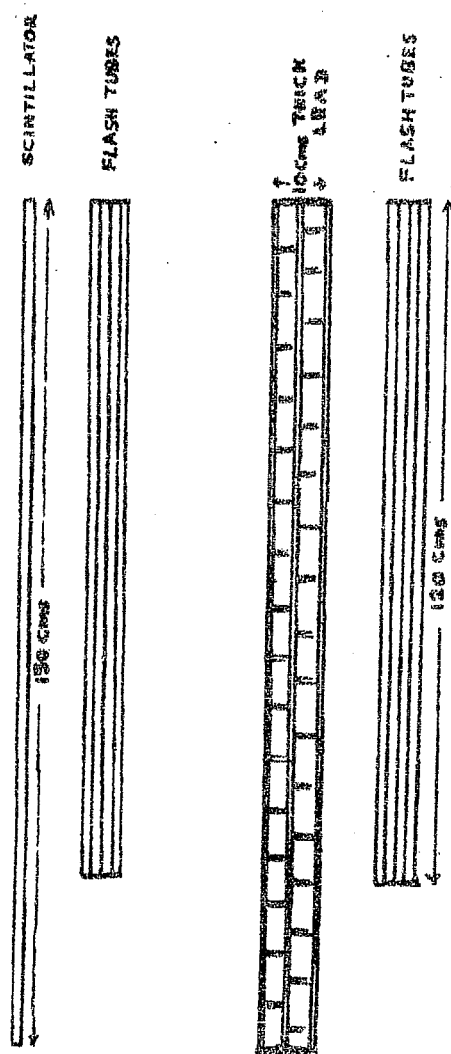


FIG. II.3(b)

by 38 cm of air, 1 cm of iron and 10 cm of lead. The lead absorber extends 15 cm. to either side of the lower tray and 30 cm. on the back of the tray as shown in Fig.II.3(b). The figure illustrates the side view of the n.f.t trays only.

II.4 Electronics used with UG Detector:

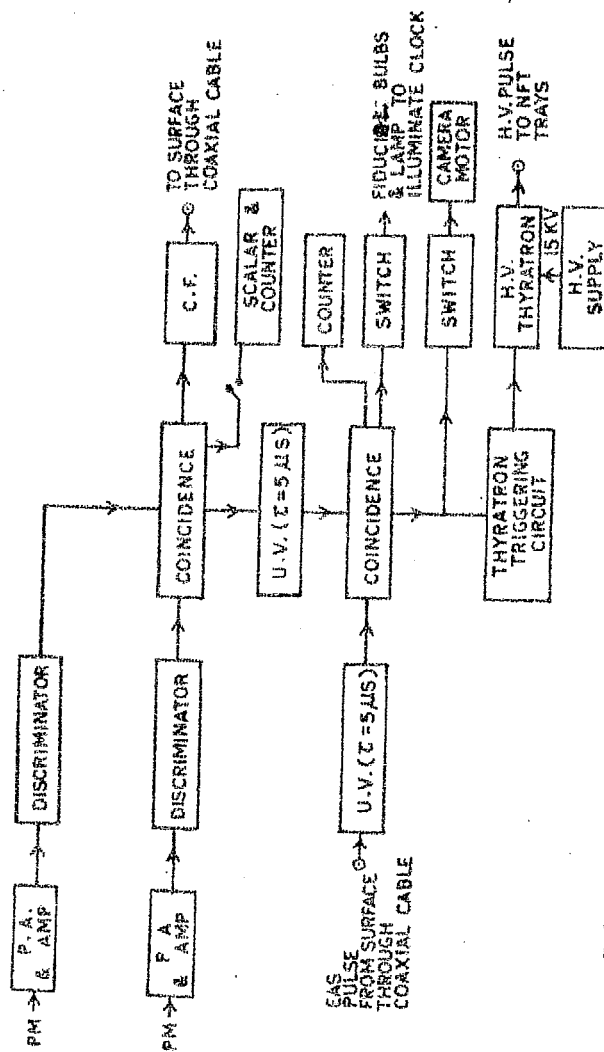
A block diagram of the electronics used with the UG-detector, for recording the muons associated with EAS, is given in Fig.II.4. The photomultiplier pulses, after being amplified by means of a preamplifier and amplifier are fed to a discriminator. The preamplifier consists of a single stage feedback amplifier and has a gain ~ 10 . The amplifier consists of two feedback stages with gains ~ 10 and ~ 100 respectively. The discriminator outputs for the two photomultipliers are fed to a coincidence circuit and a coincidence pulse then signifies the traversal of at least one charged particle through the UG-detector. These pulses are then taken to surface through a coaxial cable. A coincidence, between these underground pulses and the EAS pulses, recorded at surface, forms the trigger (to be called SU7-trigger) to operate the master pulses generator and thus the EAS associated with at least one muon at underground detector are recorded. Along with the triggering of master pulses generator at surface,

the SU7-triggers are also used to pulse the neon flash tube trays with high voltage (~ 10 KV) pulses. The neon flash tube trays are then photographed, through a mirror system, to record the tracks of the particles associated with the EAS.

II.5 Detection efficiency for UG-detector

In order to ensure maximum detection efficiency from the UG detector the biases of the discriminators connected to the UG detector are fixed in the following manner.

A vertical telescope of GM counters is used with two layers of the GM counters placed above the scintillator and one under the scintillator. For a given bias of the detector a record of three fold coincidences (c_3) between the GM counters and four-fold coincidences (c_4) between the GM counters and scintillator is made. The bias of the discriminator, under study, is adjusted till the ratio c_4/c_3 is maximum. The same procedure is repeated with the other discriminator. Efficiency at the centre of the detector is 96% and the efficiency at the edges is $\sim 77\%$. An overall efficiency of 87% is obtained.



ELECTRONICS USED WITH UG DETECTOR
(BLOCK DIAGRAM)

FIG II 4

CHAPTER III

DATA REDUCTION AND ANALYSIS

III.1 Data Reduction:

The basic data in the present experiment consists of the information regarding the particle densities, at various density detectors, for the EAS recorded with a specific trigger requirement and is on the paper tape as explained earlier (chapter II). This data is processed on the CDC 3600/160A computer installation at TIFR, Bombay, in collaboration with the EAS group of TIFR. The data is transferred on a magnetic tape from the paper tapes and former is then used for processing purposes.

a) Cross and Singles - Calibrations:

The number p_i corresponding to the density in i th density detector, punched on paper tape, represents the pulse height at the output of the Logarithmic amplifier attached to the density detector. This p_i is related to the particle density Δ_i by the relation

$$\Delta_i = A_i \times 10^{p_i/B_i}$$

where A_i and B_i are the constants characteristic of the i th detector. Thus in order to be able to determine Δ_i from p_i one must know the constants A_i and B_i . For this

purpose a singles and a cross-calibration is done for each detector. These calibrations were done by TIFR group, and constants made available by them for each detector for the duration of the present experiment have been used in the present analysis. The method followed for singles and cross-calibrations is as follows:-

A pair of linear amplifiers are used for this purpose. For singles-calibration the pre-amplifier of the detector under calibration is connected to one of the linear amplifiers. The EAS recording system is triggered by single muons passing through the detector under study. These single muons are selected by means of GM counter telescope. The linear output from the calibration amplifier is punched out and from a number of such triggers the average linear pulse height \bar{p}_i corresponding to passage of a singly charged relativistic particle through the detector is obtained. The procedure is repeated for all density detectors and the value of \bar{p}_i are determined.

For cross-calibration, the preamplifier outputs for a given pair of detectors are connected to the calibration amplifiers and shower records obtained then contain both the logarithmic as well as linear output.

A semi-log plot of these outputs with the logarithmic output along the linear scale and corresponding linear output on the log scale then gives a relation between p_i and Δ_i . The linear readings are converted into densities by dividing these readings by the single particle height \bar{p}_i^{-1} .

The cross-calibration done in this way for different detectors alongwith the singles calibration then yield the values of the constants A_i and B_i for various density detectors.

The details of singles and cross-calibrations are given by Sivaprasad (1970).

III.2 Evaluation of Shower Parameters:

An EAS can be characterised by four parameters (N, X, Y, s) at a given level of observation, where N gives the total number of charged particles in the shower and is known as its size, X and Y are the co-ordinates of the core of the shower and s the age parameter of the shower. The particle densities obtained in various density detectors, are used to obtain these parameters, by fitting the densities to the NKG distribution function (Equation 1.3.4) which is known to give a good fit to the experimental data as discussed in section 1.3. For the present observation level $\gamma_1 = 96$ m.

The fit is achieved through the minimisation of a quantity χ^2 defined as

$$\chi^2 = \sum_{i=1}^n W_i (\rho_i - \Delta_i)^2 \quad \dots (3.2.1)$$

Δ_i & ρ_i being respectively the observed and expected densities at i th density detector and W_i is the weight attached to the observed density. Following Scherb (1959) the weights are taken as

$$W_i = 1/\rho_i \quad \Delta_i \leq 25 \text{ m}^{-2} \quad \dots 3.2.2$$

$$W_i = 25/\rho_i^2 \quad \Delta_i \geq 25 \text{ m}^{-2} \quad \dots 3.2.3$$

The weights are given to take into account the fluctuations in the observed densities. For densities $\Delta_i < \Delta'$ major source of error is statistical fluctuations in the number of shower particles crossing the i th detector and the distribution for this error is nearly Poisson. For $\Delta_i > \Delta'$ the Poisson fluctuation becomes smaller than the instrumental uncertainty which is assumed to have Gaussian distribution with a constant relative standard deviation. Taking a value of 20% for relative deviation, Δ' is found to be 25 particles / m^2 .

The best fit values of the parameters (N,X,Y,s) are then those which satisfy the following equations.

$$\frac{\partial \chi^2}{\partial N} = \frac{\partial \chi^2}{\partial X} = \frac{\partial \chi^2}{\partial Y} = \frac{\partial \chi^2}{\partial s} = 0 \quad \dots 3.2.4$$

Thus we have a set of four simultaneous equations which can, in principle, be solved to obtain the values of (N, X, Y, s) . However, the equations are non-linear and solutions are not possible in all cases. To solve these equations the method of "Steepest descent" has been used. The parameters (N, X, Y, s) can be considered as co-ordinates of the vector.

$$\vec{\xi} = \vec{\xi}(N, X, Y, s) \quad \dots (3.2.5)$$

Then the surface $\chi^2 = \chi^2(\vec{\xi})$ will have a valley in the neighbourhood of the best fit values of the parameters so that equation 3.2.4 is satisfied. For achieving minimisation, an initial estimate of the vector is made. Then, quantised vector increments, in the direction of $-\vec{\nabla} \chi^2$ are given to the vector $\vec{\xi}_j$, the magnitude of the increments being adjusted in binary approximation. A new value of the vector $\vec{\xi}_{j+1}$ is obtained from the previous value $\vec{\xi}_j$ using following relation

$$\vec{\xi}_{j+1} = \vec{\xi}_j - \lambda_{j+1} \frac{\vec{\nabla} \chi^2(\vec{\xi}_j)}{|\vec{\nabla} \chi^2(\vec{\xi}_j)|} \quad \dots (3.2.6)$$

and the process is repeated till a certain criterion is satisfied implying the approach of minimum. The criterion requires three consecutive reductions in $\chi^2/(n-d)$ by magnitudes $< .01$.

A goodness of fit parameter $\chi^2/(n-d)$ is printed out for each shower. Here n is the number of density detectors used for analysis and d is the number of fitted parameters. The method is similar to one used by Scherb (1959)

For the analysis of present data a fortran programme, based on above method, written by EAS group at TIFR, is used. A fixed value of s ($s = 1.25$) is taken for all showers and the remaining three parameters (N, X, Y) are then obtained by χ^2 minimisation. The use of $s=1.25$ for all showers at the level of observation though not strictly correct, does not however introduce serious errors in the present size range as shown by Sivaprasad (1970). Sivaprasad did an extensive error analysis for the array used in the present experiment using the above mentioned fortran programme and has shown that the effect of using $s=1.25$ for all showers on an incident spectrum of artificial showers is to leave the slope of the spectrum unchanged. There is however a change in absolute intensity $\sim 25\%$ which is of the same order of magnitude as the statistical accuracy of the data under consideration.

III.3 Initial Estimate of Shower Parameters:

In order to obtain X_0, Y_0 , initial estimate of X & Y respectively a weighted average of the co-ordinates

of four density detectors having first four maxima of densities is taken. Then if Δ_i ($i = 1, 4$) represent the density maxima and (X_i, Y_i) , ($i = 1, 4$) are the co-ordinates of corresponding density detectors we have

$$\begin{aligned} X_0 &= \sum_i X_i \Delta_i / \sum_i \Delta_i \\ Y_0 &= \sum_i Y_i \Delta_i / \sum_i \Delta_i \end{aligned} \quad \dots (3.3.1)$$

For estimating N_0 the initial estimate of N use is made of the fact that equation $\frac{\partial \chi^2}{\partial N} = 0$ for the given distribution gives a cubic equation of the form

$$N^3 + a N + b = 0 \quad \dots (3.3.2)$$

which always yields a real solution. Here a and b are functions of core location and age of the shower. Thus knowing X_0 and Y_0 , an estimate of N_0 can be obtained by solving equation (3.3.2) analytically.

III.4 Errors in Fitted Parameters:

The parameters, fitted to a given shower, are subjected to errors which are not easy to evaluate by direct methods. Hence an 'error analysis' has been done, using showers generated artificially (to be called artificial shower) in the following manner. For a given shower size N and age parameter $s=1.25$, the shower cores are fixed at random locations within a certain distance

R from the array centre. Uniformly distributed random numbers between 0 and 1 are used for this purpose. Using the equation (1.3.4) the densities Δi in all density detectors are calculated. Over these densities are then superposed fluctuations proportional to two Gaussian distributions, one with a mean of $\sqrt{\Delta i}$ and other with a mean of 20% of Δi . The shower thus generated is then similar, for all practical purposes, to the showers recorded in the experiment, as it is subjected to the fluctuations similar to the fluctuations in the measured densities of the recorded showers. A number of artificial showers (~ 100 for each size) thus generated are then fed to the computer and the showers are processed like real showers. A comparison of the fitted parameters (N, X, Y) with the original parameters (N_0, X_0, Y_0) then yields an estimate of the errors in these parameters. Fig. III.1 to Fig. III.3 show histograms for $\Delta X = X - X_0$, $\Delta Y = Y - X_0$ and $\log(N/N_0)$ for three different sizes. The error analysis yields following values of the errors ΔN , ΔX and ΔY in the parameters N , X & Y respectively.

$$\Delta N = \pm 0.20 * N$$

$$\Delta X = \pm 2.50 \text{ m}$$

$$\Delta Y = \pm 2.50 \text{ m}$$

Fig. III.4 shows the distribution in $\chi^2 / (n-d)$ for SU 7 trigger showers and artificial showers.

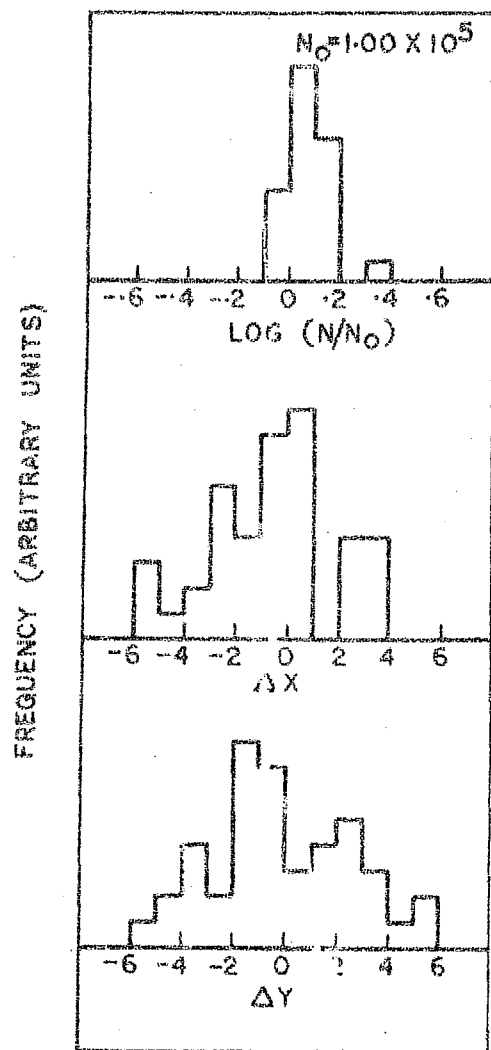


Fig. 11.1

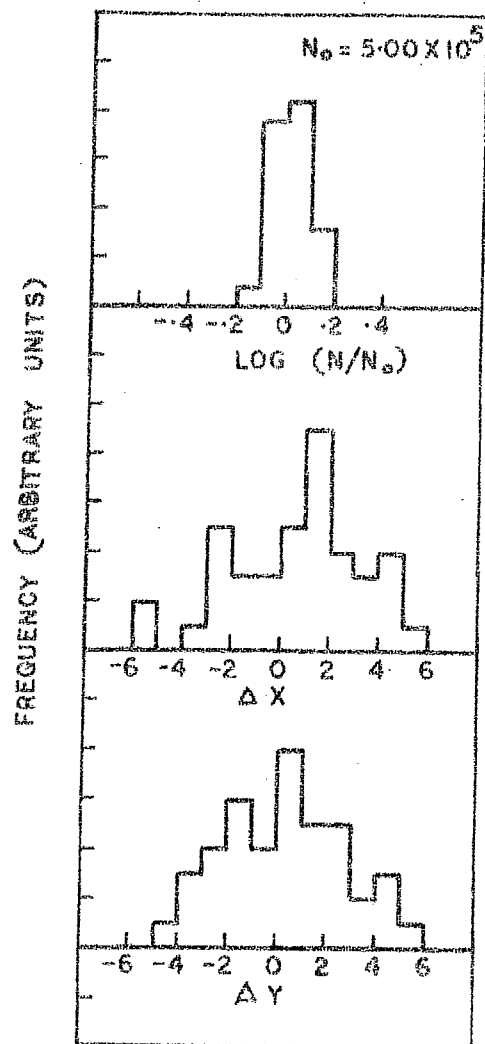


Fig. III.2

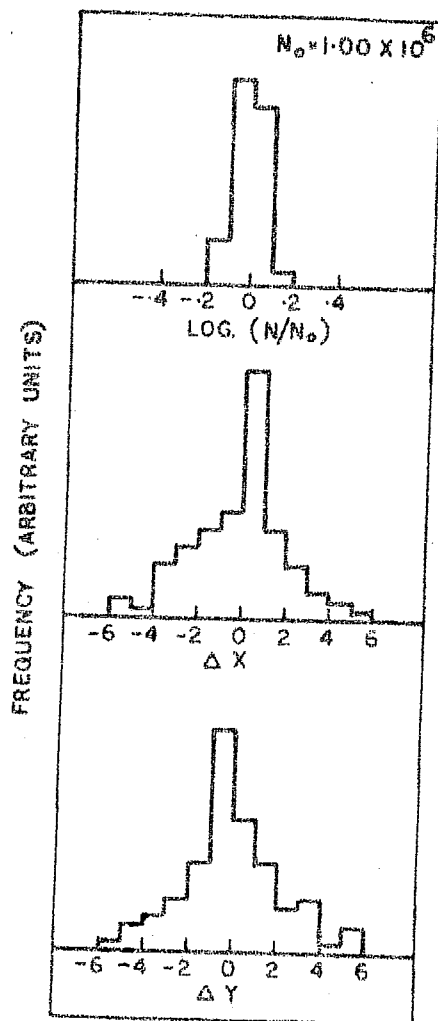


Fig. B.3

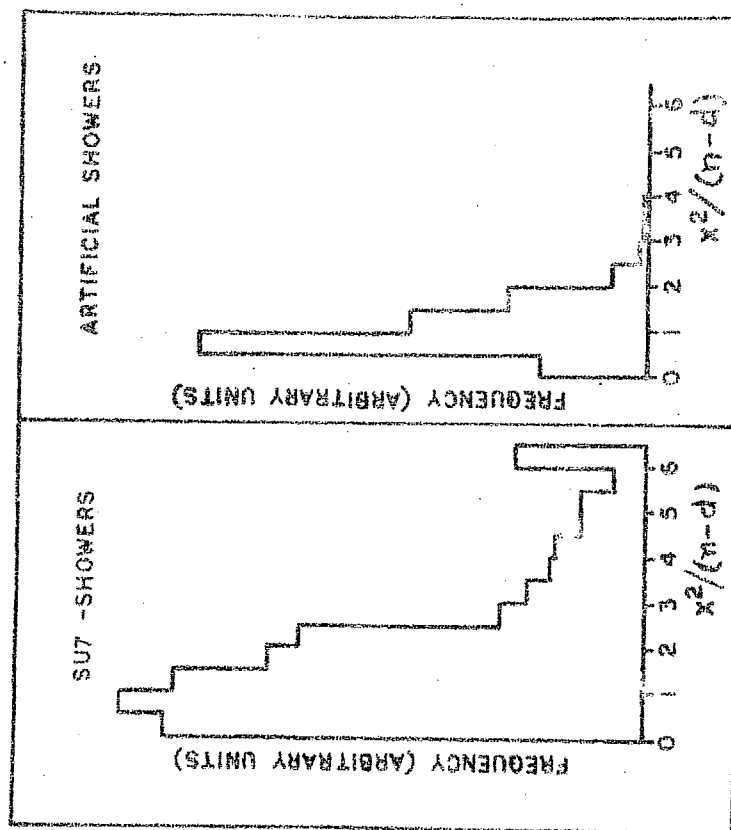


Fig. III.4

CHAPTER IV

EXPERIMENTAL RESULTS

IV.1 Shower Data

About 4000 showers have been recorded in the present investigation using SU7 triggers. The rate of chance coincidence for such triggers is estimated to be \sim one per day. Taking into account the detection efficiency of the UG-detector the total rate for the SU7 triggers is $(0.92 \pm 0.02) \text{ m}^{-2} \text{ hr}^{-1}$.

For the present analysis, about 10,000 showers, recorded by triggering the EAS system by EAS pulse only without the requirement of U.G pulse have also been used. These showers, to be called S-trigger showers, were made available by TIFR EAS group and were recorded during the operation of the present experiment.

As mentioned earlier (Chapter II), the selection criterion for the showers required a coincidence between any four of the inner nineteen density detectors. During the selection of the showers for analysis another criterion has been imposed which requires that at least three of the inner four density detectors should have ≥ 2 particles each. This helps in removing the showers which are far away from the centre of the EAS array and for which the parameters could not be evaluated very accurately.

In order to determine the size spectra, the recorded showers have been classified in eight different size groups as given in Table IV.1.

In absence of the information on the arrival directions, the showers have been assumed to be vertical. This does not introduce much error because of a very steep angular distribution for the showers. The angular distribution is given by

$$I(\theta) = I_0 \cos^n \theta$$

where $n \simeq 8$ for the present level of observation, θ is the zenith angle and $I(\theta)$ and I_0 are the flux values at an angle θ and along vertical respectively.

IV.2 The 100% area for showers:

To obtain the spectrum for the recorded showers it is essential to have an estimate of 100% area for the showers of a given size N recorded by a given EAS array. The 100% area for showers of given size N can be defined as an area such that the incident showers having cores within this area are detected with 100% efficiency by the air shower array.

If Δ_i represents the particle density in the i th density detector due to an incident shower, then the probability of occurrence of a four fold coincidence can be written as

$$\prod_i (1 - e^{-\Delta_i S_i})$$

TABLE IV.1

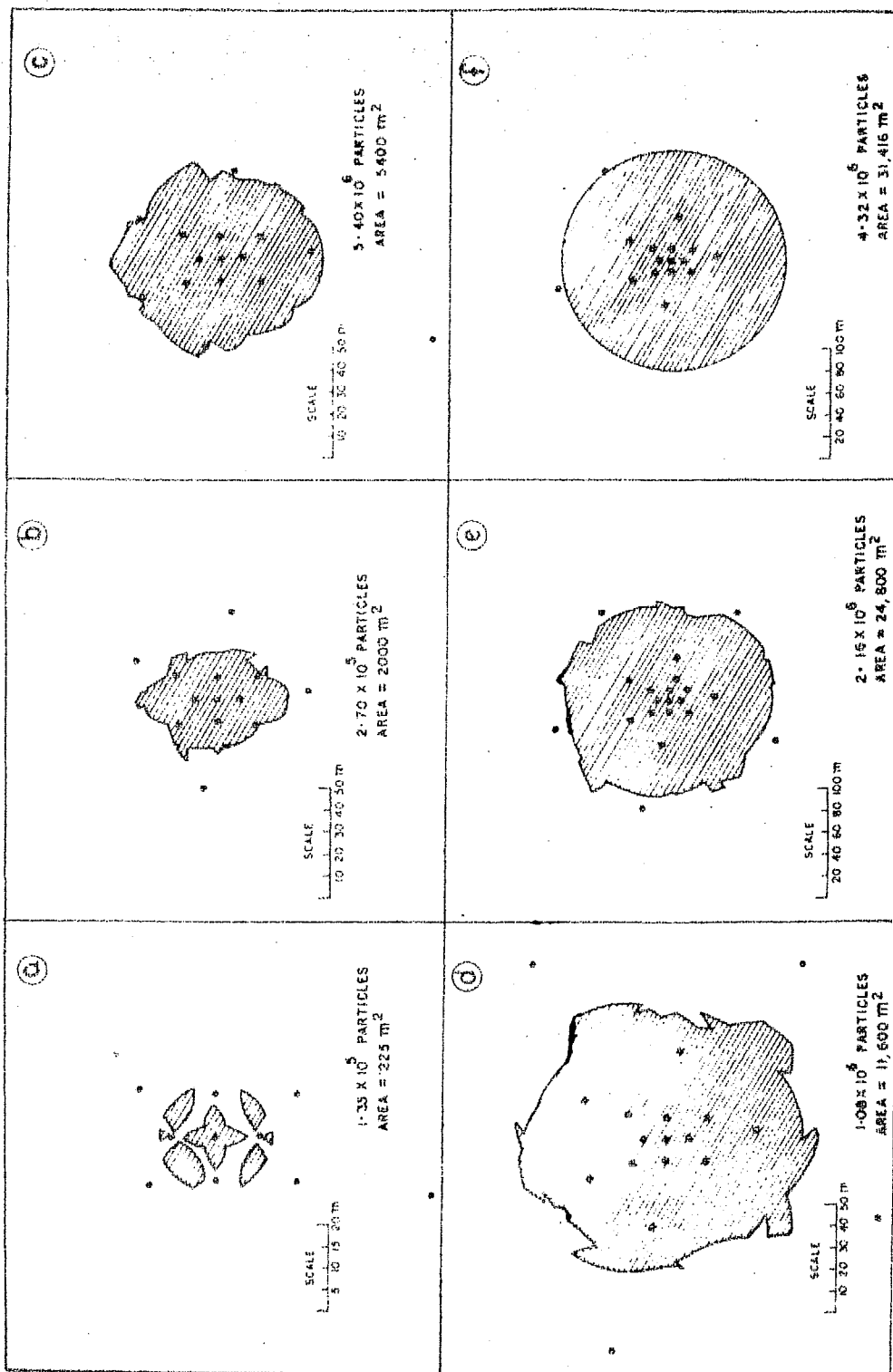
Group No.	1	2	3	4	5	6	7	8
	5.0×10^4	1.0×10^5	2.0×10^5	4.0×10^5	8.0×10^5	1.6×10^6	3.2×10^6	6.4×10^6
Size	to	to	to	to	to	to	to	to
Range	1.0×10^5	2.0×10^5	4.0×10^5	8.0×10^5	1.6×10^6	3.2×10^6	6.4×10^6	1.28×10^7

where S_i is the area of the i th density detector. This probability is equivalent to the detection efficiency $\epsilon(N)$ for the incident shower of size N . Thus if we select an area such that for showers of size N incident on this area $\epsilon(N) \simeq 1$, then this area can be termed as 100% area (to be denoted by $A(N)$). If showers of size N are incident on the array such that the density in any four of the density detectors is ≥ 20 particles/m² then for such showers $\epsilon(N) \simeq 0.99$, a value which is sufficiently close to 1. Thus for computing $A(N)$ the following procedure has been followed:

Using NKG distribution function, given by equation (1.3.4), the value of radius $R_{20}(N)$ for a given size N is determined. $R_{20}(N)$ is the distance from the core, of a shower of size N , at which the density is equal to 20 particles/m². Having evaluated $R_{20}(N)$ an area is mapped out on the EAS array diagram such that each point in this area has at least four detectors within a circle of radius $R_{20}(N)$ m, around the point. This area then represents $A(N)$ and fig. IV.1 illustrates examples of 100% areas for six different sizes. A plot of $A(N)$ as a function of size N is given in Fig. IV.2.

IV.3: The Size Spectra:

For obtaining the size spectrum for S-trigger showers a selection of the showers having cores within 100% area is done as follows.



ACCEPTANCE AREAS FOR SHOWERS

FIG. IV.1

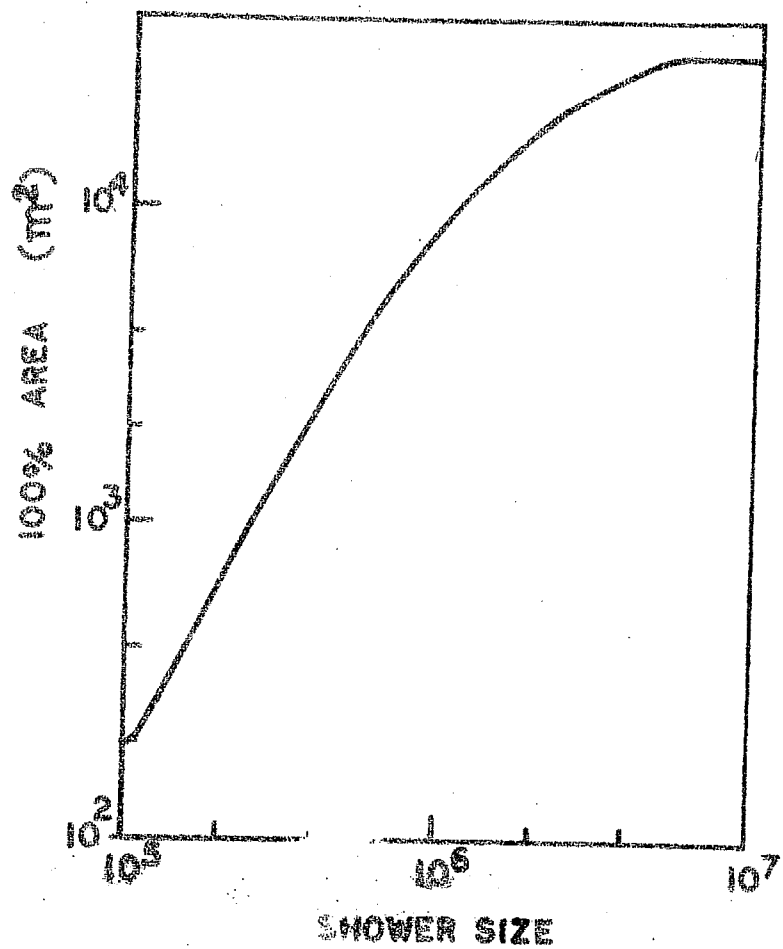


FIG. IV. 2

A shower of size N is accepted or rejected according to whether or not a circle of radius $R_{20}(N)$ drawn around the core of the shower contains at least four detectors within it. The method is adopted from one used Clark et al. (1958). Using the area, obtained as described above, and the number of S-trigger showers incident on the area, the differential size spectrum for the S-trigger showers has been obtained.

The same procedure could also be used for obtaining the size spectrum for SU7-trigger showers. However, the number of the showers for each size group, which fall within 100% area, is very small for some of the size groups. A slightly modified method has, therefore, been used for determination of SU7- spectrum. The modification consists in including the showers having cores outside the 100% area, in the analysis and correcting their number for the reduction in the detection efficiency. For this purpose correction factors $C(N)$ are worked out as follows:

For a given size group a comparison is made between the number density (number of showers per unit area) of the S-trigger showers falling within 100% area to the number density of these showers (S-trigger) having cores within a radius $R_a(N)$ of the centre of the array. The ratio of the two densities then yields the correction factor $C(N)$. The SU7-trigger showers having cores within

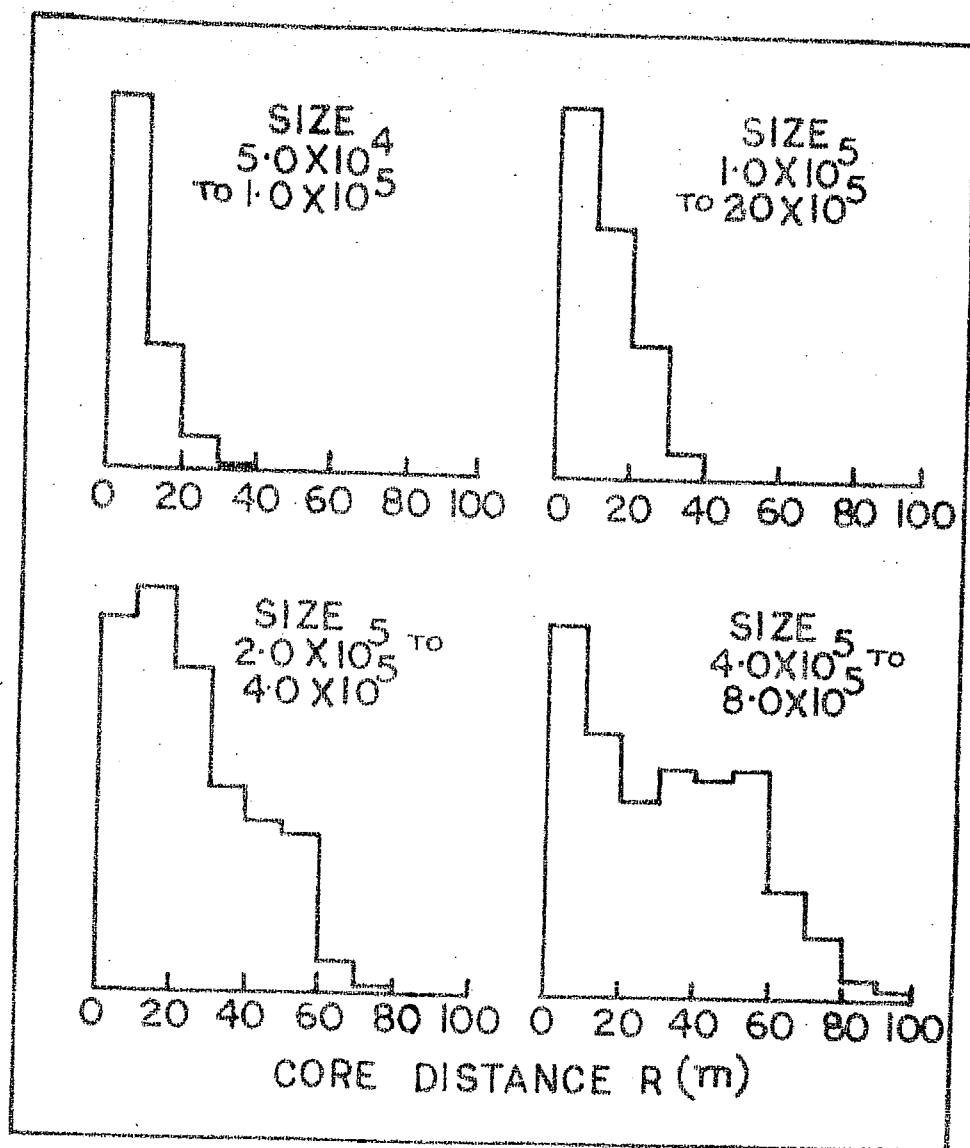
a circle of radius $R_a(N)$ around the centre of the EAS array have been accepted for the analysis. Different values of $R_a(N)$ have been taken for different size groups. The values are given in Table IV.2 together with the values of $C(N)$. The size group number refers to the number given in Table IV.1.

T A B L E IV.2

Size Group No	$R_a(N)$	$C(N)$	Size Group No	$R_a(N)$	$C(N)$
1	10 m	2.50	5	100 m	1.00
2	20 m	2.38	6	100 m	1.00
3	50 m	1.70	7	100 m	1.00
4	80 m	1.38	8	100 m	1.00

The reason for taking different values of the acceptance radius $R_a(N)$ for different size groups is that the detection efficiency decreases more rapidly, with increasing distance of the core from the air shower array centre, for showers of smaller sizes than for showers of larger sizes. This is evident from Fig. IV.3 which shows the distribution of S-trigger showers in distance, R , of the shower cores from the array centre, for showers in different size groups. A consideration in selecting

NO. OF SHOWERS/ m^2 (ARBITRARY UNITS)



DISTRIBUTION OF S TRIGGER SHOWERS OF
VARIOUS SIZES IN CORE DISTANCE R.

FIG.IV.3

$R_a(N)$ has been that the correction factor $C(N)$ should not exceed 2.50 i.e., the overall detection efficiency for showers whose cores land within distance $R_a(N)$ from the centre of the array should not be less than 40%.

Having calculated $C(N)$ for different size groups (using S-trigger showers), the number of SU7-trigger showers, having cores within a radius $R_a(N)$ of the centre of the array, is determined. The number is then corrected using the values of $C(N)$. The effect of the correction factors on the probable errors is taken into consideration. The corrected number, then, corresponds to the number expected if the whole area within a radius $R_a(N)$ were 100% area. Using the corrected number of SU7-trigger showers the size spectrum for these showers is obtained.

Fig.IV.4 shows the differential size - spectra for S-trigger and SU7-trigger showers, Representing the S-trigger spectrum as

$$F(N) dN = K \left(\frac{N}{10^5} \right)^{-\gamma} dN \quad \text{m}^{-2} \text{Sec}^{-1} \quad \dots (4.3.1)$$

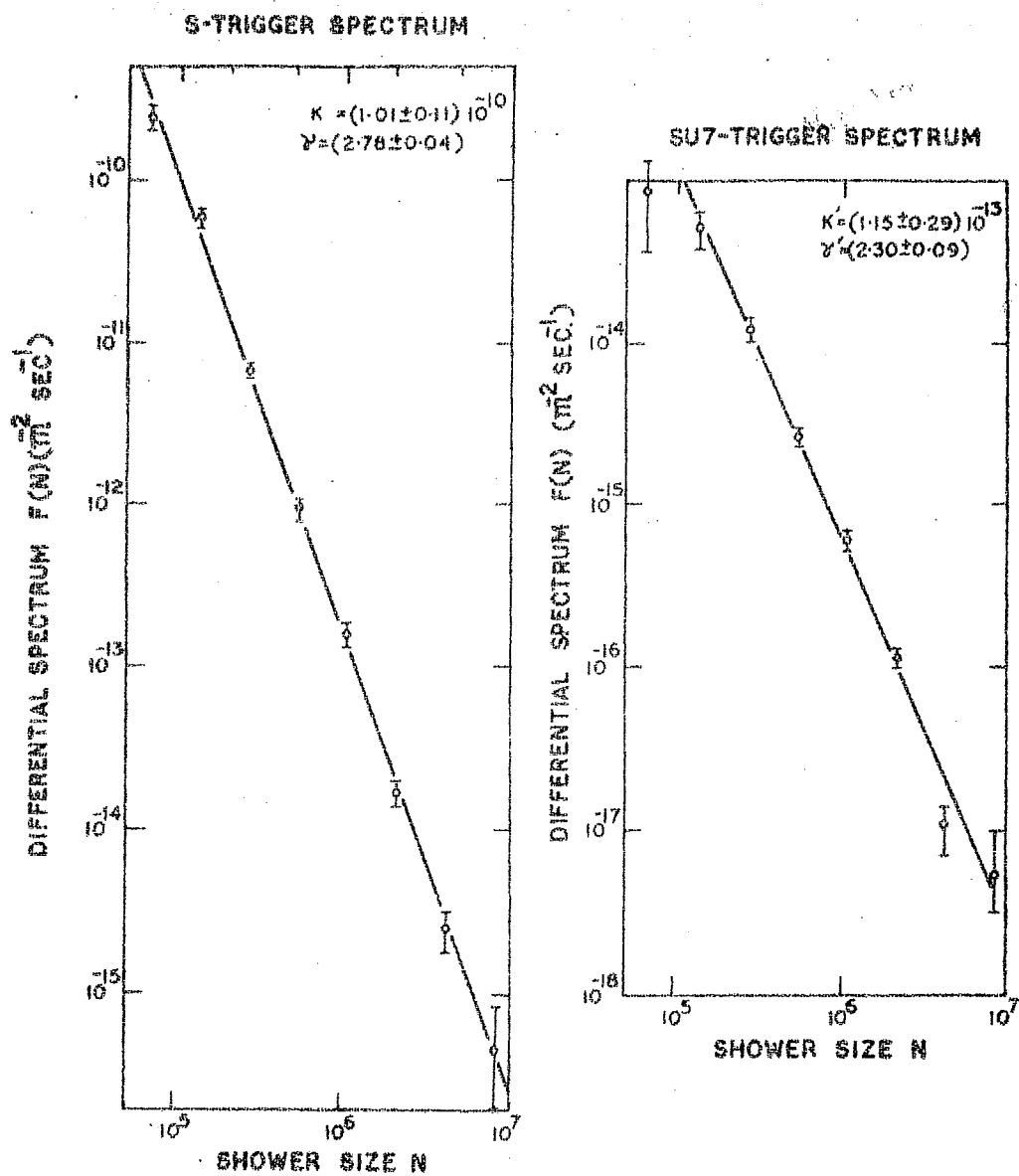
and SU7-trigger spectrum as

$$\Phi(N) dN = K' \left(\frac{N}{10^5} \right)^{-\gamma'} dN \quad \text{m}^{-2} \text{Sec}^{-1} \quad \dots (4.3.2)$$

Where K, γ and K', γ' are constants, we can write

$$K = (1.01 \pm 0.10) 10^{-10} ; \quad \gamma = 2.78 \pm 0.04 \quad \dots (4.3.3)$$

$$K' = (1.15 \pm 0.28) 10^{-13} ; \quad \gamma' = 2.30 \pm 0.09 \quad \dots (4.3.4)$$



DIFFERENTIAL SPECTRA FOR THE SHOWERS

FIG. IV.4

While fitting eqn. (4.3.2) to the SU7-trigger spectrum the point corresponding to the first size group has been ignored because a change in slope around this point is indicated.

The difference Δ in the Power indices γ and γ' can be accounted for by the increase in the probability of association, of a shower with a muon at underground level, with increasing shower size resulting in a SU7-trigger spectrum which is flatter than S-trigger spectrum. A size dependence of muon number n_μ of approximately following type is indicated

$$n_\mu \propto N^{0.48 \pm 0.02}$$

A more exact relation between n_μ and N can, however, be obtained from the spectra derived above using the procedure outlined in the following section.

IV.4 Number of muons of energy ≥ 150 Gev in showers of different sizes:

Let $S(N) dN$ denote the total rate of showers of sizes between N & $N + dN$ recorded by the EAS array, and let $S \cdot U(N)dN$ be the rate of the showers in the same size range associated with a muon detected at a depth d underground. Then the probability,

$$P_\mu (\geq E_\mu, N) = \frac{SU(N)dN}{S(N)dN} \quad \dots (4.4.1)$$

that a shower of size N is recorded in association with a muon detected at the depth d , is related to

$\eta_{\mu}(\geq E_{\mu}, N)$, the average total of muons, of energy $\geq E_{\mu}$, present in shower of size N . Here E_{μ} is the minimum energy which a muon must possess to traverse a depth d .

In the present experiment the depth $d = 194$ m corresponds to 590 m.w.e. of standard rock. Using the range-energy relation for muons given by Menon and Ramanamurthy (1967) the value of E_{μ} for present case is found to be 150 Gev.

In order to obtain the relation between $\eta_{\mu}(\geq E_{\mu}, N)$ and $P_{\mu}(\geq E_{\mu}, N)$ let us consider the geometry of the experimental set up (Fig.IV.5). S' and S are two parallel planes at surface and underground level respectively, separated by a vertical distance d . O' is the array centre at surface and O its vertical projection on S . Let $F(N)dN$ represent the vertical flux of showers having size between N & $N + dN$. Let us consider showers in this size group incident on S' at zenith angle θ such that their axes pass through an elemental area dA' around C' . The axes of these showers will fall on an elemental area dA

around C in underground plane S. The total number of such showers is then given by

$$F(N) = \frac{dA \cdot \cos \theta}{L^2} \frac{dA' \cdot \cos \theta}{2} \cos^n \theta$$

where L is the distance CC' and $\cos^n \theta$ term comes because of zenith angle dependence of shower flux. Now if r is the perpendicular distance of the detector at D from the shower axes and $\Delta_\mu(N)$ the density of muons at distance r from the shower axes at underground level then the probability that such showers will be recorded in association with a muon at underground detector D is

$$(1 - e^{-s \cos \theta \cdot \Delta_\mu(r)}) \quad \dots (4.4.3)$$

where s is the area of the detector D. This probability expression is based on the assumption that the number of muons in the showers is subject to Poisson fluctuations. Combining 4.4.2 and 4.4.3 we get

$$SU(N)dN = \iint_A \iint_A F(N)dN \frac{dA \cdot dA'}{2} \cos^{n+2} \theta (1 - e^{-s \Delta_\mu(r) \cos \theta}) \quad \dots (4.4.4)$$

Here the integration is carried over the array area A' and over an infinite plane passing through underground detector D. For the total rate of the Air showers of sizes between N & $N + dN$ we can write:

$$S(N)dN = \iint_A \iint_{\Omega} F(N)dN \cdot \cos^n \theta \cdot dA' \cos \theta d\Omega \dots (4.4.5)$$

where A' is same as above and Ω is the solid angle of the array. We can then write

$$P_{\mu}(\geq E_{\mu}, N) = \frac{\iint_A \iint_{A'} \frac{dA' \cdot dA}{l^2} \cos^{n+2} \theta (1 - e^{-S \Delta_{\mu} \cos \theta})}{\iint_{A'} \iint_{\Omega} dA' \cos^{n+1} \theta d\Omega} \dots (4.4.6)$$

This gives us a relation between $P_{\mu}(\geq E_{\mu}, N)$ and $n_{\mu}(\geq E_{\mu}, N)$. However for this we must assume an explicit form of lateral distribution of the muons of energy $\geq E_{\mu}$ in the EAS. A likely form for lateral distribution of high energy muons in EAS is the exponential distribution given by

$$\Delta_{\mu}(r) = \frac{n_{\mu}(\geq E_{\mu}, N)}{2\pi r_0^2} \exp\left(-\frac{r}{r_0}\right) \dots (4.4.7)$$

this distribution is based on the transverse momentum distribution, for pions produced in Nucleon - nucleon interactions, as given by Cocconi et al. (1961) viz.

$$f(p_t) \propto p_t \exp(-p_t/p_0) \dots (4.4.8)$$

where $\langle p_t \rangle = 2p_0$. Expression (4.4.7) is derived from (4.4.8) for the case of monoenergetic muons produced at a given level in the atmosphere. However this can also be used for the case of high energy muons as their production

levels are confined to a narrow region of atmosphere and also because they have a steep energy spectrum.

Substitution of equation (4.4.7) in right hand side of eqn. (4.4.6) yields a relation, which in conjunction with equation (4.4.1) can be used to obtain values of $\eta_{\mu}(>E_{\mu}, N)$ for a given value of E_{μ} . Using S-trigger and SU7 - trigger spectra derived above/equation (4.3.3; 4.3.4)/which correspond to $S(N)$ and $SU(N)$ respectively, the values of $P_{\mu}(>E_{\mu}, N)$ for different values of N have been obtained using eqn.(4.4.1). Also integrals on R.H.S. of Eqn.(4.4.6) have been solved numerically using n_{μ} and r_0 as free parameters. Before carrying out the integration dA' , dA , θ , r & l were expressed in terms of R , ϕ , R' , ϕ' , and R_0 using the geometry of the set up (Fig.IV.5). The area A' is the 100% area for the size group. However, the dependence of $P_{\mu}(>E_{\mu}, N)$ on A' is negligible. The area A was taken to be the area of a circle of radius $500 r_0$ around the underground detector D. The integration was carried out using Gaussian Quadrature formulae for R and R' and the trapezoidal rule for angles ϕ and ϕ' .

Before deriving the values of $\eta_{\mu}(\geq 150, N)$ by comparison of experimental values of $P_{\mu}(\geq 150, N)$ with the values of P_{μ} calculated using (4.4.6) it is necessary to specify the values of $r_0(\geq E_{\mu})$ appropriate to -

$E_\mu = 150$ Gev. This value cannot be derived from the present experimental data. We have, therefore, made an estimate of the value of $\gamma_0(\geq E_\mu)$ as follows:

We note that for a given energy E_μ , $\gamma_0(\geq E_\mu)$ is related to the mean spread, $\langle r(\geq E_\mu) \rangle$, of the muons by the relation

$$\langle r(\geq E_\mu) \rangle = 2 \gamma_0(\geq E_\mu) \quad \dots(4.4.9)$$

Fig. IV.6 gives the values of $\langle r(\geq E_\mu) \rangle$ for four different values of E_μ . The points at 50 Gev and 100 Gev are calculated from the lateral distributions obtained by Earnshaw et al. (1968). It is to be noted that $\langle \gamma(\geq E_\mu) \rangle$ decreases with increasing energy and a smooth curve drawn through the points indicates a value of $\langle \gamma(\geq 150) \rangle \simeq 24$ m giving an $r_0(\geq 150)$ value of 12 m. Fig. IV.7 gives the variation of P_μ with n_μ for six different values of r_0 . It is seen that the $P_\mu - n_\mu$ relation does not change significantly, for values of r_0 from 8 m to 14 m and for $10 \leq n_\mu \leq 200$. The experimental values of $P_\mu(\geq 150, N)$ lie between 0.9×10^{-3} and 1.6×10^{-2} and for this range of P_μ values, the $P_\mu - n_\mu$ relationship does not change significantly for $8 \text{ m} \leq r_0 \leq 14 \text{ m}$.

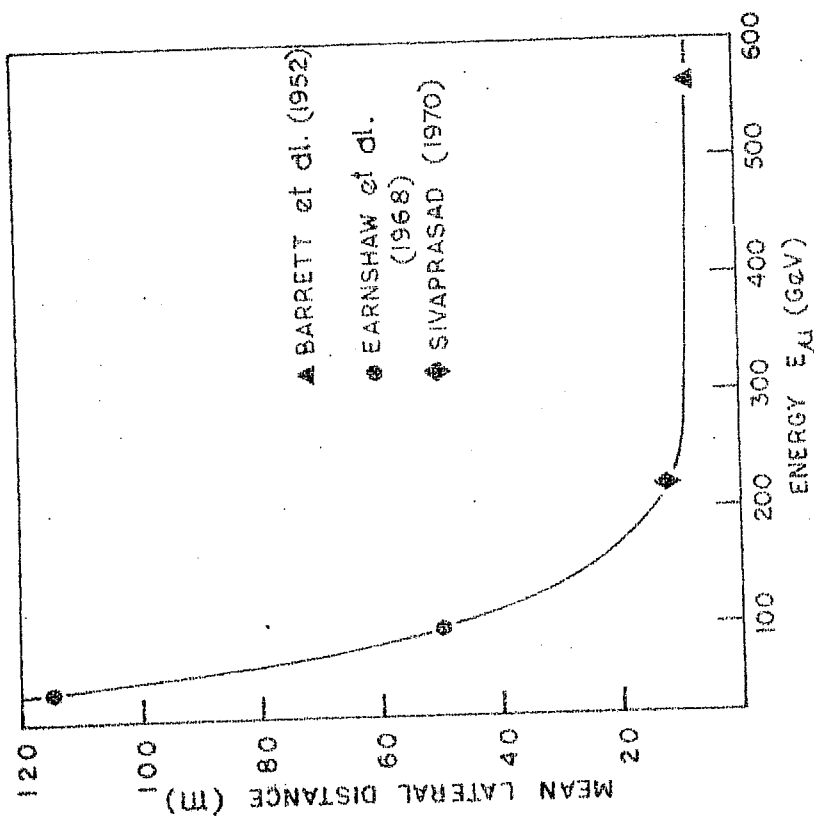


FIG. IV.6
 MEAN LATERAL DISTANCE OF MUONS OF
 ENERGY $\geq E_0$ IN EAS

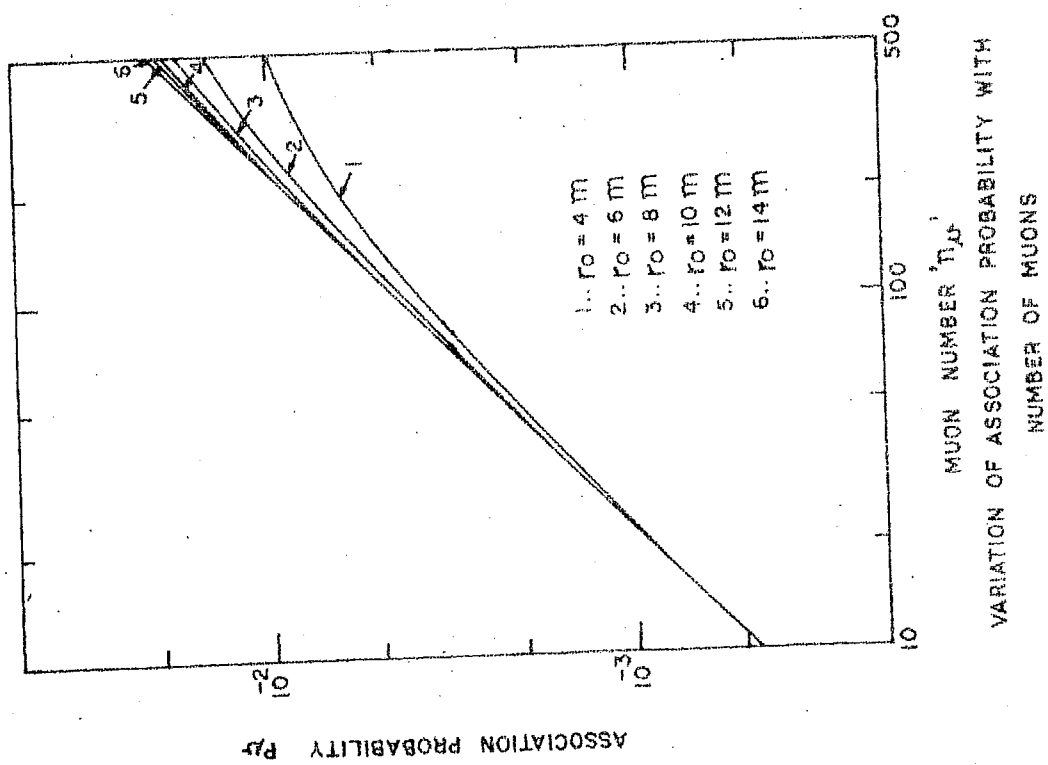
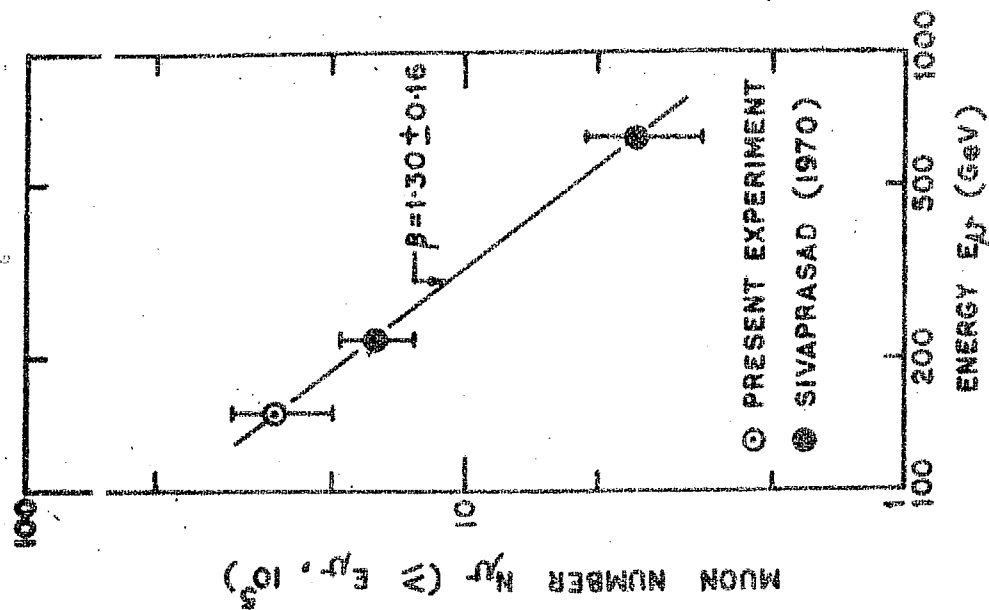
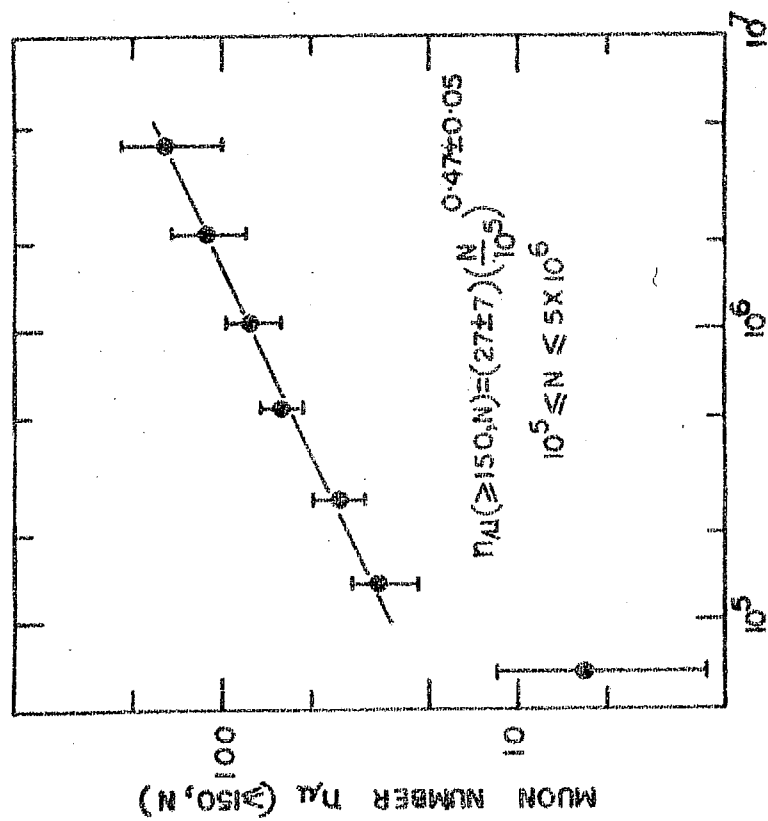


FIG. IV.7



ENERGY SPECTRUM OF MUONS
IN EAS OF SIZE 10^5 PARTICLES

FIG. IX.9

Using the curves in Fig. IV.7 and the experimental values of $P_\mu (\geq 150, N)$, the values of $n_\mu (\geq 150, N)$ have been calculated for $r_0 = 12$ m. Fig. IV.8. shows the variation of the number of muons $n_\mu (\geq 150, n)$ with the shower - size N . The relation between $n_\mu (\geq 150, N)$ and N can be expressed by a power law of the type

$$n_\mu (\geq 150, N) = (27 \pm 7) \left(\frac{N}{10^5} \right)^{0.47 \pm 0.05} \quad (4.4.11)$$

for $10^5 \leq N \leq 5 \times 10^6$

The experimental point corresponding to the first size group (Table IV.I) is much lower than expected on the basis of equation (4.4.11) and may indicate an increase in the power index for $N \leq 10^5$ particles; in this case the error factor is also much larger.

IV.5 Energy Spectrum of Muons in EAS

Sivaprasad (1970) has obtained the following relations for the variation of number of muons, of energy $E_\mu \geq 220$ Gev and $E_\mu \geq 640$ Gev, with the shower size

$$n_\mu (\geq 220, N) = (16 \pm 3) \left(\frac{N}{10^5} \right)^{0.41 \pm 0.09} \quad \dots (4.5.1)$$

$$n_\mu (\geq 640, N) = (4.1 \pm 1.2) \left(\frac{N}{10^5} \right)^{0.41 \pm 0.15} \quad \dots (4.5.2)$$

The power indices for $n_\mu - N$ relation in this case are in agreement with the power index obtained in present experiment within experimental errors and hence these values

of n_μ can be used with the value of n_μ ($\geq 150, n$), obtained in present experiment, to obtain the energy spectrum of the muons of energy ≥ 150 Gev.

Fig. IV.9 gives the energy spectrum which can be represented by a power law of the type

$$n_\mu (\geq E_\mu) = A (E_\mu / 150)^{-\beta} \quad \dots (4.5.3)$$

where $\beta = 1.30 \pm 0.16$

$$A = (27 \pm 7) \quad \& \quad N = 10^5 \text{ particles}$$

Combining equation (4.4.11) and equation (4.5.3) we can write

$$n_\mu (\geq E_\mu, N) = (27 \pm 7) \left(\frac{N}{10^5} \right)^{0.47 \pm 0.05} \left(\frac{E_\mu}{150} \right)^{-1.30 \pm 0.16}$$

for $E_\mu \geq 150$ Gev and $10^5 \leq N \leq 5 \times 10^6$

IV.6 Primary Cosmic Ray Spectrum

The differential spectrum for S-trigger showers obtained as described in section IV.3 and expressed by equation (4.3.1) can be used for obtaining the energy spectrum of the primary cosmic rays. For this purpose, however, it is necessary to have a knowledge of the relationship between the energy, E_p , of the primary cosmic ray particle and the size N , of the EAS generated by the primary particle, at the level of observation.

Lal (1967), using the curves given by Bradt et al. (1965), has obtained a relationship between E_p and N at 920 gm/cm^2 (the observation level of the present experiment). The relationship, shown in Fig. IV.10, can be represented by a power law of the type

$$N \propto E_p^\beta$$

where $\beta \simeq 1.2$.

Using this relationship and equation (4.3.1), the integral energy spectrum for primary cosmic rays has been obtained and is shown in Fig. IV.11. The spectrum can be represented by

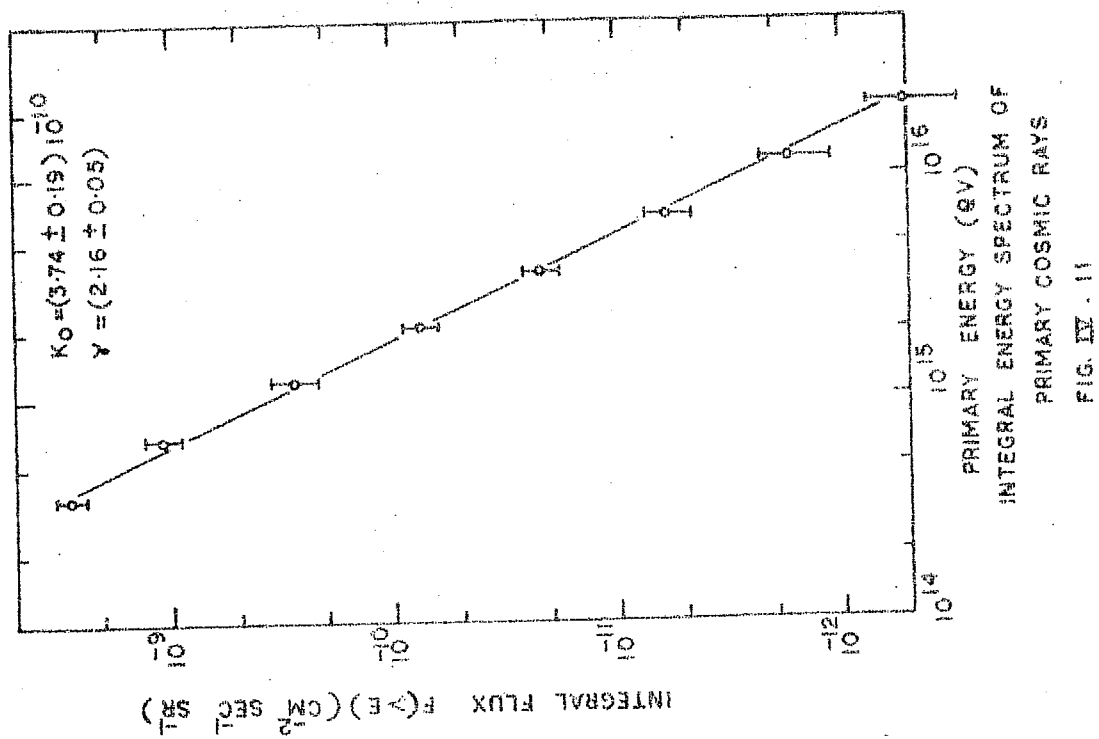
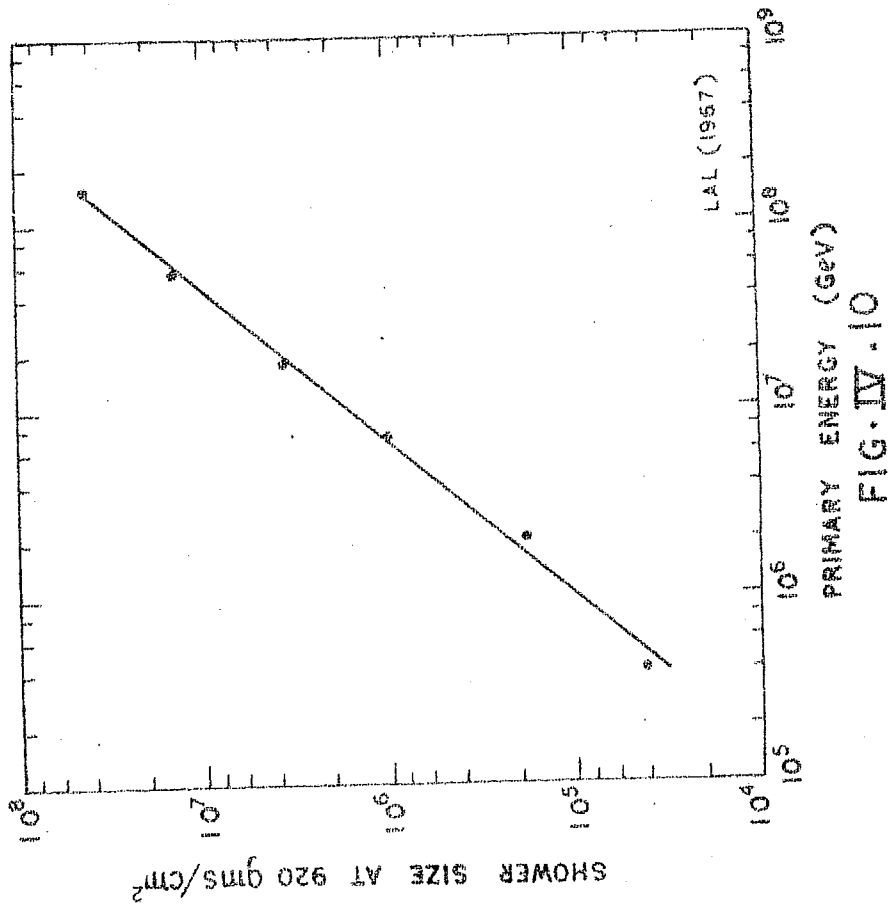
$$F(>E_p) = K_0 (E_p/10^{15})^{-\gamma} \text{Cm}^{-2} \text{Sec}^{-1} \text{Sr}^{-1} \dots (4.6.1)$$

$$\text{where } K_0 = (3.74 \pm 0.19) 10^{-10} \dots (4.6.2)$$

$$\text{and } \gamma = (2.16 \pm 0.05) \dots (4.6.3)$$

The energy E_p is expressed in eV and

$$5 \times 10^{14} \text{ eV} \leq E_p \leq 2 \times 10^{16} \text{ eV}.$$



CHAPTER V

DISCUSSION AND CONCLUSION

V.1 Comparison of present experimental results with results of other experiments:

Results of the experiments of Barrett et al. (1952) and Sivaprasad (1970) may be compared directly with the results of the present experiment.

Barrett et al. (1952) studied muons of energy ≥ 560 Gev in association with EAS and obtained the following dependence of the absolute number (n_μ) of muons on the shower size (N_e),

$$n_\mu (> 560, N_e) \propto N_e^{0.45 \pm 0.13} \quad \dots(5.5.1)$$

Further by matching the absolute flux of the muons at observation level to the air shower flux, Barrett et al. concluded that there is one muon of energy ≥ 560 Gev in a shower of size $\simeq 400$ electrons.

Sivaprasad (1970) gave the following relations for muons of energy ≥ 220 Gev and ≥ 640 Gev in EAS in the size range $10^5 \leq N \leq 10^6$.

$$n_\mu (> 220) = (16 \pm 3) (N/10^5)^{0.41 \pm 0.09} \quad \dots(5.5.2)$$

$$n_\mu (> 640) = (4.1 \pm 1.2) (N/10^5)^{0.41 \pm 0.15} \quad \dots(5.5.3)$$

The results from the present experiment may be written as

$$n_{\mu}(\geq 150) = (27 \pm 7) (N/10^5)^{0.47 \pm 0.05} \quad \dots (5.5.4)$$

for the showers in size range $10^5 \leq N \leq 5.10^6$.

We note that there is a reasonable agreement between the power indices obtained in the three different experiments. As far as the absolute number of muons is concerned, there is a good agreement between the number of muons of energy ≥ 150 Gev obtained on the basis of equations (5.5.2) and (5.5.3) and the results of present experiment. However, the number of muons of energy ≥ 560 Gev obtained from the results of Barrett et al. (1952) appears to be much larger than expected on the basis of the energy spectrum derived using the results of Sivaprasad (1970) and the present experiment.

Greisen (1960) gave the following relation for the experimental results of Barrett et al.:

$$n_{\mu}(\geq 560, N_e) = 75 (N_e/10^6)^{\alpha} \quad \dots (5.5.4)$$

where $\alpha = 0.7$ decreasing towards 0.5 for small values of n_{μ} and N_e . Considering the other available results Greisen (1960) also gave the energy spectrum for the muons associated with EAS. The spectrum turned out to be a power law with index $\beta \simeq -1.37$. Though this energy

spectrum index agrees well with the one obtained in present experiment the number of muons obtained from equation (5.5.4) for ≥ 560 Gev turns out to be much higher than expected on the basis of the present results (equation 4.5.3)

It may be pointed out that the apparatus used by Barrett et al. (1952) to detect EAS consisted of four G.M. counter trays spread over a sensitive area of 30 m radius on the surface. Thus information about the size and core location of the individual showers could not be obtained in that investigation.

The validity of the argument, put forward by Barrett et al. (1952) to obtain the absolute number of muons, has been questioned by Sivaprasad (1970). The reasoning runs as follows. Assuming that every primary particle of energy E_p (corresponding to the shower size N_0) is associated with one muon of energy ≥ 560 Gev, the steady state flux of these muons can be obtained by integrating over all primary energies. Because of a steep primary energy spectrum and a E_p^α ($\alpha < 1$) dependence of muon number on the primary energy a dominant contribution to the muon flux will come from particles of primary energies $\leq E_p$. Sivaprasad (1970) has recalculated the absolute value of $n_\mu (\geq 560)$ from the data of Barrett et al. (1952). According to this calculation the results

of Barrett et al. (1952) may be rewritten as

$$n_{\mu} (\geq 560, N_e) \simeq 7 \left(\frac{N}{10^6} \right)^{0.45 \pm 0.13}$$

and the numbers obtained using this relation are in reasonable agreement with the numbers expected on the basis of equation (4.5.3).

At Hobart conference the Russian group (Asekin et al. 1971) has reported the muon spectrum, for muons associated with EAS, to be of the type

$$n_{\mu} (\geq E_{\mu}, N_e) = (3.1 \pm 1.5) \left(\frac{E_{\mu}}{0.3} \right)^{-1.58 \pm 0.2} \left(\frac{N_e}{3 \times 10^4} \right)^{0.68 \pm 0.24}$$

for $N_e > 3 \times 10^4$ and $E_{\mu} > 0.1$ Tev.

The values of the exponents of both energy and size spectra are larger than obtained in the present experiment, but the present results are within the error limits quoted by Asekin et al. (1971). It may be noted that the above results of the Russian group are based on the size - number spectrum of the bursts produced by muons at 40 m.w.e. associated with EAS on the surface.

We may then conclude that the variation of the number of muons of threshold energies ≥ 150 Gey with the shower size (in the size range $10^5 - 10^6$) is a power law with the power index $\alpha \simeq 0.45$. The experimental results

at lower threshold energies (upto 40 Gev) give a power law with index $\alpha \simeq 0.8$. Thus there appears to be a flattening of the muon number variation for muons of threshold energies > 150 Gev.

V.2 Monte Carlo Calculations:

a) Description of the Models: In order to compare the experimental results presented in preceding chapter with the predictions of some of the models of EAS development Monte Carlo calculations based on these models were carried out. Details of the models are given in Table V.1. The models are identical to the ones used by Murthy et al. (1968) for calculations of EAS characteristics, and belong to basically two different categories viz. Fire-ball models and Isobar models.

QL and QLN models are identical with each other in all respects except that in the QLN model a production of $\bar{N}N$ (nucleon-antinucleon) is envisaged along with the production of pions. Similar difference exists between IB and IBN models.

The QL and QLN models are similar to the CKP model (described in Chapter I) and the energy spectrum of the particles created in the nucleon or pion-nucleon interaction is assumed to be an exponential function of the type

$$ns(E) dE = \frac{M}{T} \exp\left(-\frac{E}{T}\right) dE \quad \dots(5.1.1)$$

MODELS OF EAS DEVELOPMENT

	Model QLN		Model IBN		
	Nucleon	Pion	Fireball	Nucleon Isobar	Pion
Multiplicity M	$2.7 E'^{\frac{1}{4}}$		$0.25 E'^{\frac{1}{2}}$	3	$0.96 E'^{\frac{1}{3}}$
Inelasticity K	0.5	1.0	0.2	-	1
Mean Free Path (gm/cm)	80	120	80		120
Fraction of \overline{NN} produced,	$(7 (500/E'+1))^{-1}$		$(7 (500E'+1))^{-1}$		$(7 (500E'+1))^{-1}$
Energy spectrum of created particles	Exponential		Exponential	Decided by Kinametics	Exponential

E' is the energy of the projectile
Models QL and IB are, identical to models QLN and IBN
respectively except that for QL and IB models
 $f = 0$

where T is the average energy and M the total number of created particles. If the NN production is involved (as in QLN model) the energy is supposed to be distributed among pions and nucleons such that their average energies are proportional to the respective masses. Thus if m_p and m_B represent mass of a Pion and mass of a nucleon respectively the average energy T_p and T_B of pions and nucleons respectively can be written as

$$\begin{aligned} T_p &= \frac{E'K}{M} \left(m_p / (1-f) + f \cdot m_B \right) \\ T_B &= \frac{E'K}{M} \left(m_B / (1-f) + f \cdot m_p \right) \end{aligned} \quad \dots (5.1.2)$$

where E' , K and M are the initial energy, inelasticity and multiplicity respectively.

The IB and IBN models are akin to the model proposed by Pal and Peters (1964) and the interactions in these models may be described as follows. In each interaction a fireball is assumed to be created and the constituents of this fireball share 20% of the primary energy. The fireball is then assumed to emit particles isotropically in CM system. The multiplicity for these particles is assumed to be proportional to square-root of the fireball energy and the energy spectra of the particles are governed by the same relationships as for QL and QLN

models. The surviving nucleon, which retains 80% of the primary energy, is excited with a 70% probability into an excited isobar state of mass 2.4 Gev. Each isobar of mass $m_B = 2.4$ Gev and energy $E_B = 0.8 E'$ is assumed to decay into one of mass $m = 1.93$ Gev and energy E , emitting a pion of momentum $p = 400$ Mev/C isotropically in the rest system of the parent isobar. The energy distribution of the created isobar or pion may be expressed as

$$n(E) dE = \frac{m_B}{2 E_B} \frac{dE}{p^*} \quad \dots(5.1.3)$$

$$\text{for } \frac{E_B}{m_B} (E^* - p^*) \leq E \leq \frac{E_B}{m_B} (E^* + p^*)$$

where $E^* = \sqrt{m^2 + p^{*2}}$; m being the mass of created isobar or pion.

The created isobar of mass 1.93 Gev is assumed to decay into one of 1.45 Gev which in turn is assumed to decay into a nucleon, a pion of momentum p^* being emitted in each decay. Expressions similar to equation (6.1.) hold good for each decay.

b) Calculation Procedure: A primary proton of a given energy is assumed to enter the top of the atmosphere and the depth at which it suffers first collision is determined using the relation.

$$x_1 = - \lambda \ln R$$

where R is a random number distributed uniformly between 0 and 1 and λ is the mean free path of the nucleon. The depths of successive interactions of the primary as well as the secondaries is determined using the relation

$$x_{n+1} = x_n - \lambda \ln R$$

where x_n is the depth at which the preceding interactions took place and λ is the relevant mean free path.

For each collision of the primary as well as each collision of the created secondaries the number of created particles of various types, their energy etc are generated by using random numbers with appropriate distribution. Number of pions decaying into muons is calculated and muons thus produced are stored along with the values of their energies. The decay of muon is considered only for muon energies less than 10 GeV. Particles having energies less than 1 GeV are not considered for further calculations.

The calculations were carried out on CDC 3600/160A computer system at TIFR, Bombay. A random number generator, available with the system, was used for generating random numbers of desired distribution.

The shower size was calculated by superposing showers generated by photons resulting from the decay of π^0 meson. The following expression, given by

Greisen (1958), was used to calculate the number of electrons, at observation level, generated by a photon of given energy.

$$N_e(E, t) = \frac{0.31}{(\log(E/\epsilon))^{\frac{1}{2}}} \text{Exp}(t(1-1.5 \log S)) \quad \dots (5.1.4)$$

where ϵ is the critical energy, t the depth of observation level from the point of production of a gamma ray in radiation length, and S the age given by

$$S = \frac{3t}{t + 2 \log(E/\epsilon)} \quad \dots (5.1.5)$$

V.3 Results of Monte Carlo Calculations:

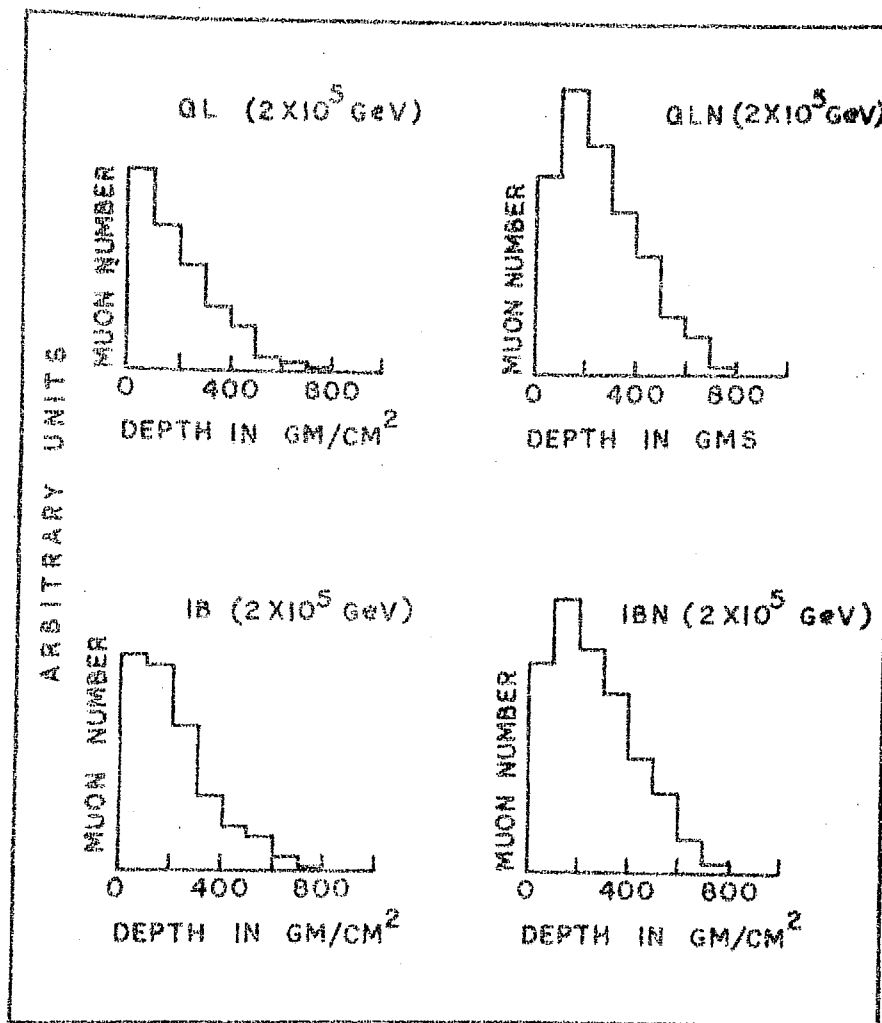
The distribution of the number of muons of energy > 150 GeV in the EAS initiated by a primary proton of energy 2.10^5 GeV in the production depths is shown in Fig.V.1 for various models. All the models predict an average production heights $\simeq 11$ Km for the muons of energy > 150 GeV, though the models envisaging $N\bar{N}$ production (i.e. QLN & IBN models) predict average production heights which are smaller than those predicted by QL and IB models.

Regarding the variation of total number of muons (n_μ) with the shower size (N_e) for various threshold

energies of muons it is seen that all the models yield a power law relationship with the exponent α having values in the range of 0.6 - 0.8. For muons of threshold energies upto 40 Gev QLN and IBN models predict muon numbers which are greater than the muon numbers predicted for the same threshold energies by QL and IB models respectively. However at larger threshold energies (≥ 100 Gev) the trend is reversed and the QLN and IBN models now yield numbers which are less than the corresponding numbers predicted by QL and IB models.

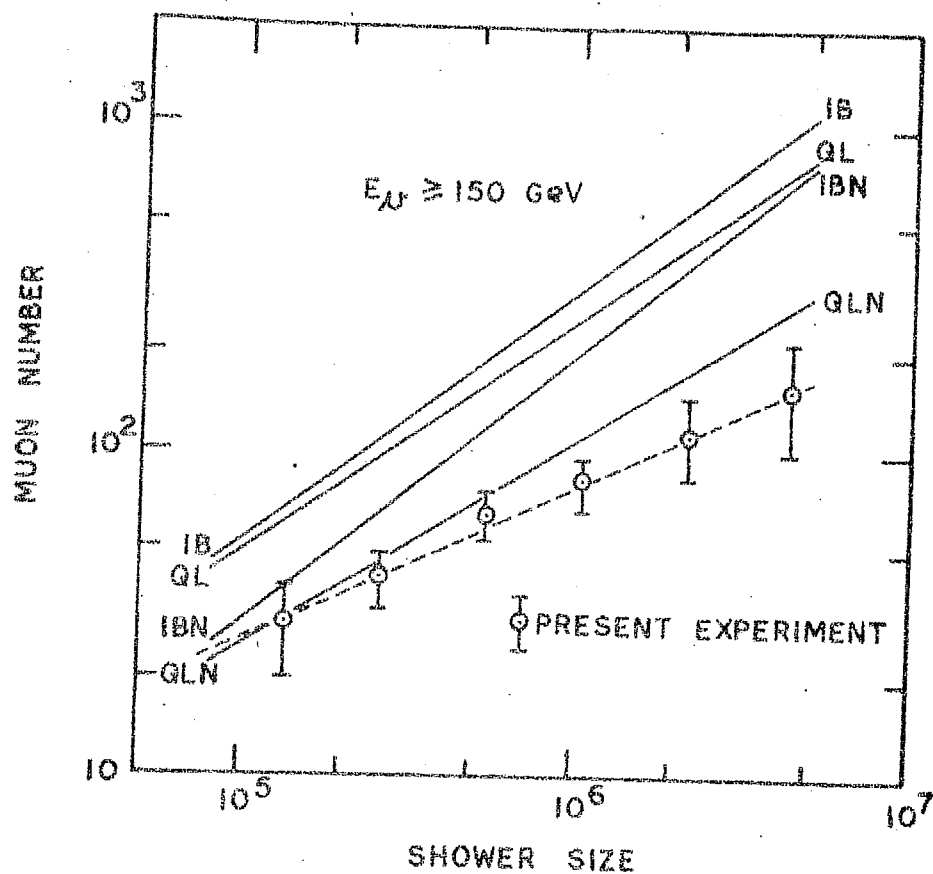
Fig. V.2 gives variation of the number of muons of energy > 150 Gev with the shower - size, in the size range $10^5 - 5.10^6$ particles. The variation is well represented by a power law with power index in the range of .62 - .82. The IBN model predicts the steepest $n_\mu - N_e$ relationship.

The predictions given in Fig.V.2 are for the proton initiated showers. Calculations were also done for a mixed primary composition. The assumed composition was similar to the one established by the Balloon born emulsion experiments at 10^{12} ev, and may be expressed as follows:-



DISTRIBUTION OF NUMBER OF MUONS OF ENERGY
 ≥ 150 GeV IN PRODUCTION DEPTH

FIG. 1



PREDICTIONS OF MONTE CARLO CALCULATIONS
ON MUONS OF ENERGY $\geq 150 \text{ GeV}$. FOR PROTON
PRIMARIES & THE EXPERIMENTAL RESULTS.

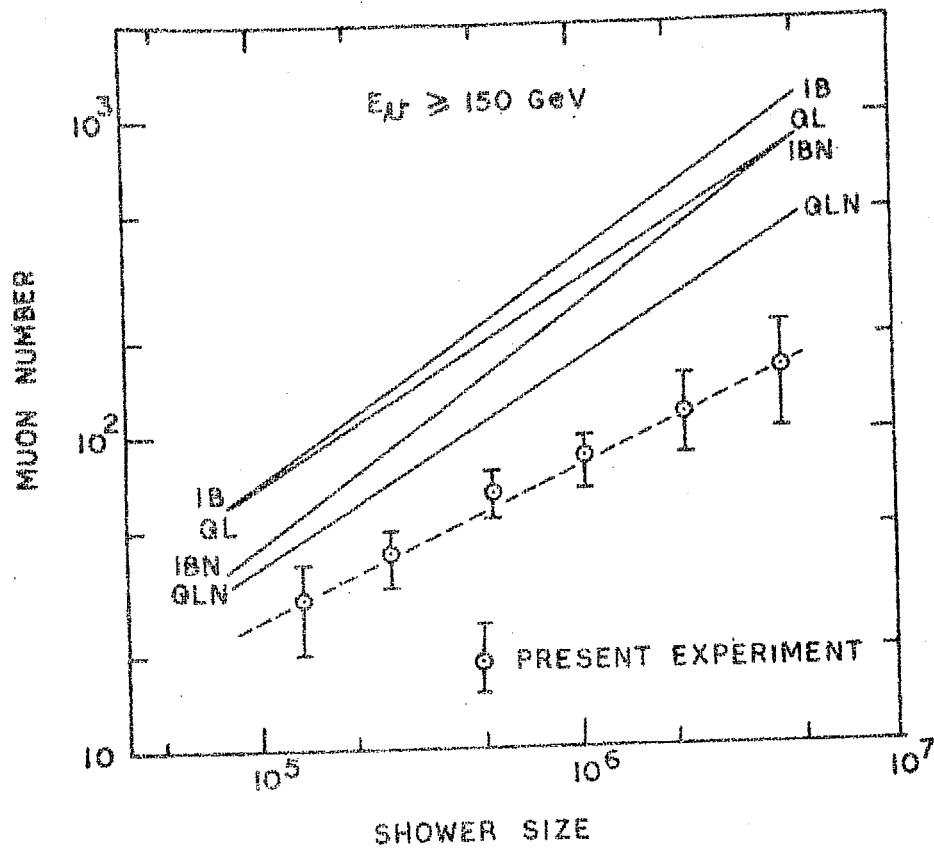
FIG. Y. 2

<u>Nuclei Mass No</u>	<u>Percentage</u>
1	49%
4	27%
14	12%
32	5%
56	7%

Using this composition showers were simulated for the four models described in Table V.1. The primary particle was selected using random number with appropriate distribution and the showers were generated by superposing showers produced by 'A' protons. The predictions of the four models for above mentioned chemical composition, for muons of energy ≥ 150 Gev are shown in Fig. V.3. It is seen that the power index for n_{μ} - Ne relationship in the case of the mixed composition lies in the range of 0.60 - 0.77 and the predicted number of muons for a given size and for a given model is larger than the corresponding number predicted by the model for proton primary.

V.4 Comparison of Experimental Results with the Predictions of the models:

The experimental results, presented in Chapter IV, are shown along with the predictions of the Monte Carlo Calculations in Fig. V.2 and V.3. Whereas the experiment gives a power index of (0.47 ± 0.05) for the n_{μ} - Ne variation for muons of energy ≥ 150 Gev, the models



PREDICTIONS OF THE MONTE CARLO CALCULATION
ON MUONS OF ENERGY $\geq 150 \text{ GeV}$, FOR A MIXED
PRIMARY COMPOSITION & EXPERIMENTAL RESULTS.

FIG. V. 3

predict power indices which are much larger than the experimental value. The absolute value of the number of muons is closer to the predicted value for showers of 10^5 particles and the discrepancy increases with the increasing shower size because of the difference in the power indices. Thus we see that the models under consideration cannot reproduce the experimentally observed variation of n_μ with N_e for the proton as well as the mixed composition primaries as found at energy $\simeq 10^{12}$ ev. We shall discuss this aspect further in a later section.

V.5 Consequences of observed $n_\mu - N_e$ relation:

As seen in the proceeding sections the variation of the muon number with the size, for muons of energy ≥ 150 Gev, in size range 10^5 to $5 \cdot 10^6$ particles, is flatter than observed for muons of lower threshold energies and the models examined do not reproduce the observed variation. Two possible explanations may be envisaged for this flat $n_\mu - N_e$ variation.

The first explanation is to invoke an energy dependent change in some characteristic of the interaction, in the relevant energy region, which may lead to a decrease in the fraction of energy going into the production of the parent particles of muons. This

will lead to a relative reduction in the muon number for higher shower sizes and will result in a flatter n_{μ} - Ne variation. An alternative explanation is to invoke a change in the mass-composition of the primary cosmic rays in the relevant energy region (10^{14} - 10^{15} GeV) such that the average mass number A of the primaries decreases from a high value at low energies to a lower value at higher energies. This will result in an enhancement in the muon number of small size showers leading to a flatter n_{μ} - Ne variation. Possibility of both the effects operating simultaneously may also be considered.

In light of the existing results and model calculations by various authors we have examined the second possibility in the following section.

V.6 Primary Mass Composition and the n_{μ} - Ne relation:

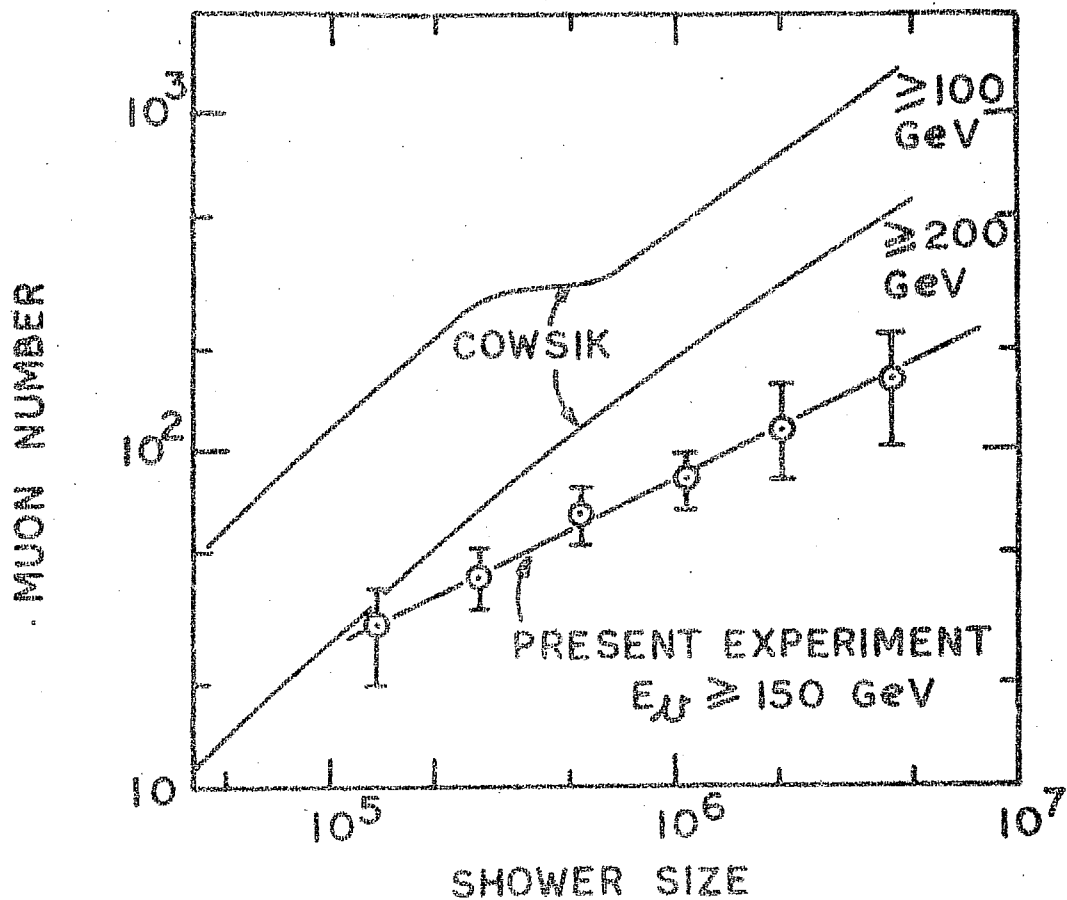
The chemical composition of primary cosmic rays has been well established at energies $\simeq 10^{10}$ eV. Studies, using large emulsion stacks flown in Balloons, indicate that the composition remains unaltered upto energies $\simeq 10^{12}$ eV. At very high energies 10^{17} eV, the smallness of the fluctuations in the characteristics of the EAS,

indicates a pure protonic nature of the primaries as discussed by Linsley and Scarci (1962) and K. Suga et al. (1970). A change in the primary chemical composition may then be expected in the intervening energy interval ($10^{14} - 10^{16}$ eV). It has long been considered that the primary cosmic rays over a certain threshold of magnetic rigidity may not be retained in our galaxy and there may exist a galactic rigidity cut-off, for the primary cosmic rays, beyond which the cosmic rays may be of extra-galactic origin. Peters (1961) envisaged such a rigidity cut-off on the basis of certain irregularities in the air shower characteristics.

Using an "Isobar-cum-Fireball" model, similar to the model of Pal and Peters (1964), and assuming a changing chemical composition due to galactic rigidity-cut-off, Cowsik (1967) calculated the size dependence of the average shower characteristics. He assumed a rigidity cut-off at 10^5 Gv and a chemical composition same as at low energies upto the cut-off. Beyond the cut-off a pure extra-galactic proton primary component was assumed. A comparison of the results from present experiment with the calculations of Cowsik (1967) is shown in Fig.V.4. The heavy lines are the calculated curves at two threshold

energies, viz. 100 Gev. and 200 Gev. Besides the disagreement with the absolute values, the observed variation is not reproduced under the assumptions and the model used by Cowsik (1967). Chatterjee (1964) also proposed a similar model for the primary energy spectrum using the galactic cut-off for protons at 3×10^{14} eV and Z times higher for the heavier particles. The cut-off was assumed to be sharp. Sivaprasad (1970) has modified this model slightly by introducing a gradual cut-off starting at 10^{14} eV for the protons. The flux was assumed to drop-off to 1% of the pre-cut-off value within an energy equal to 2.5 times the cut-off energy. Using this model Sivaprasad studied the $n_{\mu} - \text{Ne}$ variations as predicted by various models of nucleon-nucleon interactions as used by Murthy et al. (1967). The results of the calculations may be summarised as follows:

The calculations predict a flattening in $n_{\mu} - \text{Ne}$ variations at high energies and the predicted variations, for threshold energies 220 Gev and 640 Gev in the size range $10^5 - 10^6$ particles -- are in better agreement with the experimental results of Sivaprasad (1970). The predictions are not in conflict with the experimental results for muons of threshold energies upto 40 Gev and the models envisaging NN production are in better agreement with the experimental results.



COMPARISON OF EXPERIMENTAL
RESULTS WITH THE CALCULATIONS
OF COWSIK (1967).

FIG V. 4

The effect of the magnetic rigidity cut-off on the n_{μ} - Ne relation can be understood as follows. For a given level of observation, the average size of the showers initiated by a heavy primary will be different from the size of the shower initiated by a proton of same energy. Thus the primary energy, required to produce shower of a given size, will be different for the primaries of different 'A' values. It is this difference in the primary energy, for producing showers of a given size, coupled with the existence of the rigidity-cut-off that leads of a decrease in $\langle A \rangle$ with the increase in shower size, even though there is an increase in $\langle A \rangle$ with increasing primary energy. This in turn leads to a rather flatter n_{μ} - Ne relation than obtained on the basis of a constant composition.

Calculations of Sivaprasad (1970) for muons of energy ≥ 220 Gev are shown in Fig.V.5 along with the results from the present experiment for muons of energy ≥ 150 Gev. The trend of the n_{μ} - Ne variation, predicted by the calculations, is not in disagreement with the observed trend.

The Durham group (J.F. de Beer et al. 1968; C. Adcock et al. 1968) has carried out a theoretical study of the possible consequences, of a primary compo-

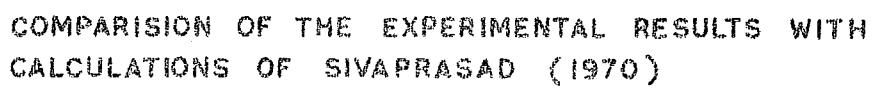


FIG 7. 3

sition subjected to a magnetic rigidity cut-off, on various parameters of EAS which can be measured above ground at sea-level. If the primary composition changes as a result of the magnetic modulation the authors anticipate a highly characteristic oscillation effect in the value of $\alpha = \partial \ln n_{\mu} / \partial \ln N_e$ as a function of N_e . Catz et al. (1970) have observed a somewhat similar oscillation in experimentally obtained values of α in the size range predicted by the Durham group. Though there are significant errors on the values of α as measured by Catz et al. (1970) and though the fluctuation in values of α is not as great as anticipated by the Durham group, the results of Catz et al. (1970) appear to support a changing primary composition subjected to magnetic rigidity cut-off. However, Thompson et al. (1970), from an examination of recent data on muons in EAS, conclude that the majority of the primaries are still protons above 10^{15} eV.

V.7 Change in the nature of the characteristics of the nuclear interaction and the n_{μ} - N_e relation:

A flatter variation of n_{μ} with size, than the one predicted by the above discussed models may be brought about by envisaging an energy dependent change in the characteristics of nuclear interaction such that the

fraction of energy going to the pion production decreases gradually in the relevant energy range. One of the possible changes which may be envisaged, is an energy dependent increase in the $\bar{N}N$ production. As seen earlier the production of $\bar{N}N$ results in the reduction in muon number for muons of threshold energies beyond 40 GeV. Thus in the energy range, relevant to the sizes $10^5 - 10^6$ at the observation level, an energy dependent increase in the production of $\bar{N}N$ may result in a flatter $n_\mu - E$ variation than predicted by usual models.

There is no experimental evidence against the increased $\bar{N}N$ production at high energies. Tonwar et al. (1971) have shown, from their experimental observations of the time structure of the hadrons in EAS, that the $\bar{N}N$ production at energies $> 10^{12}$ eV is as high as 14%. - Thus a rather rapid increase in the cross-section of the $\bar{N}N$ pairs at energies beyond 100 GeV is implied. However, to fit the observational data above the size range 10^6 , this effect of increase in $\bar{N}N$ production with increasing primary energy must saturate at an energy region in the neighbourhood of 10^{16} eV.

V.8 Energy Spectrum of Muons in Extensive Air Showers:

As mentioned earlier (Chapter I) Greisen (1960), on the basis of the available experimental results gave

an energy spectrum of muons of the type $(2/E_\mu + 2)^{1.37}$. In the present experiment (Chapter IV) we have obtained an energy spectrum for muons with threshold energies in the range 150 Gev \div 640 Gev. The spectrum goes as $E_\mu^{-1.30}$ and there appears to be a fair agreement in the two power indices. However, as seen in Fig. V.6, there appears to be some discrepancies between the experimental results at low threshold energies (upto 40 Gev) and at higher threshold energies. It is seen that though the slope at low threshold energies is in good agreement with the slope at higher energies the number of muons at higher energies do not agree with the ones expected on the basis of extrapolation of the results at lower energies. This can be understood on the basis of the difference in the power index

$\alpha = \partial \ln n_\mu / \partial \ln N_e$ for muons of lower threshold energies and higher threshold energies which results in a gap on the number - energy diagram as seen in Fig. V.6.

The experimental results of Earnshaw et al. (1968) stand out as the highest muon numbers for the respective threshold energies. The result of Barrett et al. (1952) also does not confirm to the picture at higher threshold energies as obtained from the results of Sivaprasad (1970) and the present experiment. However, if the result of Barrett et al. is modified as suggested by Sivaprasad the

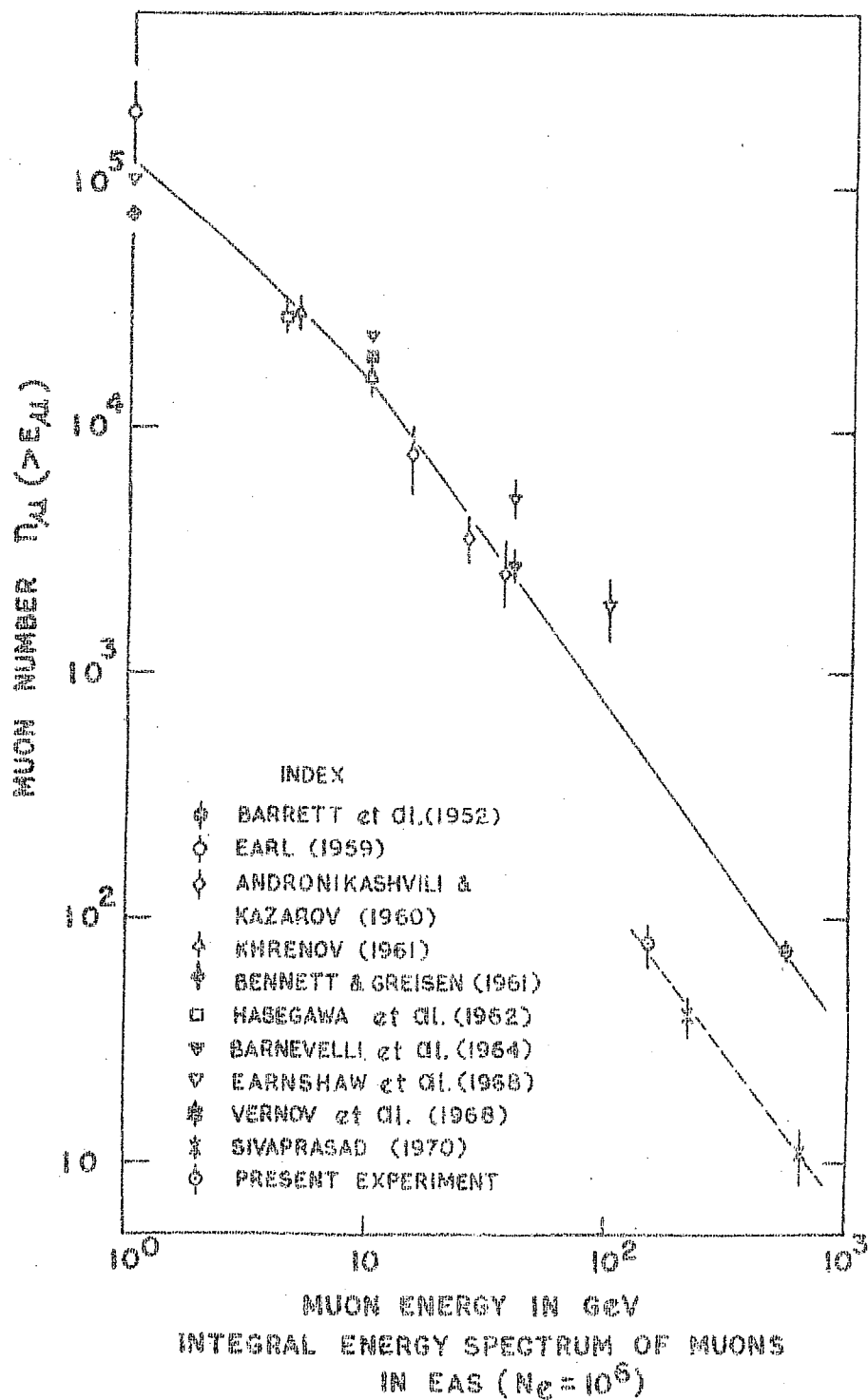


FIG. 5.6

picture becomes more consistent. For muon threshold energies < 10 Gev there appears to be a flattening in the energy spectrum.

V.9 Conclusions:

From the considerations of the preceding sections we conclude that the n_{μ} - Ne variation as observed in the present experiment for high energy muons (> 150 Gev) is flatter than one predicted by the "present-day-known" models using a constant primary composition.

The possibility of a changing primary composition resulting in a n_{μ} - Ne variation similar to the observed one is examined and it is seen that a primary composition subjected to a gradual galactic rigidity-cut-off may reproduce the observed variation. At this point it may be pointed out that if the observed n_{μ} - Ne variation in this size range is due to the rigidity cut-off in the relevant primary energy range (10^{14} - 10^{15} ev) then outside this range the n_{μ} - Ne variation for muons of higher energies (beyond threshold energies of 40 Gev) should be a power law with index $\alpha \simeq 0.6 - 0.8$. This is expected because outside the cut-off region a constant primary composition exists and such a composition will result in a power law index $\alpha \simeq 0.6 - 0.8$.

The possibility of a change in the characteristic of the nuclear interaction with energy cannot be ruled out.

V. 10 Suggestions for future investigations:

Two possible explanations for the observed n_{μ} -Ne variations in the size range $10^5 - 10^6$ particles have been given in preceding sections. If the primary composition changes with energy in the energy interval 10^{14} eV to 10^{15} eV and remains constant outside this region the expected n_{μ} -Ne variation for muons of energy ≥ 150 GeV, will have a power index $\simeq 0.6 - 0.8$ for shower sizes $< 10^5$ particles and $> 10^6$ particles. This aspect of the n_{μ} -Ne variation should be looked-for in the extended measurement on muons of energy ≥ 150 GeV in showers over a wide size range. Moreover, it is necessary to have narrower grouping in the shower sizes than obtained in the present experiment.

It is also desirable to study the behaviour of the other components of EAS as a function of the size in the region $10^5 - 10^6$. Specially an investigation on charged to neutral ratio of hadrons of energy ≥ 100 GeV in the region $10^5 - 10^6$ may be helpful to understand the different models of muon production.

Study of the fluctuations in the various characteristics of the EAS in different size range will also be useful in understanding the composition of the primary cosmic rays at high energies ($\geq 10^{14}$ eV).

CHAPTER VI

NFT HODOSCOPE DATA

RESULTS AND DISCUSSION

VI.1 The NFT Data

The photographs of the neon flash tube (NFT) hodoscope, obtained by triggering the neon flash tube trays with SU-7 triggers, contain the tracks of muons and accompanying particles associated with the EAS. During the operation of the EAS array, shown in Fig.II.1, in association with the UG-detector the NFT hodoscope was operated only for a short period. Preliminary results from the obtained data were presented by Chowdhuri and Saxena (1971). The TIFR group has, since, modified the EAS array at K.G.F. and the new arrangement of the detectors in the array is shown in Fig. VI.1. Using this array and the UG-detector the NFT hodoscope pictures were obtained for an effective operational period of 1.48×10^6 secs. during which ~ 1760 events, (coincidences between EAS and the UG-detector), were recorded. We have examined 740 of these events to obtain information about the muons of energy ≥ 150 Gev and the EAS associated with these events.

The events have been classified according to the number of particle tracks seen in the NFT hodoscope photographs and details are given in Table VI.1.

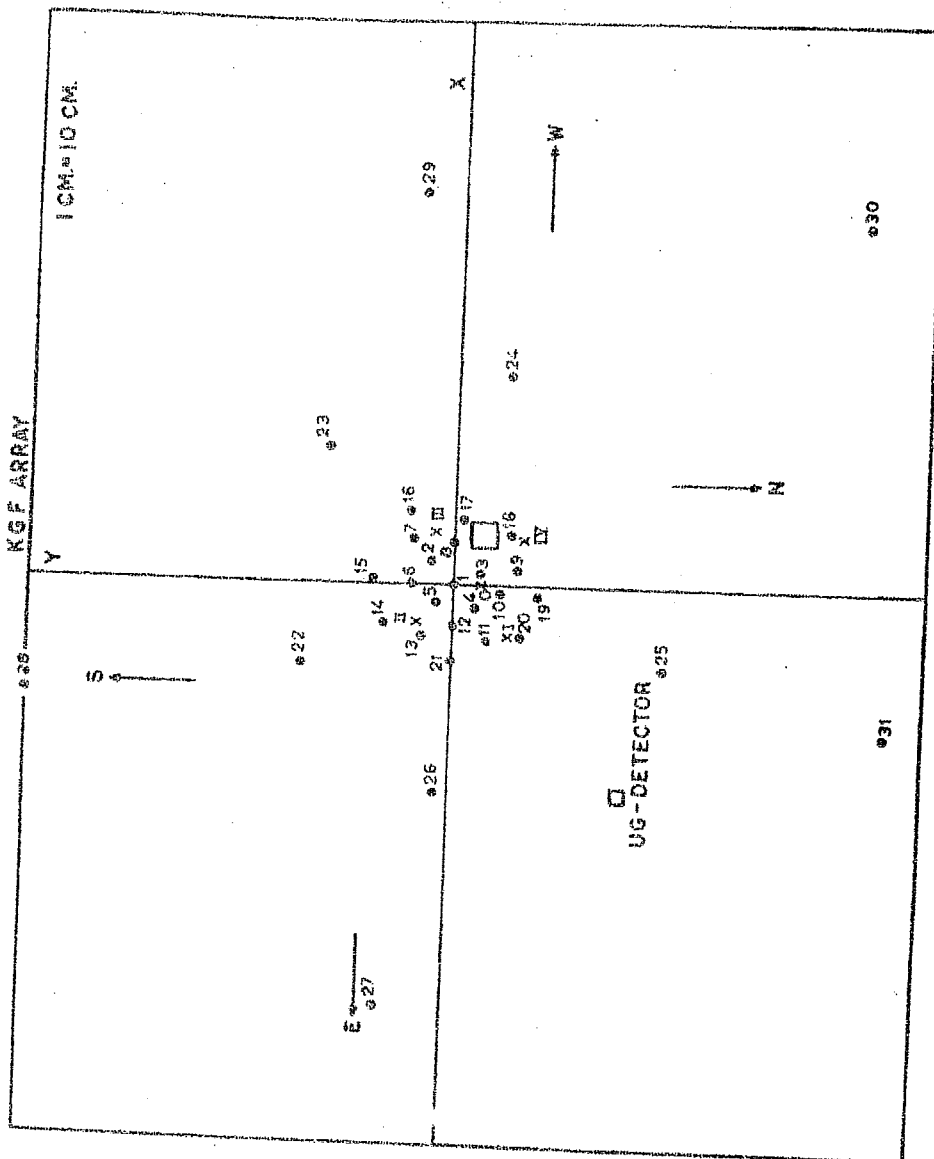


FIG. 1

TABLE VI.1NFT HODOSCOPE DATA

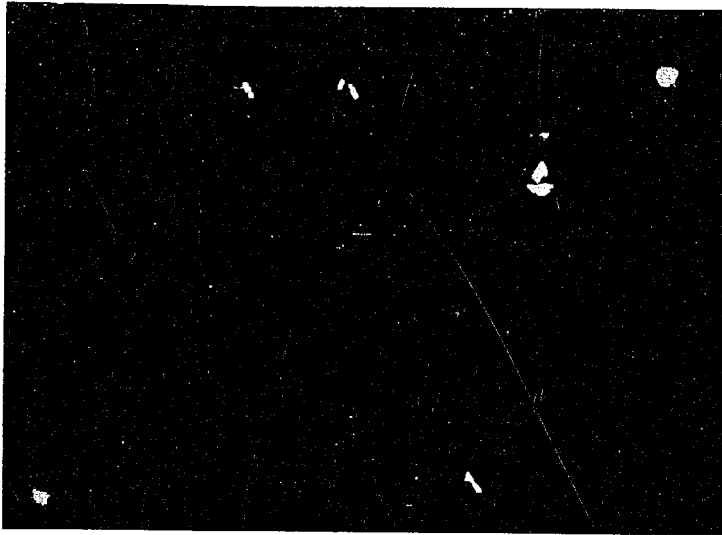
Type of the event	Single track events	Pair track events	Multiple track events	Miscellaneous
Number	606	58	6	71

The single track, pair track and multiple track events refer to passage of one, two, or more than two penetrating particles respectively, through the UG-detector. The events listed under "Miscellaneous" are the case where the tracks are seen only in one of the NFT trays. It may be mentioned that NFT trays do not cover the total area under the scintillator (Fig. II.3) and there were cases of single particle tracks where the inclination of the particles were such that particle passed only through one of the NFT trays and missed the other. However, the particle tracks listed under "Miscellaneous" were well within the geometry of the apparatus. These ~~w~~ events then could be the cases where the muon, associated with the EAS, went through the scintillator without crossing the NFT trays and an accompanying electron, produced by the muon locally triggered one of the trays.

VI.2 The Single-track Events:

Majority of the examined events showed single particle tracks implying the passage of a penetrating particle through the detector. Examples of single particle tracks are shown in Fig. VI.2 where the particles are seen triggering four-tubes in each NFT tray. From a preliminary analysis of the data of the EAS associated with the single-track events it is seen that the sizes of the EAS lie in the range $5 \cdot 10^3$ particles to $5 \cdot 10^4$ particles.

Projected angles which the single-particle tracks make with Zenith in a vertical plane in N-S direction, were measured and the events were grouped in various groups of the zenith angle. Details of the classification are given in Table VI.2.



Single Particle Track
Fig. VI. 2(a)



Single Particle Track
Fig. VI. 2(b)

TABLE VI-2
SINGLE TRACK EVENTS

Projected angle			Number of muons	
			Incident from south	Incident from north
0°	-	5°	38	15
5°	-	10°	43	9
10°	-	15°	83	21
15°	-	20°	76	17
20°	-	25°	74	17
25°	-	30°	63	5
30°	-	35°	50	2
35°	-	40°	25	0
40°	-	45°	13	0
Total			465	86
Tracks Along Vertical		 9

In addition to the events listed above there were 56 single particle events with position and inclination of the tracks such that the particles could traverse either the upper NFT tray (52 events) or the lower NFT tray (4 events). From the table one can see that in majority of the cases the particles are incident on the

UG-detector from South and projected angles of majority of the particles incident from the North are limited to angles $\leq 25^\circ$. The mean angle for the particles incident from South turns out to be 20° with a R.M.S. deviation of 10° . The mean angle for particles from North is 14° with an R.M.S. deviation of 8° .

Let us examine these observations taking the geometry of the experimental set up into account. It is to be noted that the UG- detector is located ~ 70 m North-East of the vertical projection of the centre of the EAS array. The line joining UG-detector to the centre of EAS array makes an angle of 19.5° with the vertical. Thus the observation that majority of the particle tracks are incident from South with an average angle of $20^\circ \pm 10^\circ$ implies that in most of the cases the particle enters ground very near the centre of the EAS array. The detection efficiencies for the EAS, having cores near the centre of the EAS array, are high and the efficiency drops off with increasing distance of the core from the centre. Thus we note that the NFT hodoscope records particles which form part of EAS and which are in neighbourhood of the respective EAS cores.

Taking account of the solid angles involved and detection efficiencies of the EAS the number of single track - events in various zenith angle bins has been corrected. The zenith angle distribution of the particles is as shown in Fig. VI.3. The correction factors for various zenith angle bins have been expressed in terms of the correction factor for $40^\circ - 45^\circ$ bin so that the number of events in this bin remains unaltered. The distribution can be expressed by a power law of the type

$$I(\theta) = I_0 \cos^n \theta \quad \dots(6.2.1)$$

$$\text{where } n = 7.6 \pm 1.4 \quad \dots(6.2.2)$$

As shown earlier the muons recorded by the UG-detector in association with EAS are in the vicinities of the respective EAS cores. Thus if the directions of these muons may be taken as the representatives of the directions of the EAS cores then eqn. (6.2.2) indicates a steep zenith angle distribution of the recorded EAS.

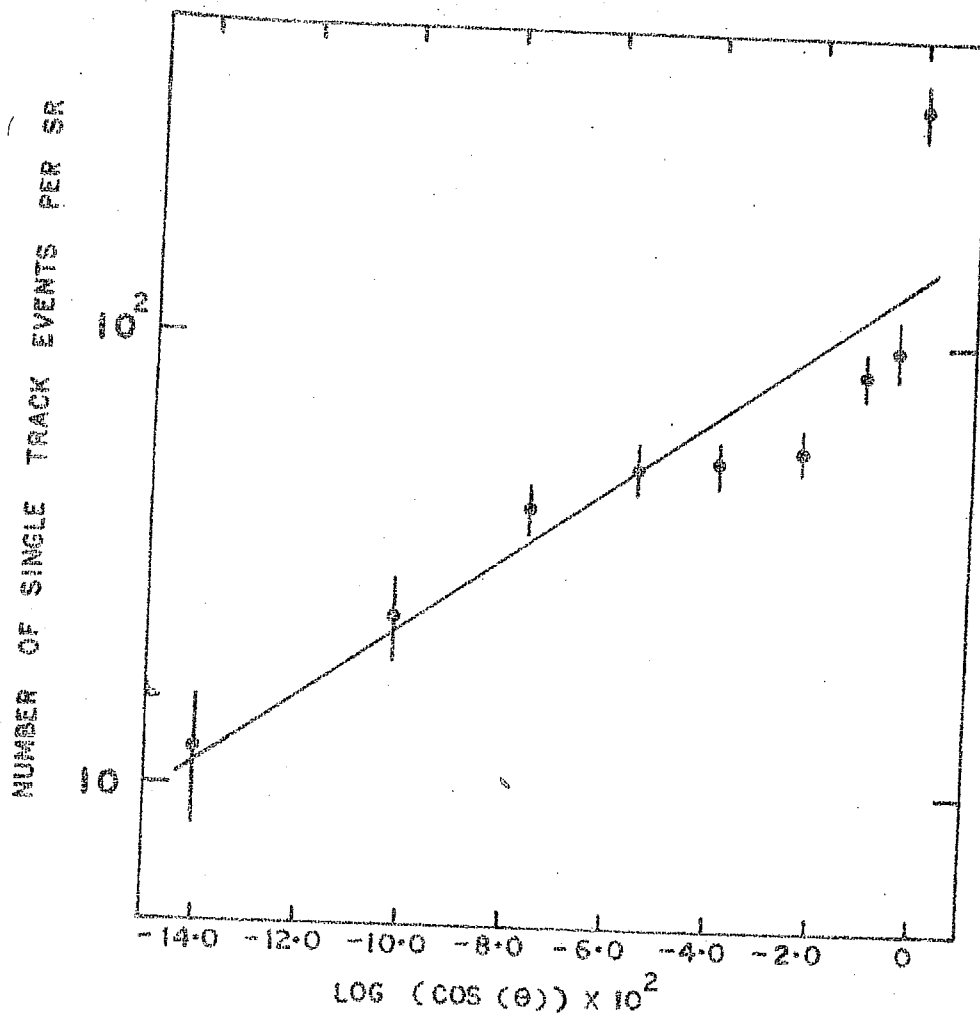
At a comparable depth of 816 m.w.e. Achar et al. (1965) measured the angular distribution of all cosmic ray muons which penetrate that depth. Operation of their experimental apparatus does not require association with an EAS at the surface level. The angular distribution

was found to be well represented by an expression of the type $I(\theta) = I_0 \cos^n \theta$, with $n = 1.93 \pm 0.22$. This distribution is much flatter than the results of the present experiment for muons, at 580 m.w.e., associated with EAS. This discrepancy is due to the difference in triggering system in the two experiments. In the present experiment angular distribution of UG-muons, associated with EAS at surface, actually gives angular distribution of the EAS cores.

Measurements on angular distribution of EAS, by means of cloud-chamber and G.M. counter techniques, by various workers show that the value of 'n' lies in the range 6-9. Bassi et al. (1953) have obtained the angular distribution of air showers at sea-level by measuring the space angles of air-shower axes. The measurement yields a distribution of the type

$$I(\theta) \propto \cos^n \theta ; n \simeq 8.3$$

This value is slightly larger than the value 7.6 obtained in the present experiment. Though the present distribution is obtained on the basis of the projected angles, we do not think that this will effect the value of the exponent 'n' significantly. The slightly flatter distribution may be due to the fact that in this



experiment an EAS is recorded only when it is associated with a muon at U.G.level. Thus the probability of recording larger zenith angle showers in this experiment is expected to be higher, as the muon density increases with the increasing zenith angle. In an experiment at sea-level, Earl (1959) found that even near the shower cores (20-150 m) the muon density (for $E \geq 1$ Gev) increased by a factor of 1.3, as the zenith angle of EAS changed from 0° to 40° .

VI.3 Pair-tracks Events:

About 7.8% of the total events were pair-tracks events exhibiting simultaneous passage of two penetrating particles through UG detectors. In most of these cases the particles were parallel to each other (Table VI,3 a).

TABLE VI.3 (a)

PAIR TRACKS EVENTS

Nature	Parallel pairs	Convergent pairs	Divergent pairs
No. of Events	47	7	4

The criterion adopted for the parallelism was that the angle between the two tracks be 1° . The distribution of the parallel-pairs in the separation between the pairs is shown in Fig. VI.4 (a). The minimum projected separation is 4 cm. Fig. VI.4 (b) shows the angular distribution of the parallel-pairs. It is seen that the distribution is having a rather sharp peak between $20^\circ - 30^\circ$. These Parallel Pairs might have originated either in the atmosphere or in the rock beyond 5 - 6 m from U.G. detector. In order to get a better idea about the origin of these particles we have analysed these events further.

Let us consider the Parallel Pair-tracks events with pairs having projected angles within 35° . There are in total 40 such events and we can write

$$(D_\mu)_{\text{obs}} = (2.02 \pm 0.32) \cdot 10^{-5} \text{ Sec}^{-1} \dots (6.3.1)$$

for the observed rate of the events. Number of such events expected, on the basis of the assumption that the observed particles are muons produced in the atmosphere as part of the EAS and that the number of muons in EAS is subjected to Poissonian fluctuations, may be written as

$$(D_\mu)_{\text{exp.}} = F (\geq N) \frac{A_{\text{eff}}}{l^2} \times P_{\mu 2} \cdot 2\pi r dr$$

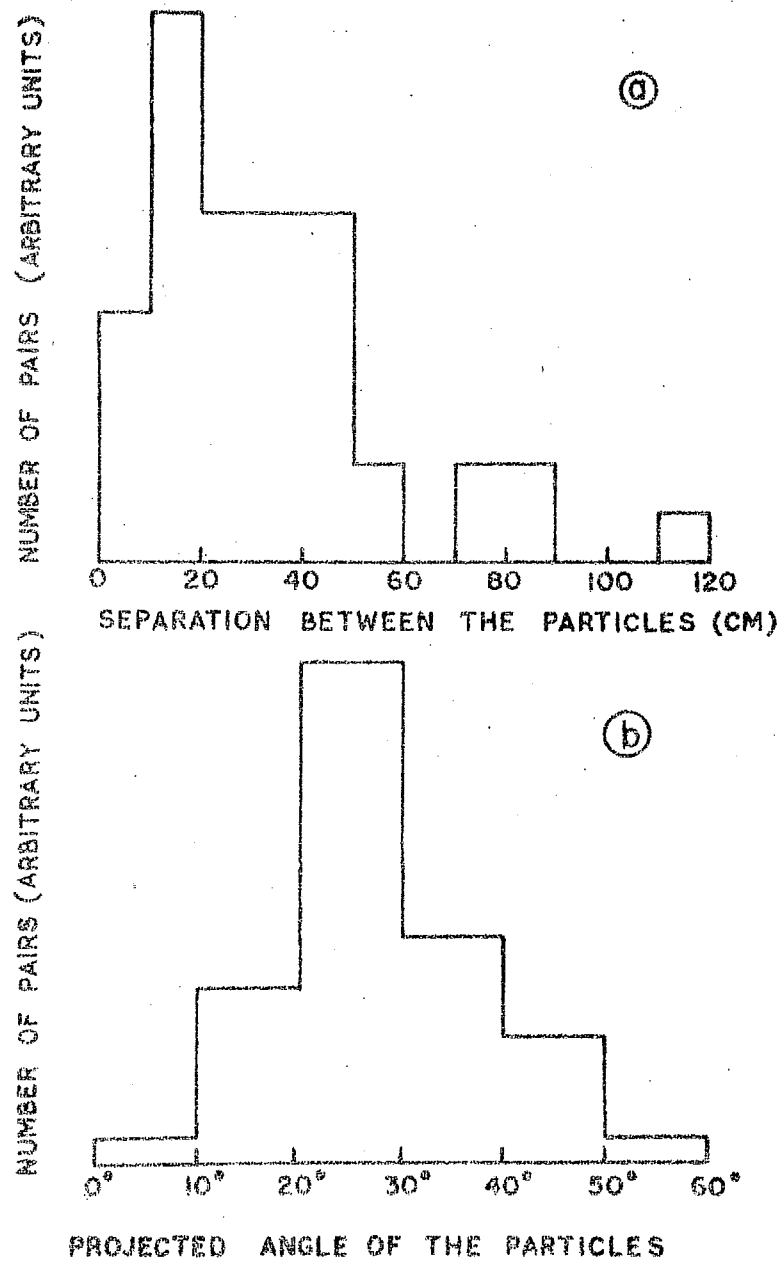


FIG. VI. 4

where (A_{eff}/L^2) is the effective solid angle for the EAS, $F(\geq N)$ is the integral flux of the EAS and $P_{\mu 2}$ is the probability that the underground detector will record two muons for showers having cores within r and $r + dr$ from the detector. $P_{\mu 2}$ may be written as

$$P_{\mu 2} = \frac{\exp(-S \Delta_{\mu})}{2!} (S \Delta_{\mu})^2 \quad \dots(6.3.3)$$

where S is the effective area of the detector.

In order to estimate the expected number we have assigned unique average values to $\langle A_{\text{eff}}/L^2 \rangle$ and $\langle r \rangle$ for the observed events as explained below.

Approximate distances of the core from the Parallel-Pair particles were obtained by calculating the distance between the intercept of one of the particles, with surface, and the point of incidence of EAS core. The distances were found to lie within 40 m. A weighted mean value of 11 m was obtained and we may then assign

$$\langle r \rangle = 11 \text{ m}$$

to all the events under consideration.

Muon density at distance r may be written as

$$\Delta_{\mu}(r) = \frac{N_{\mu}}{2\pi r_0^2} \exp\left(-\frac{r}{r_0}\right) \quad \dots(6.3.4)$$

and from Chapter IV, we may write

$$r_0 \simeq 12 \text{ m}$$

$$N_\mu = 27 \left(\frac{N}{10^5} \right)^{0.47}$$

The sizes of EAS associated with the events under consideration lie in the range $8.7 \times 10^3 - 5 \times 10^5$ particles. The integral flux $F (\geq N)$ turns out to be $\simeq 10^{-4} \text{ m}^{-2} \text{ St}^{-1} \text{ Sec}^{-1}$. A weighted mean size $\langle N \rangle \simeq 5.10^4$ particles may assigned to the events. We then have $N_\mu \simeq 20$ particles. Equation (6.3.4) then yields


$$\Delta_\mu \simeq 0.01 \text{ m}^{-2}$$

which in conjunction with equation (6.3.3) gives

$$P_{\mu 2} \simeq 2.25 \times 10^{-4}$$

In order to obtain the values of $\langle A_{\text{eff}} / L^2 \rangle$ we have classified the observed events in various zenith angle groups and calculated the solid angles for each group as given in table VI.3 (b). The triggering efficiency (ϵ) is taken into consideration. From

TABLE VI.3 (b)PARALLEL - PAIRS EVENTS

Projected zenith Angle	Number	$\frac{A_{eff}}{2\pi l^2}$	$\langle \frac{A_{eff}}{2\pi l^2} \rangle$	$\langle A_{eff}/l^2 \rangle$
10° - 15°	3	0.53 x 10 ⁻²		
15° - 20°	10	1.34 x 10 ⁻²		
20° - 25°	14	1.05 x 10 ⁻²	1.04 x 10 ⁻²	6.53 x 10 ⁻²
25° - 30°	9	0.85 x 10 ⁻²		
30° - 35°	4	1.08 x 10 ⁻²		
35° - 40°	3		Not considered for the present calculations.	
40° - 45°	1			
45° - 50°	3			

these values of solid angles a weighted mean is evaluated which may then be taken as the effective solid angle $\langle A_{eff}/l^2 \rangle$ for the events.

$$\langle A_{eff}/l^2 \rangle \simeq 6.53 \times 10^{-2} \text{ St.}$$

Substituting the values of various parameters obtained above in equation (6.3.2) we have

$$(D_{\mu})_{exp} \simeq 0.74 \times 10^{-5} \text{ Sec}^{-1}.$$

Though the observed result is nearly three times the one expected on the assumption that parallel-pairs are part of the incident EAS, it is approximately within three standard errors of the observed value.

It may, however, be noted that we can measure only projected zenith angles of the trajectories in a vertical plane in N-S direction and the actual space angles are not known. Moreover, information about the arrival directions of the associated EAS is not available. Thus the estimated core distances are very rough and Δ_{μ} is calculated only for an average r value because of a limited number of events. The effective operture estimate is also based on the projected angles and events associated with EAS of various sizes (having a large size range) are lumped together. Further the muon number - EAS size relation used here may not be very accurate in the size range under consideration. Considering all these approximations the agreement between the observed and expected rate may not be very unsatisfactory.

Thus we conclude that most of the parallel pairs originate in the atmosphere as part of EAS. However, the possibility that a small fraction may be due to local production in the rock at heights $\gtrsim 10$ m can not be ruled out. It will be possible to get more definite

information if space angles of the particles are known and if events could be classified in various size-groups.

There are seven cases of parallel pairs with projected zenith angle $\geq 35^\circ$. Out of these we have the surface EAS data for three events only. Core distances in these cases were found to be ≥ 50 m. These are most probably the particles accompanied by very much inclined showers and hence these are not included in the analysis.

The convergent-pairs appear to converge in the rock above the detector and the convergence in the cases is $> 1^\circ$. These pair events, which converge in the rock at angles greater than the limit of parallelism, seem to be produced in the rock by single muons of EAS. Particles in these events penetrate 10 cm lead absorber without undergoing the multiplication and hence they can not originate in electromagnetic interactions. These particles have to be non-electronic in nature and hence must have originated in photo-nuclear interaction of fast muons accompanying the EAS. As the number of observed events is small attempt has not been made to derive production cross-section due to nuclear interaction. For divergent pairs, the divergence appears too large to be accounted for by the multiple scattering suffered by the particles in the rock. Moreover, the accidental coincidence rate for such event is too small to account for the observed number.

VI.4 Multiple - Tracks Events:

In addition to the single-track and pair-tracks events six events, each showing three tracks, and one event showing five tracks were also observed. The particles in these events appeared to be parallel to each other and details of the separations between the tracks are given in Table VI.4.

TABLE VI.4

MULTIPLE TRACKS EVENTS

Nature	Projected angle	Separations between the tracks			
		1 & 2	2 & 3	3 & 4	4 & 5
Three Parallel Particles	34°S	46 Cm	35 Cm.	--	--
	16°S	5 "	23 "	--	--
	28°S	7 "	54 "	--	--
	30°S	74 "	40 "	--	--
	23°S	76 "	3 "	--	--
	25°S	20 "	32 "	--	--
Five Parallel Particles	30°S	37 "	5 "	2 cm	2 cm

Four of the particles in the five-particles event are close to each other, the fifth one being separated quite a bit from this group. In the present sample of the data events containing four-particles were not seen.

If the parallel particles, observed in the data, are produced in air as part of the EAS then the observed numbers in various categories appear to suggest a very steep number-density spectrum for these particles in EAS. However, any further conclusions about the nature of the spectrum of these particles, in EAS, must await the availability of a much larger sample of the data.

VI.5 Electromagnetic interactions of the high energy muons

From a study of the particles accompanying the muons, detected underground one may hope to derive information about the interactions of the muons with matter. In the present case where the muons, of energy ≥ 150 Gev associated with EAS, are being studied the interactions will correspond to interactions of muons having an average energy ≈ 500 Gev. This estimate of the average energy is based on the energy spectrum of muons in EAS, of the type $E_{\mu}^{-1.3}$ (Chapter IV). It is to be noted here that Chowdhuri and Saxena (1971) gave an estimate of 330 Gev for the average energy of the muons for the present experiment on the basis of the muon spectrum $E_{\mu}^{-1.5}$.

With a better estimate of $\beta \approx 1.3$ the average energy is found to be larger.

The particles accompanying the muons have been classified in different categories as shown in Table VI.5.

TABLE VI.5

Nature	Number	Percentage Probability
a) Showers produced in rock	30	0.040 ± 0.008
b) Showers produced in lead	40	0.055 ± 0.009
c) Knock-on Electrons produced in rock	19	0.026 ± 0.006
d) Knock-on Electrons produced in lead	30	0.040 ± 0.008
e) Knock-on Electrons produced in surrounding material	6	----
f) Electrons incident from rock	36	----
g) Electrons incident from lead	35	----
h) δ -rays in upper tray	13	----
i) δ -rays in lower tray	13	----

The events listed in category f) and g) correspond to the "Miscellaneous" category of Table VI.1 and for these events penetrating particles were not seen. In

addition to the events listed above there were 7 cases where electrons showers, incident from rock and hence seen only in upper tray, were not accompanied by a penetrating particle. Similar cases for showers incident from the lead numbered five. One event showing the electron-showers in both the upper and the lower tray was also recorded. The probability for such a double-process can then be written as (0.0013 ± 0.0013) .

The results given in table VI.5 may be compared with those of Creed et al. (1965). Creed et al. (1965) have studied the probabilities of a muon accompanied by electrons from the rock or generating them in the lead absorber, at three different depths at Kolar Gold Mines viz 816, 1812 and 4160 m.w.e. The mean energies of the muons observed at these depths were 130 Gev, 220 Gev and 300 Gev respectively. The probability of electrons accompanying a muon from the rock was found to increase with increasing depth as expected from the increasing average energy. The probabilities obtained in present experiment for various categories turn out to be greater than those observed by Creed et al. (1965) for muons of average energy 300 Gev. This is consistent with the fact that the average energy in the present experiment is greater than the average muon energies in the experiment of Creed et al.

The probabilities of electron-showers accompanying a muon from the rock and for the electron-showers produced by muons in 10 cm. lead absorber have been calculated for muon energy $E = 500$ Gev. The cross sections for knock-on, Bremsstrahlung and Pair-production processes, as given by Bhabha (1938), Christy and Kusaka (1941) and Bhabha (1935) respectively, have been used. The probabilities in the rock and the lead turn out to be 4.5% and 6.7% respectively. The calculated probability for lead is in reasonable agreement with the observed value. However the observed probability in lead appears to be slightly smaller than the predicted one.

VI.6 Large Size Bursts:

Besides the events discussed in proceeding section we have observed some cases of rather large number of particles (Bursts) triggering either the upper-tray or the lower tray or both the trays of the neon flash tube hodoscope. Some examples of such events are shown in Fig.VI.5 - Fig. VI. 10.

Out of these three categories, bursts which are detected simultaneously in both upper and lower n.f.t. trays, (separated by 10 cm. lead absorber) are most interesting. Number of the particles detected in the lower tray varies from 4 to 7. However, in some cases

the bursts are very dense. These bursts could be generated in the rock by a highly energetic Bremsstrahlung process or in some other different type of interaction in the cores of EAS. Further investigation will be able to give more definite explanation about this phenomenon. We have not included detailed analysis of these events here as further investigation is being continued.

VI.7 Conclusion and Summary:

Distribution of zenith angles of single penetrating particles at 580 m.w.e associated with EAS, is found to be of the form

$$I(\theta) = I_0 \cos^n \theta$$

with $n = 7.6 \pm 1.4$. This is a steeper distribution than obtained for all cosmic ray muons at 816 m.w.e by Achar et al. (1965). However, the distribution obtained in present experiment gives the angular distribution of EAS core. Other experiments indicate an exponent $\sim 8-9$. The discrepancy between these results and the result from present experiments can be explained on the basis of the difference in the recording systems. In the present experiment the EAS are recorded only when accompanied by a muon at underground level. Thus the

the present recording system has a natural bias for larger angle showers.

The probabilities of small shower production by muons in rock and in the lead are found to be $(4.0 \pm 0.8)\%$ and $(5.5 \pm 0.9)\%$ respectively. These values are in good agreement with the expected probabilities, for muons of average energy ≈ 500 Gev, calculated on the basis of the cross-sections given by Bhabha and Christy and Kusaka.

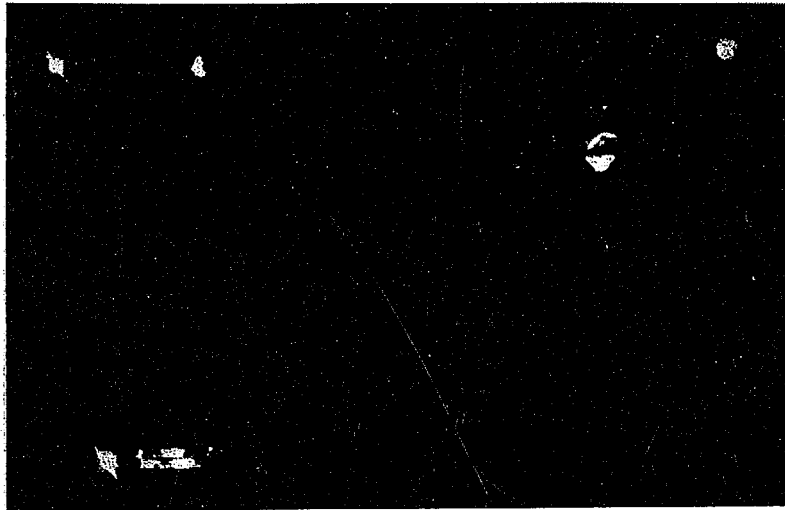
The rate of double parallel penetrating particles, associated with EAS, is found to be of the order of $(2.02 \pm 0.32) \times 10^{-5}$ per sec. The value, expected on the basis of the assumption that these particles are produced in atmosphere as a part of the EAS, is found to be 10^{-5} Sec^{-1} . The observed value thus appears to be larger than expected value. Since it has not been possible from the present data to classify the events in various EAS size groups, and further as the information is limited to the projected zenith angles of these tracks, the difference between the observed and expected values is not unreasonable. We, thus, conclude that the parallel pairs are particles produced in the atmosphere in the EAS cores.

A few cases of convergent pairs have also been observed. It is felt that these pairs are produced by the interaction of the incident muon in the rock through photo-nuclear interaction. Apart from these double penetrating particles a few multiple particle events have also been observed.

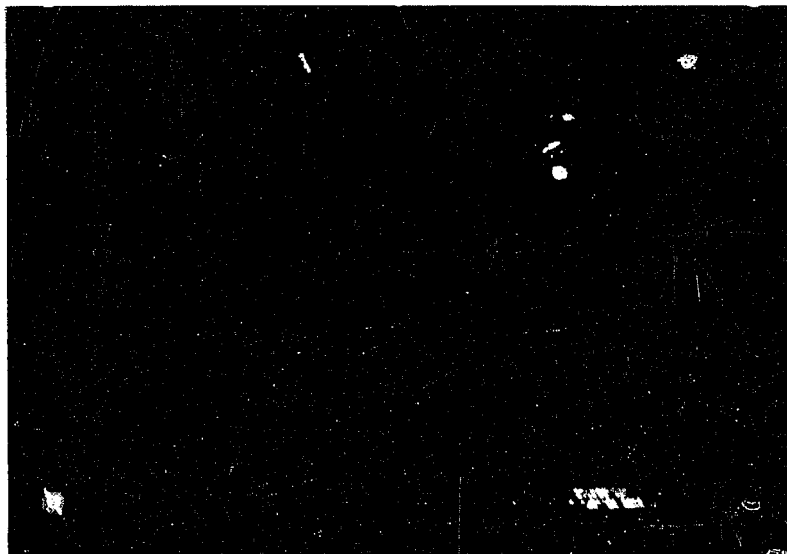
Some cases of very large bursts detected simultaneously in both the n.f.t. trays are reported. Such events are being investigated further.

VI.8 Suggestions for further investigation:

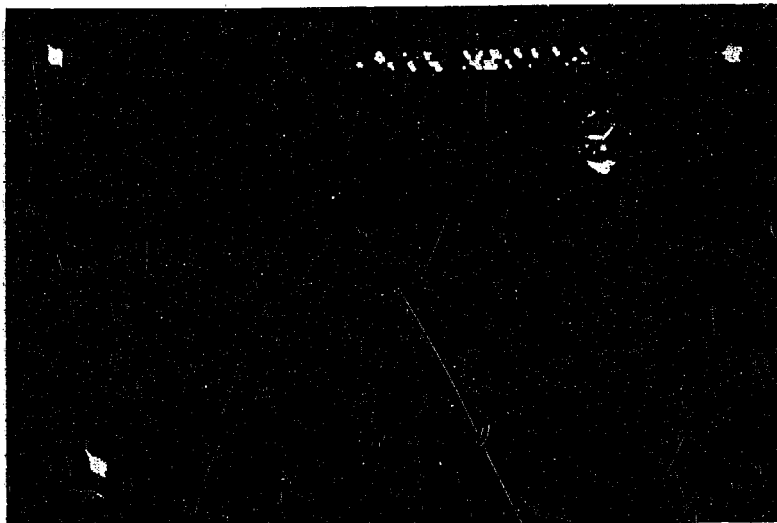
The large bursts observed in the present experiment represent a phenomenon which is hard to understand on the basis of present quantity and quality of the data. It is, therefore, desirable to look for these type of events in an improved way. At present the information about the spread of the bursts is available only in the projected plane. Use of a crossed-tray N.F.T. hodoscope can provide further information which may be useful in a better understanding of these events. Another tray of neon flash tubes under the lower tray separated by at least 5 cm of lead absorber will also be useful in understanding the nature of the detected particle.



'Burst' Produced in Lead
Fig. VI. 5



'Burst' Produced in Lead
Fig. VI. 6



'Burst' Incident from Rock
Fig. VI. 7



'Burst' Incident from Rock
Fig. VI. 8

• P 5773 LA 490-100000-1 68-100000-1 •

[illegible]

14-00000

1. The first group of people who are not in the labor force are those who are not in the labor force because they are not in the labor force.

These events have been observed for muons associated with the EAS. For a better understanding of these events it is desirable to know the location of the particles, observed in these events with respect to the core of the associated EAS. One may, therefore, use an EAS array which provided information about the direction and inclination of the EAS core.

It will, also, be interesting to look for these types of events in the underground experiments where association with the EAS is not a requirement. A comparison of the rates of these events in both these types of experiments (associated with EAS, and without EAS association requirement) will give useful clues about the nature of the particles in these events.

Parallel double and multiple penetrating particles, observed in present experiment, can give much important information about the production process and about the nature of primaries which generate the associated ultra high energy EAS. For this purpose it is necessary to know distances, of these particles from EAS cores, very accurately. To get these information a future investigation may be carried out to measure the space angles of these penetrating particles as well as arrival directions of the associated EAS. This will not only yield the accurate core distances but also the proper separation between the tracks in the parallel multiple events.

CHAPTER VII

SUMMARY

A study on muons of energy ≥ 150 Gev, associated with EAS, has been made for showers in the size range $10^5 - 5.10^6$. The study was made using an air shower array at the surface in coincidence with a muon detector placed at a depth of 194 m underground in Kolar Gold Fields, India. The investigation was carried out in collaboration with TIFR, Bombay.

The results presented in the thesis are based on the analysis of ~ 4000 showers recorded in coincidence with underground detector and $\sim 10,000$ showers recorded without the requirement of coincidence with the underground detectors. The results presented in the thesis are:

i) the differential spectrum for the showers, recorded in coincidence with a muon of energy ≥ 150 Gev, is a power law expressed as

$$\Phi(N) dN = (1.15 \pm 0.28) 10^{-13} \left(\frac{N}{10^5} \right)^{-2.30 \pm 0.09} dN$$

$$\text{m}^{-2} \text{Sec}^{-1}$$

ii) the differential spectrum for all the showers recorded by the array is given by

$$F(N) dN = (1.01 \pm 0.10) 10^{-10} \left(\frac{N}{10^5} \right)^{-2.78 \pm 0.04} dN \text{ m}^{-2} \text{ Sec}^{-1}$$

iii) the number of muons n (≥ 150 Gev) varies with the shower size N as

$$n_{\mu}(\geq 150 \text{ Gev}) = (27 \pm 7) \left(\frac{N}{10^5} \right)^{0.47 \pm 0.05}$$

in the size range $10^5 \leq N \leq 5 \cdot 10^6$,

iv) the energy spectrum of muons in the energy region $150 \leq E_{\mu} \leq 640$ Gev. may be expressed as a power law $(E_{\mu}^{-\beta})$ with a power index $\beta = 1.30 \pm 0.16$.

Number of muons, with threshold energies ≥ 150 Gev, has been calculated on the basis of four different models of the nuclear-interaction. The calculations have been carried out both for the proton primaries as well as for a mixed primary composition which remains constant throughout the primary energy range considered. The model calculations predict a n_{μ} - N variation, which goes as $N^{0.6 - 0.8}$, and the assumed models do not reproduce the observed variation. Two possibilities for obtaining the

observed n_{μ} - Ne variation are considered. It is shown that if one assumed a primary composition, which is varying with energy and is subjected to galactic rigidity cut-off in the relevant energy range, it is possible to reproduce the observed variation by selecting a proper model. However, the second possibility, viz. that of a possible change in the characteristic of the nuclear interactions at high energies ($\geq 10^{14}$ eV), cannot be ruled out.

Experimental data, on the particles detected at underground level in association with EAS, obtained by means of a NFT hodoscope are presented. It is shown that majority of the particles, recorded by the UG detector in association with EAS, are located in the vicinities of the respective cores. The distribution of the muon directions with the zenith is found to be of the type

$$I(\theta) \propto (\cos \theta)^{7.6 \pm 1.4}$$

This distribution is indicative of a steep zenith angle distribution for the recorded EAS. Order-of-magnitude calculations are given to show that the parallel-pair particles detected in association with EAS form part of EAS and are produced in the atmosphere. The electromagnetic interactions of the muons with matter are found to be consistent with the theoretical predictions. Some cases of large bursts, of high energy particles, recorded during the investigation have been presented.

LIST OF REFERENCES

- Abrosimov A.T., N.N. Gorimov, 1958 JETP, 34, 1077
V.A. Dimitriev, V.I. Solovena,
B.A. Khrenov & G.B. Khristiansen
- Abrosimov A.T., G.B. Basilevskaya 1960 JETP, 38, 100
V.I. Solovena & G.B. Khristiansen
- Achar C.V., V.S. Narasimhan, 1965 Proc. IX Int. Conf.
P.V. Ramanmurthy, D.R. Greed, Cosmic Rays (Lond),
J.B.M. Pattison, and 2, 989
A.W. Wolfendale
- Adcock C., J.F. de Beer, M. Oda, 1968 J. Phys. A, Ser 2,
J. Wdowczyk, A.W. Wolfendale 1, 82.
- Andronikashvili E.L. and 1960 JETP, 38, 703
R.E. Kazarov
- Auger P., R. Maze and 1938 Compt. Rend. 206,
T. Grivet-Meyer 1721
- Auger P., R. Maze and 1939a Compt. Rend. 207, 228.
J. Robley
- Auger P., R. Maze, J. Daudin, 1939b Compt. Rend. 208, 164
J. Robley & A. Freon
- Auger P., R. Maze, P. Ehrenfest, 1939c J. Phys. Rad. 10, 39
and A. Freon
- Barneveli T., M.F. Bibilashvili, 1964 Izv. Akad. Nauk
G.A. Grubelashvili, SSSR Ser. Fiz.
A.K. Javrishvili, R.E. Kazarov, 28, 1894
R.V. Kuridze and I.I. Khaldeeva
- Barton J.C. 1968 J. Phys. A. (Proc.
Phys. Soc.) Ser.
2, 1, 43.
- Barrett P.H., L.M. Bollinger, 1952 Rev. Mod. Phys. 24,
G. Cocconi, Y. Eisenberg and
K. Greisen

- | | | |
|---|-------|---|
| Bassi P., G. Clark,
and B. Rossi | 1953 | Phys.Rev. <u>92</u> , 441 |
| Bennett S. and K. Greisen | 1961 | Phys.Rev. <u>124</u> , 1982 |
| Bhabha H.J. | 1935 | Proc. Roy. Soc. <u>152A</u>
559 |
| Bhabha H.J. | 1938 | Proc. Roy. Soc. <u>164A</u> ,
257 |
| Blake P.R., H. Ferguson and
W.F. Nash | 1971 | Proc. XII.Int. Conf.
C.R. Hobart, <u>3</u> ,
1062 (EAS-35) |
| Bonzack B., R. Firkowsky,
J. Gawin, J. Hibner,
R. Maze, J. Wdowczyk and
A. Zawadzki | 1969 | J. Phys. A. <u>2</u> , <u>2</u> ,334 |
| Bridge H., W. Hazen and
B. Rossi | 1948 | Phys.Rev. <u>73</u> , 1352 |
| Broadbent D. and
L. Janossy | 1947a | Proc. Phys. Soc.
<u>A190</u> , 497 |
| Broadbent D. and
L. Janossy | 1947b | Proc. Phys. Soc.
<u>A191</u> , 517 |
| Broadbent D. and
L. Janossy | 1948 | Proc. Phys. Soc.
<u>A192</u> , 364 |
| Brown and McKay | 1949 | Phys. Rev. <u>76</u> , 1034 |
| Catz Ph., R. Maze,
J. Gawin | 1970 | Acta Physica Acad.
Sc. Hungaricae <u>29</u> ,
Suppl. <u>3</u> , 395 |
| Chatterjee B.K. | 1964 | Ph.D. Thesis
Bombay University |
| Chatterjee B.K., G.T. Murthy,
S. Naranan, B.V. Sreekantan,
and M.V. Srinivasa Rao | 1963 | Proc. Int. Conf.
C.R. Jaipur, <u>4</u> , 227 |
| Chatterjee B.K., S. Lal,
T. Matano, G.T. Murthy,
S. Naranan, K. Sivaprasad,
B.V. Sreekantan,
M.V. Srinivas Rao, and
P.R. Viswanath | 1965 | Proc. IX Int.Conf.
C.R. (Lond.) <u>2</u> ,
627 |

- Chatterjee B.K., G.T. Murthy,
S. Naranan, B.V. Sreekantan,
M.V. Srinivas Rao, S.C. Tonwar
and R.H. Vatcha 1968a Can. Jn. Phys.
46, S136
- Chatterjee B.K., G.T. Murthy,
S. Naranan, K. Sivaprasad,
B.V. Sreekantan, A. Suri and
P.R. Viswanath 1968b Can. Jn. Phys. 46,
S13.
- Chowdhuri B. 1948 Nature 161, 680
- Chowdhuri B. 1950 Proc. Phys. Sco.
A63, 165
- Chowdhuri B., R.C. Saxena and
A. Subramanian 1952 Proc. Ind. Acad.
Sc. A36, 457
- Chowdhuri B., and
Y.C. Saxena 1971 Proc. Ind. Acad.
Sc. A73, 69
- Christy and Kusaka 1941 Phys. Rev. 59, 405
- Ciok, Coghen, Gierula,
Holynski, Jurak, Miesowicz,
Saniswka and Pernegar 1958 Nuovo Cimento, 10,
741
- Clark G., J. Earl,
W. Kraushar, J. Linsley,
B. Rossi and F. Scherb 1957 Nature, 180, 353,
406
- Clark G., J. Earl,
W. Kranshar, J. Linsley,
B. Rossi and F. Scherb 1958 Nuovo Cimento
Suppl. 8, 623
- Cocconi G. 1958 Nuovo Cimento
Suppl. 8, 472
- Cocconi G. 1958a Phys. Rev. 111,
1699
- Cocconi G. 1961 Handbuch. d. Phys.
XLVI/1, Cosmic
Rays Ed.S. Flugg.

- | | | |
|---|-------|--|
| Cocconi G., Tongiorgi and Greisen | 1949a | Phys. Rev. <u>75</u> , 1063 |
| Cocconi G., Tongiorgi and Greisen | 1949b | Phys. Rev. <u>76</u> , 1020. |
| Cocconi, G., Koester and Perkins | 1961 | UCID Report No.28
pt.II |
| Cowsik R. | 1968 | Cand. Jn. Phys. <u>46</u> ,
S142 |
| Creed D., J.B.M. Pattison,
A.W. Wolfendale, C.V. Achar,
V.S. Narasimham and
P.V. Ramanmurthy | 1965 | Proc. IX Int. Conf,
C.R. (London) <u>2</u> ,
980 |
| Danilova T.V., S.I. Nikolskii | 1963 | Proc. Int.Conf.
C.R.Jaipur, <u>4</u> , 221 |
| Daudin J. | 1944 | Ann. Phys. <u>19</u> , 110 |
| Daudin J. | 1945 | Compt. Rend. <u>216</u> ,
483, 830, 832 |
| Daudin, J. | 1946 | Ann. Phys. <u>20</u> , 563 |
| De Beer, J.F., B. Holyok,
H. Oda, J. Wdowczyk and
A.W. Wolfendale | 1968 | J. Phys. A, Ser 2,
1, 72 |
| Dobrovolskii, Nikol'skii,
Tukish and Yakovlev | 1956 | JETP <u>31</u> , 939 |
| Dovzhenko and Nikol'skii | 1955 | Dokl. Akad. Nauk.
SSSR <u>102</u> , 241 |
| Earl J.A. | 1959 | M.I.T. Tech.Report
No.70 (Ph.D.Thesis) |
| Earnshaw J.C., K.J. Orford,
G.D. Rochester, A.J. Somogyi,
K.E. Turver, A.B. Walton | 1967 | Proc. Phys.Soc.
<u>90</u> , 91 |

- | | | |
|--|-------|---|
| Earnshaw J.C., K.J. Orford,
G.D. Rochester, K.E. Turver
and A.B. Walton | 1968 | Can. Jn. Phys.
<u>46</u> , S 122 |
| Eidus L.K., M.L. Adamovitch,
I.A. Ivanowskaya, V.S. Nikolaev
and M.S. Tulyankina | 1952 | JETP <u>22</u> , 440 |
| Fermi E. | 1950 | Prog. Theo. Phys.
<u>5</u> , 570 |
| Firkowski R., J. Gawin,
R. Maze, and A. Zawadzki | 1962a | J. Phys. Sco.
Japan <u>17</u> , Suppl.
A III, 123 |
| Firkowski R., J. Gawin and
A. Zawadzki | 1962b | Nuovo Cimento <u>26</u> ,
1422 |
| Firkowski R., J. Gawin and
A. Zawadzki | 1963 | Nuovo Cimento <u>29</u> ,
19 |
| Firkowski R., J. Gawin,
B. Grochalska, J. Hibner,
J. Kempa, R. Maze,
S. Pachala, W. Tkaczyk,
J. Wdowczyk | 1970 | Acta Phys. Acad.
Sc. Hungaricae,
<u>29</u> , Suppl.3, 509 |
| Fukui, Hasegawa, Matano,
Miura, Oda, Suga, Tanashi
and Tanaka | 1960 | Prog. Theo. Phys.
Suppl. <u>16</u> , 1. |
| Fujioka G. | 1953 | Int. Conf. Theo.
Phys. Japan, 125 |
| Gawin J., R. Maze, J. Wdowczyk,
and A. Zawdzki | 1968 | Cand. Jn. Phys. <u>46</u> ,
S75 |
| Greisen K. | 1956 | Prog. Cosmic R.
Physics <u>III</u> , 3. |
| Greisen K. | 1960 | Ann. Rev. Nucl.
Sc. <u>10</u> , 63. |

- Greisen K., D.D. Walker and S.P. Walker 1950 Phys. Rev. 80, 535
- Hara T., S. Kawaguchi, S. Mikano, M. Nagano, K. Sugi, G. Tanahashi, K. Uchino and H. Akiyama 1970 Acta Physica Acad. Sc. Hungaricae 29, Suppl 3, 361
- Hasegawa H., S. Naranan, T. Matano, I. Miura, M. Oda, S. Shibata, G. Tanahashi and Y. Tanaka 1962 J. Phys. Soc. Japan 17, Suppl. A.III, 189
- Hasegawa H., T. Matano, I. Miura and S. Shibata 1963 Proc. Int. Conf. C.R. Jaipur, 4, 284.
- Higashi S., T. Oshio, H. Shibata, T. Watanabe and Y. Watase 1957 Nuovo Cimento 5, 597
- Higashi S., T. Oshio, H. Shibata, T. Watanabe and Y. Watase 1960 Proc. Moscow C.R. Conf. 2, 170.
- Higashi S., T. Kikunura, Y. Mishima, S. Iyomoto, T. Oshio, H. Shibata and Y. Watase 1962 Jn. Phys. Soc. Japan 17, Suppl. A.III, 209
- Hulsizer R.I. and B. Rossi 1948 Phys. Rev. 73, 1402 (L)
- Ise J. & W.B. Fretter 1949 Phys. Rev. 76, 933
- Janossy J. and A.C.B. Lovell 1938 Nature 142, 716
- Kamata K., S. Shibata, O. Savedara, V. Dominik, K. Suga, K. Murakami, Y. Toyoda, M. La Pointe, J. Gaebel and I. Escobar 1968 Can. J. Phys. 46, 572.

- | | | |
|---|------|--|
| Kasnitz and Sitten | 1954 | Phys. Rev. <u>94</u> , 977 |
| Khrenov B.A | 1961 | Soviet Phys.JETP
<u>14</u> , 1001. |
| Khrenov B.A. | 1965 | Jn. Nucl. Phys.USSR
<u>1</u> , 540. |
| Khristiansen G.B. | 1958 | Nuovo Cimento Suppl.
<u>8</u> , 598. |
| Khristiansen G.B.,
O.V. Vedeneev,
G.V. Kulikov, V.I. Nazarov,
and V.I. Solovjeva | 1971 | Proc. XII Int. Conf.
C.R. Hobart, <u>3</u> , 1074,
(EAS-37) |
| Kolhorster W., Matthes and
E. Weber | 1938 | Naturwiss. <u>26</u> , 576 |
| Kraushar and Mark | 1954 | Phys. Rev. <u>93</u> , 233 |
| Lal S. | 1967 | Nuovo Cimento <u>48</u> ,
A, 466 |
| Landau L. | 1953 | Izv. Akad. Nauk
SSSR <u>17</u> , 57. |
| Lehane J., D.D. Miller, and
M.H. Rathgeb | 1958 | Nature <u>182</u> , 1699 |
| Linsley J. and L. Scarci | 1962 | Phys. Rev. Lett. <u>9</u> ,
123 |
| Manchanda N.K. | 1967 | M.Sc. Thesis Bombay
University |
| Machin A.C., K.J. Orford,
D.R. Pickersgill and
K.E. Turver | 1969 | Proc. of Budapest
Conf.(Acta Phys.
Acad. Sc. Hungaricae,
<u>29</u> , Suppl.3, 579,
1970) |

- | | | |
|---|------|--|
| Milone | 1952 | Nuovo Cimento <u>9</u> ,
237 |
| Molier G. | 1946 | Cos.Rad.,Ed.W.
Heisenberg 26. |
| McCusker C.B.A. | 1950 | Proc.Phys.Soc. <u>A63</u> ,
1240 |
| McCusker C.B.A. and
D.D. Miller | 1951 | Proc. Phys. Soc.
<u>A64</u> , 915. |
| Murthy G.T., K. Sivaprasad,
M.V. Srinivas Rao,
S.C. Torwar, R.H. Vatcha
and P.R. Viswanath | 1968 | Cand. Jn. Phys <u>46</u> ,
S147, S153, S159 |
| Nishimura J. and K. Kamata | 1950 | Prog.Theo.Phys. <u>5</u> ,
899 |
| Nishimura J. and K. Kamata | 1951 | Prog.Theo.Phys. <u>6</u> ,
262, 628 |
| Nishimura J. and K. Kamata | 1952 | Prog.Theo.Phys. <u>7</u> ,
185 |
| Nikol'skii S.I. | 1962 | USP.Fiz.Nauk SSSR.
<u>78</u> , 365. |
| Niu K. | 1958 | Nuovo Cimento <u>10</u> ,
944 |
| Pal Y. and B. Peters | 1964 | Kgl.Danske Viden-
skab. Selskab -
Mat.- Figs Medd.
<u>33</u> , No.15. |
| Peters B. | 1961 | Nuovo Cimento <u>22</u> , 800 |
| Peters B | 1962 | J.Phys.Soc.Japan, <u>17</u> ,
Suppl.A.III, 282. |
| Porter,N.A., T.E. Crawnshaw
and W. Galbraith | 1957 | Phil.Mag. <u>2</u> , 900 |

- | | | |
|---|------|---|
| Rochester G.D. | 1946 | Proc.Roy.Soc. <u>A187</u> ,
464 |
| Rogoginsky A. | 1944 | Phys.Rev. <u>65</u> , 291 |
| Scherb F. | 1959 | MIT Tech.Report
No.71 |
| Sitte K | 1950 | Phys.Rev. <u>78</u> , 721 |
| Sitte K. | 1952 | Phys.Rev. <u>82</u> , 977 |
| Sivaprasad K | 1970 | Ph.D.Thesis
Bombay University |
| Skobeltsyn D., G.T. Zatsepin
and V.V. Miller | 1947 | Phys.Rev. <u>71</u> , 5, 315 |
| Sreekantan B.V | 1971 | Paper presented at
XII Int.Conf.C.R.,
Hobart (EAS 1) |
| Staubert R., J. Trumper,
L. Wiedecke, W. Wolter,
E. Bohm, R. Fritze,
F. Mie and M. Samorski | 1970 | Acta Physica Acad.
Sc. Hungaricae, 29,
Suppl. 3, 661 |
| Suga K., I. Escobar,
K. Murakami, V. Domingo,
V. Toyoda, G. Clark and
M. La Pointe | 1963 | Proc.Int. Conf.C.R.
Jaipur, <u>4</u> , 9. |
| Suga K., S. Shibata,
S. Mikamo, Y. Toyoda,
K. Murakami, M. La Pointe,
K. Kamata and V. Domingo | 1970 | Acta Phys. Acad.Sc.
Hungaricae <u>29</u> , Suppl.
3, 423. |
| Takagi S. | 1952 | Prog. Theo Phys. <u>7</u> ,
123 |
| Thompson M.G., M.J.L. Turner,
A.W. Wolfendale and
J. Wdowczyk | 1970 | Acta Phys.Acad.Sc.
Hungaricae 29,
Suppl 3, 615 |

- Treat J.E. and K. Greisen 1948 Phys.Rev.74, 414
- Toyoda Y., K. Suga, K. Murakami, 1965 Proc. IX Int. Conf,
H. Hasegawa, S. Shibata, C.R.(Lond.); 2,
V. Domingo, I. Escobar, K. Kamata 708
H. Bradt, G. Clark and
M. La Pointe
- Tongiorgi V.C. 1948a Phys.Rev.73, 923
- Tongiorgi V.C. 1948b Phys.Rev.74, 227
- Tongiorgi V.C 1949 Phys.Rev.75, 1532
- Tonwar S.C., S. Naranan and 1971 Lett.Nuovo Cimento
B.V. Sreekantan 1, 13, 531
- Vavilov Yu.N 1962 JETP 43, 1009
- Vavilov Yu.N., Evstigneev, 1957 JETP 32, 1319
and S.I. Nikol'skii
- Vernov S.N. 1967 Proc. Int.Conf.C.R.
Calagary (invited
talk) 345
- Vernov S.N., I.P. Ivananko, 1960 JETP, 39, 509
G.V. Kulikov, and
G.B. Khristiansen
- Vernov S.N., V.I. Soloveva, 1961 Soviet Phys.JETP,
B.A. Khrenov and 14, 246
G.B. Khristiansen
- Vernov S.N., Li Don Hua, 1962 JETP, 42, 758
B.A. Khrenov and
G.B. Khristiansen
- Vernov S.N., G.B. Khristiansen, 1963 Proc.Int.Conf.C.R.
Abrosimov, Atrashkevich, Jaipur 4, 173
Beliaeva, Vendeneev, Bmitriev,
Kulikov, Netchin, Solovjeva,
Soloviev, Fomin and Khrenov

- Vernov S.N., G.B. Khristiansen, 1964 Izv. Akad. Nauk
A.T. Abrosimov, I.F. Beliaeva, SSSR, Ser. Fiz. 28,
V.A. Dimitriev, G.V. Kulikov, 1886
Yu. A. Nechin, V.I. Soloveva
and B.A. Khrenov
- Vernov S.N., Yu.A. Netchin, 1965 Proc. IX Int. Conf.
D.A. Stoyanova, B.A. Khrenov, C.R. (Lond.) 2,
Yu.A. Fomin and G.B. Khristi- 624.
ansen
- Vernov, S.N., G.B. Khristiansen 1968 Can. Jn. Phys. 46,
A.T. Abrosimov, V.B. Atrash- S197
kevitch, I.F. Beljaeva,
G.V. Kulikov, K.V. Mandritskaya,
V.I. Solovjeva and B.A. Khrenov
- Vernov S.N., G.B. Khristiansen, 1970 Acta Phys. Acad. Sc.
O.V. Vedneev, N.N. Kalnuykov, Hungaricae, 29,
G.V. Kulikov, K.V. Mandrit- Suppl. 3, 429
skaya, V.I. Soloveva
- Vernov S.N. and G.B. Khristi- 1969 Presented at XI Int.
ansen Conf, Budapest.
- Wdowczyk J., Wolfendale A.W. 1971 J. Phys. A, Vol. 4,
No. 2.
- Zatsepin G.T. 1962 J. Phys. Soc Japan
17, Suppl. A III,
495.
- Zatsepin G.T. Rozenthal, 1953 Izv. Akad. Nauk,
Saritcheva and SSSR, Ser. Fiz. 17,
G.B. Khristiansen 39.
- Asekun V.S., Erdyken A.D., 1971 Proc. XII Int. Conf.
Kulichenko A.K., C.R., Hobart,
Machavariani S.K., 6, 2132 (EAS-40)
Nikol'sky S.I. and
Ramakhin V.A.